

國立交通大學機械工程學系

博士論文

具齒面修整之齒輪刮削研究

Research on Gear Shaving for Gears with
Tooth Modifications




研究生：劉嘉宏

指導教授：洪景華 博士

中華民國九十七年十二月

中文摘要

齒輪齒面修整亦稱為齒輪隆齒，能夠大幅地提高齒輪的性能；齒輪刮削是具備高效率的齒輪精加工法，其中橫向式刮齒與直進式刮齒是齒輪刮削的基本形式，能夠以高效率的方式完成齒輪齒面修整。本論文針對此兩種形式之刮齒方法進行研究，探討其對於齒輪之隆齒的影響。論文中研究了在橫向刮齒製程中的機器設定參數與刀具裝備誤差對齒面修整的影響，並以實驗設計法對製程中各項參數進行最佳化研究，提高了齒輪的傳動性能。以本研究中的範例說明，在相同條件下的傳動誤差可以得到相當程度的改善



對於直進式刮齒，本論文提出一設計最佳化方法，針對具隆齒的齒輪調整直進式刮齒刀的齒面修形，藉由降低刮齒刀之輪磨齒面與理論齒面之間的拓樸誤差，可進一步改善工件齒輪齒面誤差；本研究亦分析了直進式刮齒的切削路徑，針對刮齒刀齒面插槽設計參數進行最佳化設計，能夠有效地提高刮齒效率，使其切削比(cutting-down ratio)可得到相當程度的改善。

ABSTRACT

Gear tooth modification, also called gear tooth crowning, can cause great improvement of gear performance. Gear shaving is one of the most efficient and economical process for gear finishing after the rough cuttings of hobbing or shaping, in which transverse shaving and plunge shaving are the most widely adopted methods. Through gear shaving, tooth crowning can be achieved very efficiently. This dissertation has investigated gear tooth crowning induced by transverse and plunge gear shaving. For transverse gear shaving, the influences of machine setting parameters and cutter assembly errors have been observed. Design optimization for robustness of gear transmission error has also been accomplished, in which the transmission error has been greatly improved.

For plunge gear shaving, in order to manufacture gears with tooth crowning, a method of design optimization is proposed to reduce the topographic error between the theoretical and the ground shaving cutter tooth surfaces, in which the analytical description of the gear with tooth crowning is constructed, and then the grinding wheel profile is parameterized and optimized. The cutting trace of plunge shaving cutter has also been analyzed by optimizing the arrangement of cutter serration, so that the cutting-down ratio can be reduced and therefore the cutting efficiency can be improved.

CONTENTS

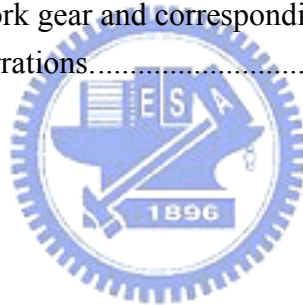
中文摘要	II
ABSTRACT	III
CONTENTS	IV
LIST OF TABLES	VI
LIST OF FIGURES	VII
CHAPTER 1 INTRODUCTION	1
1.1 Backgrounds	1
1.2 Literature review	2
1.3 Research objectives	4
CHAPTER 2 GEAR SHAVING: FUNDAMENTALS	5
2.1 Gear shaving cutter	5
2.2 Methods of gear shaving	6
2.2.1 Transverse shaving	6
2.2.2 Diagonal Shaving	6
2.2.3 Underpass shaving	7
2.2.4 Plunge shaving	7
CHAPTER 3 TRANSVERSE GEAR SHAVING WITH TOOTH MODIFICATIONS	11
3.1 Transverse shaving with lead crowning	11
3.1.1 Construction of coordinate systems and the shaved gear tooth profile	11
3.1.2 Effects of machine setting parameters on the tooth lead crowning	14
3.1.3 Simulation of gear shaving with cutter assembly errors.....	16
3.2 Transverse shaving with double crowning	17
3.3 Design optimization for robustness of gear transmission error.....	19
3.3.1 Transmission error analysis of the shaved gear.....	19
3.3.2 Design optimization for robustness	21
3.4 Concluding remarks.....	22
CHAPTER 4 PLUNGE GEAR SHAVING WITH TOOTH MODIFICATIONS	40
4.1 Surface interpolation of modified gear tooth.....	41
4.2 Topographic error analysis of the plunge shaving cutter.....	43
4.3 Design optimization of the cone-grinding wheel	45
4.4 Concluding remarks.....	48
CHAPTER 5 DESIGN OF SERRATIONS ON GEAR PLUNGE SHAVING CUTTER..	70
5.1 Design parameters for the shaving cutter serrations.....	70
5.2 Numerical examples and discussion.....	72
5.3 Concluding remarks.....	74
CHAPTER 6 CONCLUSIONS AND FUTURE WORKS.....	80

6.1	Conclusions	80
6.2	Future works	81
REFERENCES		83



LIST OF TABLES

Table 3.1 Parameters of work gear and shaving cutter.	24
Table 3.2 Machine setting parameters in gear shaving.	24
Table 3.3 Basic data of the gear pair (Example 3.6).	25
Table 3.4 Factors and their levels in transmission error analysis.	25
Table 3.5 The S/N ratios of the transmission error analyses.	26
Table 3.6 Factor response table for the transmission error analyses.	27
Table 4.1 Basic data of the target surfaces.	50
Table 4.2 Data of gear tooth modifications of the target surfaces.	50
Table 4.3 Conditions and errors of B-spline surface interpolation (Σ_{S2}^I).	51
Table 4.4 Data of cutter and grinding wheel for Example 4.1.	52
Table 4.5 Results of the second level optimization in Example 4.2.	52
Table 4.6 Achieved tooth modifications of gear after the experiment for validating Example 4.3.	53
Table 5.1 Basic data for the work gear and corresponding shaving cutter.	75
Table 5.2 Basic data for the serrations.	75



LIST OF FIGURES

Figure 2.1 Sliding on the tooth flanks of the crossed-axes meshing.....	8
Figure 2.2 Shaving cutter serrations.....	8
Figure 2.3 Transverse gear shaving.....	9
Figure 2.4 Diagonal gear shaving.....	9
Figure 2.5 Underpass gear shaving.....	10
Figure 2.6 Plunge gear shaving.....	10
Figure 3.1 Crowning mechanism of the traditional shaving machine.....	28
Figure 3.2 Parametric representation of the crowning mechanism.....	28
Figure 3.3 Coordinate system of the gear shaving machine with considerations of cutter assembly errors.....	29
Figure 3.4 Lead crowning of the shaved gear.....	29
Figure 3.5 Lead crowning under different conditions ($d_v=188mm, C=385mm, \theta=2^\circ 50'$, $d_h=350\sim 600mm, \Delta d_h=50mm$).....	30
Figure 3.6 Lead crowning under different conditions ($d_h=545mm, C=385mm, \theta=2^\circ 50'$, $d_v=50\sim 300mm, \Delta d_v=50mm$).....	30
Figure 3.7 Lead crowning under different conditions ($d_v=188mm, d_h=545mm, \theta=2^\circ 50'$, $C=200\sim 400mm, \Delta C=100mm$).....	31
Figure 3.8 Lead crowning under different conditions ($d_v=188mm, d_h=545mm, C=385mm$, $\theta=1^\circ 50'\sim 4^\circ 50', \Delta\theta=1^\circ$).....	31
Figure 3.9 Variations of circular tooth thickness from vertical error (a) $\Delta v = 0.02^\circ$ (b) $\Delta v = -0.02^\circ$	32
Figure 3.10 Tooth lead crowning affected by vertical cutter assembly error.....	33
Figure 3.11 Tooth lead crowning affected by horizontal cutter assembly error.....	33
Figure 3.12 Tooth lead crowning affected by cutter assembly error of the center distance....	34
Figure 3.13 Normal section of the parabolic rack cutter.....	34
Figure 3.14 Coordinate systems of the rack cutter from normal to axial section.....	35
Figure 3.15 Coordinate systems of the generating motion between the rack cutter and the shaving cutter.....	35
Figure 3.16 Double crowning of the saved gear.....	36
Figure 3.17 Coordinate systems of the meshing gear pair.....	36
Figure 3.18 Meshing of the two gear tooth surfaces.....	37
Figure 3.19 Transmission error of the gear pair (gear 2 lead crowned only).....	37
Figure 3.20 Transmission error of the gear pair (gear 2 double crowned).....	38
Figure 3.21 Fishbone diagram of the factors.....	38
Figure 3.22 Factor response graph for the transmission error analyses.....	39
Figure 3.23 Transmission errors caused by original and optimized parameters.....	39
Figure 4.1 SAP and EAP of a shaving cutter tooth.....	54

Figure 4.2 Model of gear tooth crowning (Wagaj, 2002).....	54
Figure 4.3 Flowchart of interpolation error analysis.....	55
Figure 4.4 Cylindrical coordinate used for sampling data points.....	55
Figure 4.5 Interpolation error of Σ_{D2}^I by changing m ($n=3, p=q=4$).....	56
Figure 4.6 Validations of interpolated surfaces (Σ_{S2}^I vs. Σ_{L2}^I).....	56
Figure 4.7 Validations of interpolated surfaces (Σ_{S2}^I vs. Σ_{D2}^I).....	57
Figure 4.8 Coordinate systems of gear shaving machine.....	58
Figure 4.9 Coordinate systems of shaving cutter re-sharpening machine.....	59
Figure 4.10 Topographic errors between theoretical and ground shaving cutter tooth surfaces (Σ_{S1}^T vs. Σ_{S1}^G).....	60
Figure 4.11 Topographic errors between theoretical and ground shaving cutter tooth surfaces (Σ_{D1}^T vs. Σ_{D1}^G).....	60
Figure 4.12 Flowchart of design optimizations of the cone grinding wheel.....	61
Figure 4.13 Topographic errors between theoretical and ground shaving cutter tooth surfaces optimized by θ_c (Σ_{S1}^T vs. Σ_{S1}^G).....	61
Figure 4.14 Topographic errors between theoretical and ground shaving cutter tooth surfaces optimized by θ_c (Σ_{D1}^T vs. Σ_{D1}^G).....	62
Figure 4.15 Parameterized profile of grinding wheel for optimization.....	62
Figure 4.16 Topographic errors between theoretical and ground shaving cutter tooth surfaces by profile optimization (Σ_{D1}^T vs. Σ_{D1}^G).....	63
Figure 4.17 Plunge shaving cutter used in the experiment (a) overview (b) scaled view.....	64
Figure 4.18 Pre-shaved gear used in the experiment (a) overview (b) detailed view.....	65
Figure 4.19 Measured data of the pre-shaved gear used in the experiment.....	66
Figure 4.20 Plunge shaving cutter ground by the grinding wheel of the re-sharpening machine.....	67
Figure 4.21 NACHI shaving machine used in the experiment (a) machine overview (b) cutter and work gear setup.....	68
Figure 4.22 Measured data of the shaved gear after the experiment.....	69
Figure 5.1 Diagram of a shaving cutter and a work gear (Hsu, 2006).....	76
Figure 5.2 Diagram of a shaving cutter with helix-staggered serrations (Hsu, 2006).....	76
Figure 5.3. Design parameters of plunge shaving cutter serration (a) serration pitch (b)	

serration displacement. 77

Figure 5.4 Cutting path calculations (Hsu, 2006) (a) path of the cutting edge on the work gear (b) end of the first cutting cycle simulation (c) end of the second cutting cycle simulation. 78

Figure 5.5 Optimized cutting-down ratio of Example 5.2 (a) 1st cut (b) 1st peak (c) 2nd peak. 79



CHAPTER 1

INTRODUCTION

1.1 Backgrounds

With the increasing requirements of transmission systems for high rotation speed and compact size, the precision of gears, which are the most important components in transmission systems, is also highly required. Gear shaving is one of the most efficient and economical process for gear finishing after the rough cuttings of hobbing or shaping. The shaving process has the ability to correct errors in index, helix angle, tooth profile, and eccentricity by removing fine hair-like chips from gear tooth surfaces (Townsend, [1]). Through this process, the highest gear precision that can be achieved is DIN 6 or DIN 7. There are four basic shaving methods: transverse shaving, diagonal shaving, underpass shaving and plunge shaving.

Gear tooth modification, also called gear tooth crowning, can be accomplished by gear shaving. It can be used to eliminate edge contact of the teeth, and hence significantly increases operation cycles. Gear tooth crowning can also produce significant improvements in transmission. It can be induced efficiently by a CNC shaving machine. However, it is indeed costly for gear manufacturer to replace a traditional shaving machine by a CNC one. To induce crowning in transverse (or diagonal) shaving by a traditional shaving machine, it requires rocking of the machine worktable. The coordinated motions of traditional shaving machine is driven by mechanism instead of controller, which is relatively much cheaper. However, the crowning effect needs to be studied further.

In tangential or plunge shaving, however, the cutter has to be modified several times to meet the demand resulting in much consumed time and inevitable higher cost. Therefore, an analytical method is needed to obtain the right shaving cutter tooth surface geometry.

1.2 Literature review

The meshing between cutter and work gear in shaving can be viewed as a meshing pair of gears in a 3-D crossed-axis manner. The rotary shaving of an involute pinion was studied by Dugas [2]. Litvin [3] proposed the basic meshing conditions of a 3-D crossed-axis helical gear pair and it has been widely adopted as the fundamental assumption for simulation of gear shaving. Tsay [4] studied tooth contact and stress analysis of helical gears. Miao and Koga [5] and Koga *et al.* [6] calculated the crossed-axis angle at operating pitch circle, and developed a mathematical model of a plunge shaving cutter. In addition to these researches on fundamental theories of gear shaving, software for designing shaving cutter has been provided by Kim *et al.* [7], where meshing between cutter and work gear was approximated as an equivalent 2-D spur gear model. Moriwaki *et al.* [8, 9] proposed a stochastic model to predict the effect of shaving cutter performance on the finished tooth form. Hsu [10] proposed a mathematical model of serration cutting edge of plunge shaving cutter taking into account necessary hollow tooth form. The majority of literature focused on studying the shaving cutter itself and the corresponding effects on the shaved gears. However, high quality shaved gear can also be made through researches on the gear shaving machine. Lin [11] constructed a mathematical model of a gear shaving machine by firstly deriving an analytical representation of an additional angle of rotation in shaving.

Transmission error is one of the most important indication of gearing quality. Through optimum or robust design, the transmission error can be significantly improved. Chang *et al.* [12] studied the transmission error in a modified helical gear train, and the system was optimized by adjusting the helical angles of the gears. Sundaresan *et al.* [13] explored the influences of gear profile parameters on transmission error, and robust design of the whole assembly was then achieved.

Litvin [14] provided a double crowned gear modified both in lead and in profile with

improved transmission error. Wagaj and Kahraman [15] investigated the durability of helical gear affected by tooth crowning. Kahraman *et al.* [16] presented a gear wear model analyzing the influences of tooth crowning.

Plunge shaving is the most advanced gear finishing technique which only needs radial infeed. Its advantages include increased productivity, accuracy, long tool life, and a simple machine structure (Bianco [17]). In recent years, how to induce gear tooth crowning by shaving has become an important subject of research. Litvin *et al.* [18] proposed a method for shaving gears with double crowning by CNC shaving machine. For shaving methods other than plunge shaving, the gear tooth crowning is accomplished by tooth modifications of the shaving cutter and the coordinated motions between cutter and gear. For the plunge shaving method, however, it only depends on the surface geometry of the plunge shaving cutter. Traditionally, the cutter surface geometry results from a cutter re-sharpening machine by trial and error.

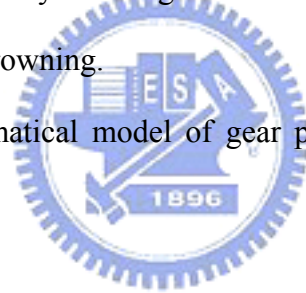
Focusing on the surface geometry of shaving cutter, Koga *et al.* [6] explored the errors in the cutter's tooth profile that resulted from the grinding machine setup. Hsu [10] investigated the topographic error of cutters from a re-sharpening machine for shaving involute gears. Radzevich [19, 20] proposed a methodology for calculating the parameters of the plunge shaving cutter and the respective form grinding wheel from measured discrete points of the modified gear. Nevertheless, without an analytical description of the modified gear and the plunge shaving cutter, further investigations are still limited.

Numerical approximation and interpolation are commonly used to construct an analytical description of discrete data points. Piegl and Tiller [21] provided basic theories for numerical approximations and interpolations. Barone [22] used B-spline curve fitting and swept surface to model gears with profile crowning. Wang, *et al.* [23] studied the geometric relationship and conjugate motion of DGTS (Digital Gear Tooth Surface) composed of discrete points.

1.3 Research objectives

Although the previous studies have significantly improved understanding of the characteristics of the shaving process, they largely focused on theoretical analyses and manufacture of shaving cutter. However, a complete mathematical model of gear shaving has not been established, which can facilitate the control of gear tooth crowning and predict the real finished tooth forms. The main objectives of this dissertation including:

1. Investigating the important influences of shaving machine setting parameters and cutter assembly errors on gear tooth crowning.
2. Investigating the transmission error of the gear pair shaved by traditional shaving machine, and also carrying out robust design.
3. Improving the efficiency of design and manufacture of plunge shaving cutter for shaving gears with crowning.
4. Constructing mathematical model of gear plunge shaving to improve the cutting efficiency.



CHAPTER 2

GEAR SHAVING: FUNDAMENTALS

2.1 Gear shaving cutter

During all shaving processes, the work-piece and the cutter rotate together like a pair of helical gears with crossed axes. The shaving cutter receives the motion from the motor and drives the work-piece which is coupled onto a freely-moving shaft. The meshing is therefore free, which is the main reason why indexing errors are not easy to improve.

The reason why axes are crossed is to create an action of relative sliding between the cutter tooth flank and the gear tooth. As shown in Fig. 2.1. the cutter prolonged along its axis in such a way as to form a cylinder if the b axis were free to move, the wheel coupled on it would have a movement around the cutter axis in the V direction linked to the cross angle γ . Speed V is the result of two components, precisely V_1 and V_s . V_s is compensated by the natural cutter rotation, while the V_1 component would move the workpiece along the cutter axis. In fact, wheel b cannot move in that direction because it is clamped on its axis and the axis, in turn, is fixed. It is quite clear that in order to compensate for this missing movement, a sliding action will occur between the two tooth flanks.

The shaving cutter teeth are manufactured with slots, normally called serrations as shown in Fig. 2.2, which run along the tooth profile. These serrations form a series of cuffing edges. These are the edges that generate the removal of metal in the form of tiny chips, as a result of the sliding effect between the gear tooth flank and the cutter tooth flank. The shape, dimensions and manufacturing methods of these serrations will be dealt with at a later stage.

The crossed-axes angle is the difference between the cutter helix angle and the gear helix angle. The range of the values of such angle is normally between 10° and 15° . If the value is higher than 15° , cutting is easier, cutting capacity increases and the sliding speed increases,

thereby shortening the life of the cutting edges. However, the control of the profile and the lead direction is lost because of the reduced guiding action. On the other hand, if the angle decreases from 10° onwards, a progressive upsetting effect is obtained that tends to reproduce the conditions of parallel axes. In cases where gears do not permit a regular crossed-axes angle due to their shape, it can go as down to 3° thus obtaining a shiny surface.

2.2 Methods of gear shaving

There are various shaving methods which substantially differ according to the direction of the movement given to the cutter. The choice of one method or another depends on the work- piece shape, on the machine characteristics and on the type of production of that has to be performed, i.e. small batches or big series. For some methods the cutter has to be studied carefully as regards both serrations and the tooth surface geometry.

2.2.1 Transverse shaving

The relative feed motion between the cutter and the gear takes place in the direction of the gear axis as shown in Fig. 2.3. The gear to be shaved reciprocates in the direction of its own axis while the gear and the tool are in mesh. With each reciprocation, a small amount of radial feeding of the shaving cutter occurs. The theoretical table stroke is as long as the face width of the gear to be shaved and it is recommended to calculate 1 extra stroke per module in order to guarantee clean shaving of the edges. This method is unsuitable for shaving shoulder gears.

2.2.2 Diagonal Shaving

As shown in Fig. 2.4, the gear to be shaved reciprocates obliquely in relation to its own axis while the gear and the tool are in mesh. The diagonal angle is achieved either by positioning the workpiece table obliquely or by interpolating two machine axes. With each reciprocation, radial feeding of the shaving cutter occurs. In general the diagonal angle can be

between 0 and 40 degrees but should not be above 25 degrees for reasons of wear.

2.2.3 Underpass shaving

As shown in Fig. 2.5, underpass shaving is basically the same as diagonal shaving but with a diagonal angle of 90 degrees. With underpass shaving, there is no axial table reciprocation. Instead the workpiece reciprocates perpendicularly to its own axis. The shaving cutter must be wider than the gear to be shaved and its serrations must be placed on a helix. All tooth corrections must be made to the shaving cutter as it will not be possible to realize them through axial movements on the machine.

2.2.4 Plunge shaving

As shown in Fig. 2.6, with this method there is no worktable translation but only a radial feed of the workpiece against the shaving cutter. The shaving cutter must be wider than the gear to be shaved and the serrations of the shaving cutter must be in the form of a helix in order to produce the relative tooth flank feed. Plunge shaving is particularly suited to shaving shoulder gears. In this case, however, all tooth modifications also must be made to the shaving cutter as it will not be possible to realize them through axial movements on the machine.

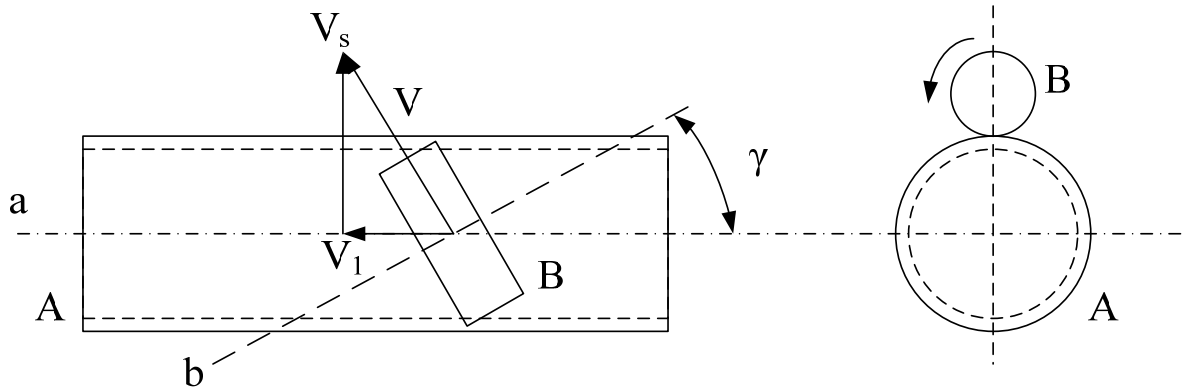


Figure 2.1 Sliding on the tooth flanks of the crossed-axes meshing.

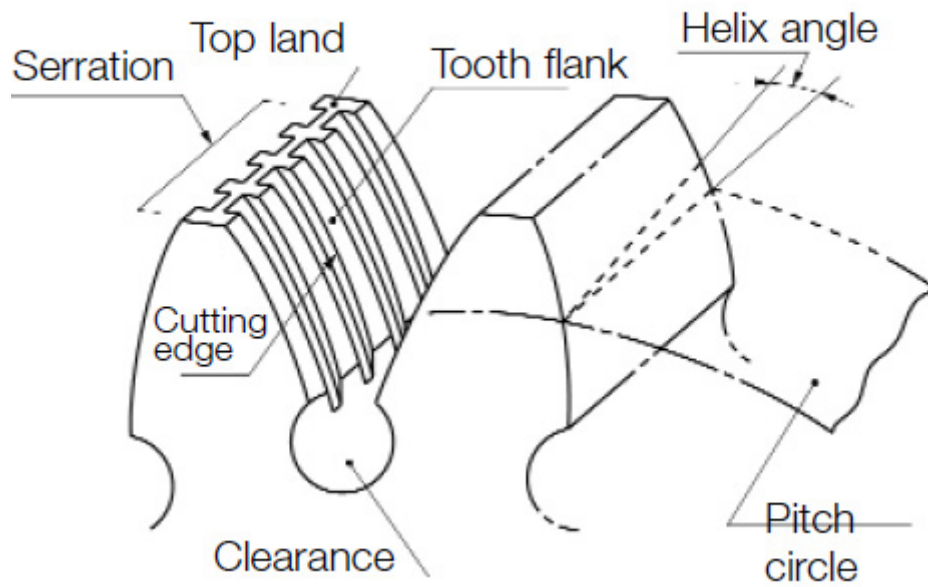


Figure 2.2 Shaving cutter serrations.

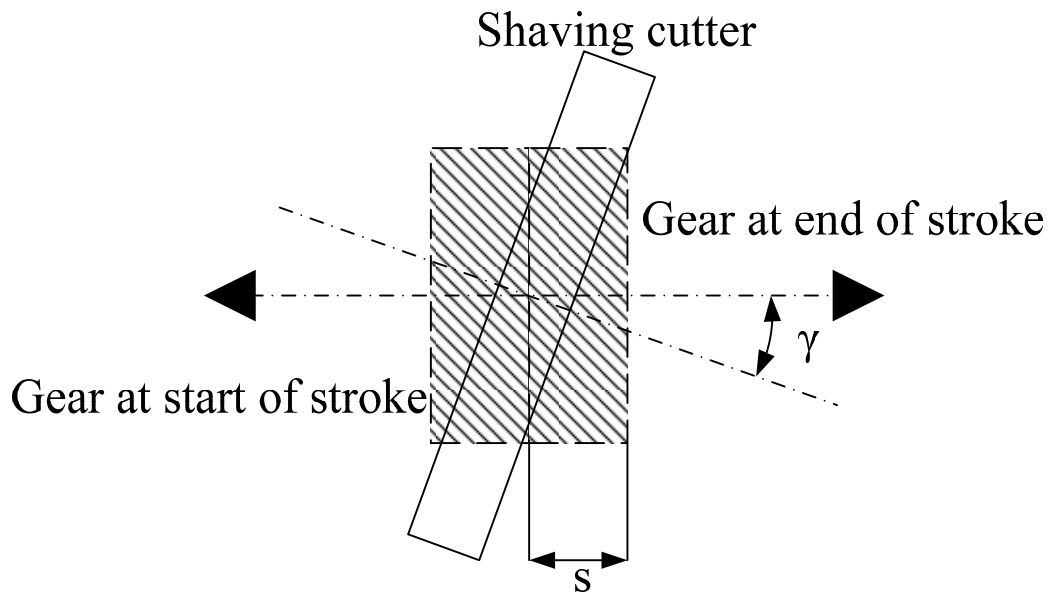


Figure 2.3 Transverse gear shaving.

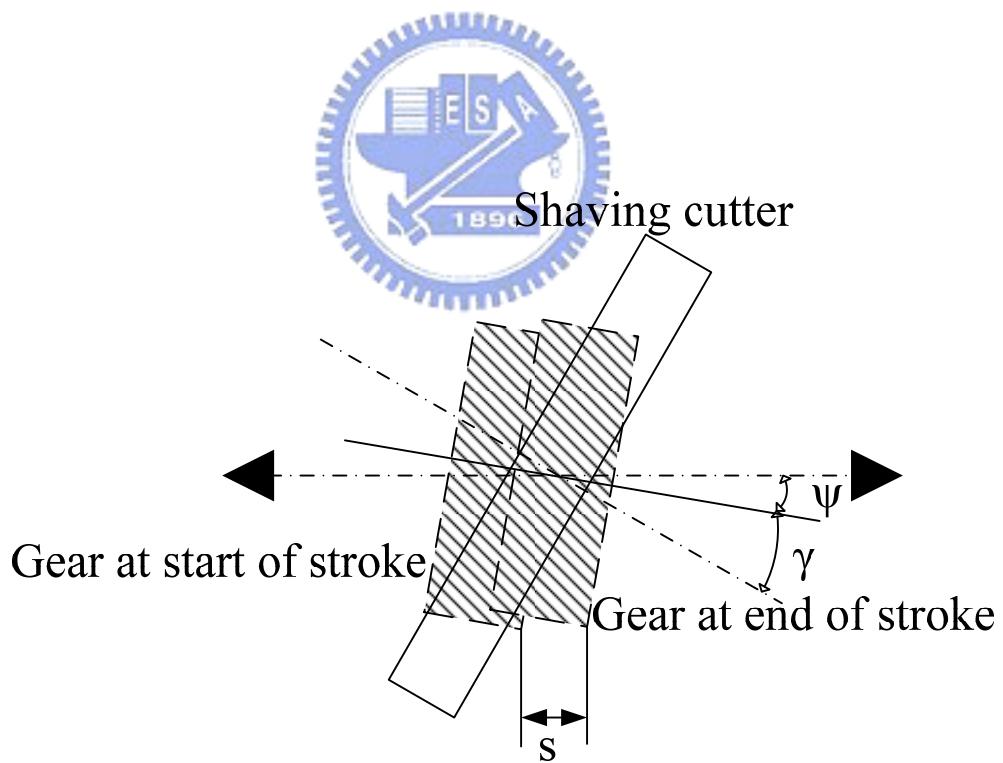


Figure 2.4 Diagonal gear shaving.

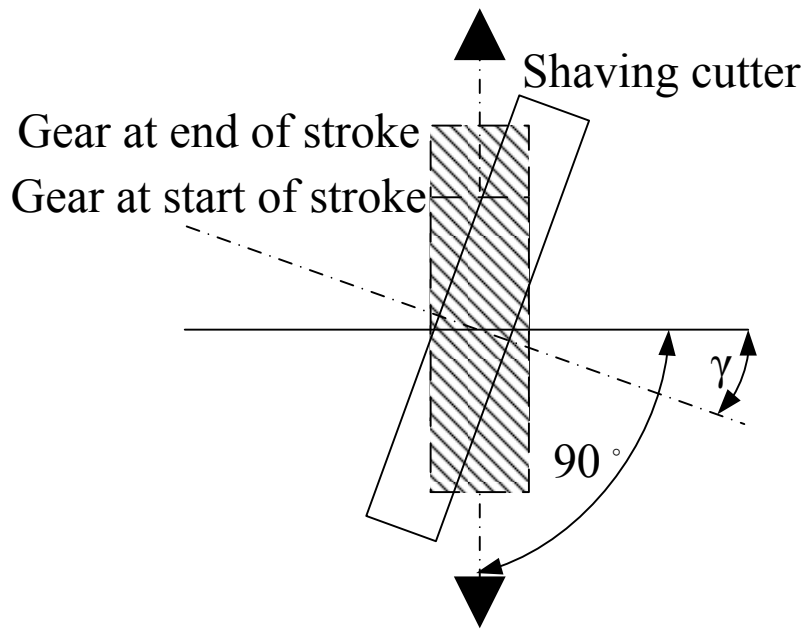


Figure 2.5 Underpass gear shaving.

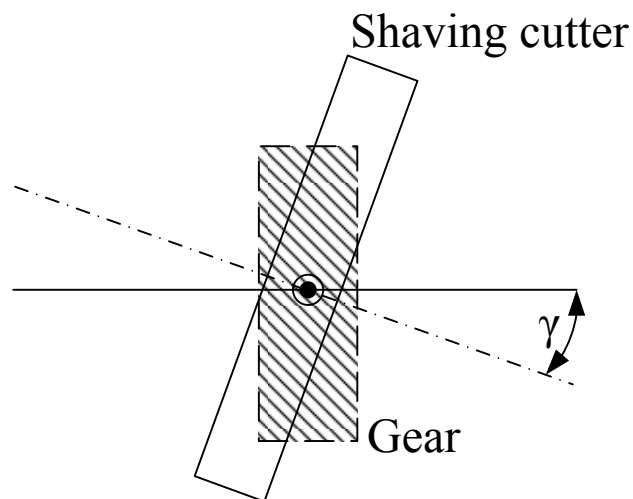


Figure 2.6 Plunge gear shaving.

CHAPTER 3

TRANSVERSE GEAR SHAVING WITH TOOTH CROWNING

Transverse gear shaving has been widely adopted for shaving helical/spur gears with large face width because the whole gear can be finished by the axial infeed of shaving cutter. If plunge shaving is to be adopted under this condition, without axial infeed, the face width of shaving cutter must be large enough to shave the whole gear tooth surface, which inevitably causes much higher cutter cost. To induce lead crowning of the shaved gear by transverse shaving on a traditional shaving machine, the crowning mechanism is needed as shown in Fig. 3.1, in which the work table will rock in the shaving process. The pivot can be fed horizontally only, and the pin will move along the guideway. Once the angle θ between the guideway and the horizontal is specified ($\neq 0$) in the shaving process, the rocking motion of the work table can be achieved. When $\theta = 0^\circ$, the work table will move horizontally without rocking and will therefore not produce any crowning effect. This can also be achieved by a modern CNC shaving machine by simulating the rocking motion, however, with a much higher cost. On the other hand, to induce gear tooth crowning in profile direction, the profile of shaving cutter itself should be modified at the first place. This chapter proposes the mathematical model of the traditional shaving machine. Then, both gear tooth lead and profile crownings are investigated by analyses of parameters. Finally, design optimization for robustness of gear transmission error has also been conducted.

3.1 Transverse shaving with lead crowning

3.1.1 Construction of coordinate systems and the shaved gear tooth profile

The crowning mechanism can be further parameterized as shown in Fig. 3.2, where d_v and d_h are the vertical and horizontal distances between the pin and pivot at the initial position. While the pivot (work table) moves z_i horizontally in shaving from position I to

position II, the pin will move a distance d_p along the guideway. The rotating angle of the work table ψ_t can be derived as shown in Eq. 3.1 (Lin, [11]).

$$\psi_t = \sin^{-1}\left(\frac{d_v}{\sqrt{d_h^2 + d_v^2}}\right) + \sin^{-1}\left(\frac{d_h \sin \theta - d_v \cos \theta + z_t \sin \theta}{\sqrt{d_h^2 + d_v^2}}\right) - \theta \quad (3.1)$$

The coordinate system of the shaving process can be simplified and illustrated as shown in Fig. 3.3, where the cutter assembly errors including horizontal, vertical, and center distance errors, are considered. The coordinate systems S_s and S'_2 are connected to the shaving cutter and the work gear, respectively, while S_d is the fixed coordinate system; S'_h and S'_v are auxiliary coordinate systems for importing assembly errors into the horizontal and vertical directions; the angle Δh denotes the horizontal assembly error, the angle Δv denotes the vertical assembly error, and ΔE_0 indicates the error in the center distance. Other parameters in Fig. 3.3 are also described as follows: z_t denotes the traveling distance of the shaving cutter along the axial direction of the work gear; C denotes the distance between the pivot and center of the work gear; γ denotes the angle between the two crossed axes; E_0 represents the center distance; ϕ_s and ϕ_2 represent the angles of rotation of the cutter and the gear, respectively, which are related to each other in the shaving operation.

If the shaving cutter is assumed to be a helical involute gear, the surface profile and its unit normal can be represented by Eqs. 3.2 and 3.3 derived by Litvin [3], where u_s and v_s are surface parameters.

$$\mathbf{r}_s(u_s, v_s) = [x_s \quad y_s \quad z_s]^T \quad (3.2)$$

$$\mathbf{n}_s = [n_{sx} \quad n_{sy} \quad n_{sz}]^T \quad (3.3)$$

Tooth profile \mathbf{r}_s and surface unit normal \mathbf{n}_s of the shaving cutter represented in the coordinate system S_s can be transformed into the coordinate system of work gear S'_2 constructed in Fig.3.3 by Eq. 4:

$$\mathbf{r}'_2(u_s, v_s, \phi_s, z_t) = M_{2's}(\phi_s, z_t) \cdot \mathbf{r}_s(u_s, v_s) = [x'_2 \quad y'_2 \quad z'_2 \quad 1]^T \quad (3.4)$$

, in which

$$M_{2's} = M_{2'd} M_{ds}$$

$$M_{ds} = M_{dv'} M_{v'h'} M_{h'e'} M_{e'f'} M_{f'i'} M_{i's}$$

$$M_{2'd} = M_{2'a'} M_{a'b'} M_{b'c'} M_{c'd}$$

There are two major kinematical parameters ϕ_s and z_t in transverse shaving gear with lead crowning so that two meshing equations (Eqs. 3.5 and 3.6) are required to calculate the enveloping surface of the work gear, where \mathbf{n}'_2 is derived from \mathbf{n}_s through the same coordinate transformation mentioned above.

$$f_1(u_s, v_s, \phi_s, z_t) = \mathbf{n}'_2 \cdot \frac{\partial \mathbf{r}'_2}{\partial \phi_s} = 0 \quad (z_t \text{ constant}) \quad (3.5)$$

$$f_2(u_s, v_s, \phi_s, z_t) = \mathbf{n}'_2 \cdot \frac{\partial \mathbf{r}'_2}{\partial z_t} = 0 \quad (\phi_s \text{ constant}) \quad (3.6)$$

The parameters ϕ_s and ϕ_2 denote the angles of rotation of the cutter and the gear, respectively, which are related to each other in the shaving operation by Eq. 3.7 when the gear ratio is assumed fixed value, where T_s and T_2 denote the numbers of shaving cutter and gear, respectively. Eq. 3.7 needs to be modified as shown in Eq. 3.8 if there exists feeding of the shaving cutter along the rotation axis of the work gear, where ϕ_{2s} denotes the additional rotation angle of the work gear in transverse shaving and its representation is shown in Eq. 3.9 (Lin, 2006), in which r_{p2} and β_{p2} denote the radius and the helical angle on the pitch circle, respectively.

$$\frac{\phi_2}{\phi_s} = m_{2s} = \frac{T_s}{T_2} \quad (3.7)$$

$$\phi_2 = \frac{T_s}{T_2} \phi_s \pm \phi_{2s} \quad (3.8)$$

$$\phi_{2s} = \frac{[(C + r_{p2}) \sin \psi_t + z_t \cos \psi_t] \tan \beta_{p2}}{(C + r_{p2}) \cos \psi_t + z_t \sin \psi_t - C} \quad (3.9)$$

Considering Eq. 3.4 to Eq. 3.9 simultaneously, the tooth surface of the shaved gear with lead crowning can be obtained under the ideal conditions ($\Delta h = \Delta v = 0^\circ$ and $\Delta E_0 = 0 \text{ mm}$). Simulation of gear shaving is carried out with properties of the work gear, the shaving cutter and machine settings listed in Tables 3.1 and 3.2. Comparing with standard gear tooth surface ($\theta = 0^\circ$), the deviations are calculated according to Eq.3.10:

$$\Delta \varepsilon = \sqrt{(x_2 - x_2')^2 + (y_2 - y_2')^2} \quad (3.10)$$

, in which (x_2, y_2) and (x_2', y_2') represent the points of the same z cross-section and radius on gear tooth surfaces with and without lead crowning, respectively. As illustrated in Fig. 3.4, the dashed line represents the standard tooth surface, while the solid line represents the gear tooth with lead crowning. The effect of lead crowning is obvious that deviations are large at $z = 10 \text{ mm}$ and $z = -10 \text{ mm}$, and no crowning is produced at $z = 0 \text{ mm}$.

3.1.2 Effects of machine setting parameters on the tooth lead crowning

From the developed mathematical model, in this section, four important machine setting parameters are investigated including the angle between the guideway and the horizontal θ , the vertical and horizontal distances between the pivot and the pin d_v and d_h , and the distance between the pivot and the center of the work gear C . The effects of these parameters are illustrated through the following examples.

Example 3.1

The fundamental properties of the shaving cutter and the work gear are listed in Table 3.1 and parameters d_v and d_h are changed to investigate the variations of lead crowning of the left tooth surface on the operating pitch circle within the tooth face width (-10mm~10mm) as shown in Figs. 3.5 and 3.6.

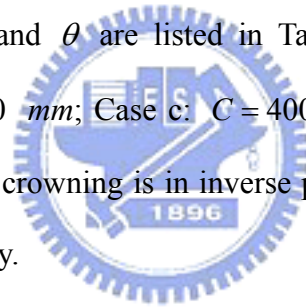
Case1~Case6: $d_v = 188\text{ mm}$, $C = 385\text{ mm}$, $\theta = 2^\circ 50'$, d_h varies from 350 mm to 600 mm in steps of 50 mm .

Case7~Case12: $d_h = 545\text{ mm}$, $C = 385\text{ mm}$, $\theta = 2^\circ 50'$, d_v varies from 50 mm to 300 mm in steps of 50 mm .

It is found that the effects of parameter d_v on crowning are extremely small compared to that induced by d_h , and the variation of the parameter d_h is in inverse proportion to the amount of lead crowning. It is thought to be more effective to control this parameter in the design or assembly of the crowning mechanism.

Example 3.2

The properties of the shaving cutter and the work gear are listed in Table 3.1, and the machine parameters d_v , d_h and θ are listed in Table 3.2. With variations of C (Case a: $C = 200\text{ mm}$; Case b: $C = 300\text{ mm}$; Case c: $C = 400\text{ mm}$), as shown in Fig. 3.7, the result shows that the amount of lead crowning is in inverse proportion to the value of the variation of C but with a low sensitivity.



Example 3.3

The properties of the shaving cutter and the work gear are listed in Table 3.1, while the machine parameters d_v , d_h and C are listed in Table 3.2. With variations of θ (Case A: $\theta = 1^\circ 50'$; Case B: $\theta = 2^\circ 50'$; Case C: $\theta = 3^\circ 50'$; Case D: $\theta = 4^\circ 50'$), as shown in Fig. 3.8, it is observed that the parameter θ indeed has great influences on the amount of tooth lead crowning in positive proportion manner.

From Examples 3.1 to 3.3, it can be summarized that:

- (1) The amount of gear tooth lead crowning is moderately sensitive to machine setting parameter d_h in the inverse proportion sense.
- (2) The amount of gear tooth lead crowning is very sensitive and proportional to the machine setting parameter θ .

In gear shaving, parameters θ and d_h can be adjusted to approach the desired amount of lead crowning. Results of this section can be further utilized with the technique of optimization to determine the best setting of the shaving machine for different work gears and shaving cutters.

3.1.3 Simulation of gear shaving with cutter assembly errors

Two more examples are provided in this section to show the influences of cutter assembly errors on the quality of shaved gear. In Example 3.5, cutter assembly errors including horizontal (Δh), vertical (Δv) and center distance (ΔE_0) are investigated by comparing them with the perfect work gear (shaved without assembly errors). However, the cutter assembly errors take effects not only on lead crowning, but also on circular tooth thickness. Consequently, the theoretical work gear must be derived beforehand (without lead crowning, but still with cutter assembly errors). This is demonstrated in Example 3.4. The influences of cutter assembly errors on lead crowning can then be studied by subtracting the tooth surface derived in Example 3.4 from that obtained considering lead crowning and assembly errors.

Example 3.4

The properties of the shaving cutter and the work gear are listed in Table 3.1, and the machine setting parameters are: $\theta = 0^\circ$ (no lead crowning of gear tooth), $d_v = 188$ mm, $d_h = 545$ mm and $C = 385$ mm. Cutter assembly errors are considered in the following cases.

- (i) vertical error $\Delta v = \pm 0.02^\circ$
- (ii) horizontal error $\Delta h = \pm 0.02^\circ$
- (iii) error of center distance $\Delta E_0 = \pm 1$ mm

Taking condition (i) as an example, as shown in Figure 3.9, the pressure angle of the right tooth surface is increased while it is decreased on the left tooth surface. Simulations of the other two conditions are completed in the same way, and demonstrated in the next

example.

Example 3.5

The properties of the shaving cutter and the work gear are listed in Table 3.1, and the machine setting parameters are listed in Table 3.2. The same cutter assembly errors as those in Example 3.4 are considered. Variations of lead crowning are shown in Figs. 3.10, 3.11 and 3.12, in which the values of ideal condition are included for comparison. It can be seen that the horizontal and the center distance errors Δh and ΔE_0 have more significant effects on lead crowning than those caused by the vertical error Δv . From the results shown in examples 3.4 and 3.5, it can be concluded that the cutter assembly errors have significant effects on both the circular tooth thickness and tooth lead crowning.

By simulating transverse shaving with the crowning mechanism, the effects of machine setting parameters and cutter assembly errors on the tooth lead crowning of the work gear have been investigated through numerical examples. The crowning effect has been shown sensitive to the angle θ between guideway and horizontal as well as the horizontal distance d_h between pivot and pin. The horizontal and the center distance errors Δh and ΔE_0 are also proved significant to gear tooth crowning.

3.2 Transverse shaving with double crowning

The double crowned gear (gear teeth crowned both in lead and profile directions) is an excellent example of significant improvements in transmission by gear tooth crowning (Litvin, 2001), and it can be manufactured efficiently by gear shaving with CNC shaving machine (Litvin, 2001). However, it is indeed costly for gear manufacturer to replace a traditional shaving machine by a CNC one. The coordinated motions of traditional shaving machine is driven by mechanism instead of controller, and, nevertheless, only lead crowning can be conducted. In this section, gear tooth surface with double crowning manufactured by traditional shaving machine is derived and then examined.

To manufacture a double crowned gear by this machine, the shaving cutter needs to be modified in the tooth profile direction, and it can be generated by the parabolic rack cutter shown in Fig. 3.13. a_c is the parabolic coefficient used to control the profile of the rack cutter. Involute profile of shaving cutter can also be generated by simply setting $a_c = 0$, represented as Eq. 3.11.

$$\mathbf{r}_a = [u_c \quad -a_c u_c^2 \quad 0 \quad 1]^T \quad (3.11)$$

Through the coordinate transformations from rack cutter to shaving cutter, which is shown in Figs. 3.14 and 3.15, the locus can be obtained shown as Eqs. 3.12 and 3.13.

$$\mathbf{r}_c = \mathbf{M}_{ca}(\theta_c) \mathbf{r}_a(u_c) = [x_c(u_c, \theta_c) \quad y_c(u_c, \theta_c) \quad z_c(u_c, \theta_c)]^T \quad (3.12)$$

$$\begin{aligned} [\mathbf{r}_s \quad 1]^T &= \mathbf{M}_{sc}(\psi_s) [x_c(u_c, \theta_c) \quad y_c(u_c, \theta_c) \quad z_c(u_c, \theta_c) \quad 1]^T \\ &= [x_s(u_c, \theta_c, \psi_s) \quad y_s(u_c, \theta_c, \psi_s) \quad z_s(u_c, \theta_c, \psi_s) \quad 1] \end{aligned} \quad (3.13)$$

By deriving the normal vector Eq. 3.14 and the meshing equation Eq. 3.15, the tooth surface of shaving cutter \mathbf{r}_s can be obtained.

$$\mathbf{n}_s = \frac{\partial \mathbf{r}_s}{\partial u_c} \times \frac{\partial \mathbf{r}_s}{\partial \theta_c} \quad (3.14)$$

$$f_1(u_c, \theta_c, \psi_s) = \mathbf{n}_s \cdot \frac{\partial \mathbf{r}_s}{\partial \psi_s} = 0 \quad (3.15)$$

The transverse shaved gear tooth surface can then be derived through the process similar to those in the previous section. The locus equation of shaving cutter:

$$[\mathbf{r}_2(u_c, \theta_c, \psi_s, \varphi_s, z_t) \quad 1]^T = \mathbf{M}_{2s}(\varphi_s, z_t) [\mathbf{r}_s(u_c, \theta_c, \psi_s) \quad 1]^T \quad (3.16)$$

, and the meshing equations:

$$f_2(u_c, \theta_c, \psi_s, \varphi_s, z_t) = \mathbf{n}_2 \cdot \frac{\partial \mathbf{r}_2}{\partial \varphi_s} = 0 \quad (z_t = \text{constant}) \quad (3.17)$$

$$f_3(u_c, \theta_c, \psi_s, \varphi_s, z_t) = \mathbf{n}_2 \cdot \frac{\partial \mathbf{r}_2}{\partial z_t} = 0 \quad (\varphi_s = \text{constant}) \quad (3.18)$$

Note that the normal vector on S_2 is derived by Eq. 3.19, in which the 3×3 matrix \mathbf{L}_{2s} is the sub-matrix of 4×4 matrix \mathbf{M}_{2s} .

$$\mathbf{n}_2 = \mathbf{L}_{2s}(\varphi_s, z_t) \mathbf{n}_s(u_c, \theta_c, \psi_s) \quad (3.19)$$

Considering Eq. 3.11 to Eq. 3.19 simultaneously, the tooth surface of the shaved gear with double crowning can be obtained. Simulation of gear shaving is carried out with data of the work gear, the shaving cutter and machine settings listed in Tables 3.1 and 3.2 with $a_c = 1.4 \times 10^{-3}$. As shown in Fig. 3.16, the effect of crowning especially in the profile direction can be clearly observed at $z = 0 \text{ mm}$.

3.3 Design optimization for robustness of gear transmission error

3.3.1 Transmission error analysis of the shaved gear

Transmission error of the shaved gears can be calculated by simulation of gear meshing. Considering a gear pair composed of a double crowned gear (gear 2) and an involute gear (gear 4, directly generated by rack cutter with $a_c = 0$), the coordinate systems can be illustrated as Fig. 3.17. Coordinate system $S_2(X_2, Y_2, Z_2)$ is fixed on gear 2, and $S_4(X_4, Y_4, Z_4)$ is fixed on gear 4. The two gears rotate about axes Z_2 and Z_4 respectively. $S_h(X_h, Y_h, Z_h)$ and $S_v(X_v, Y_v, Z_v)$ are auxiliary coordinate systems for simulating assembly errors between gear 2 and gear 4 including horizontal error $\Delta\gamma_h$, vertical error $\Delta\gamma_v$ and the center distance error ΔE . ϕ'_2 and ϕ'_4 denote the real rotation angles of the two gears in operating. Transforming the vectors and unit normal vectors of the gear tooth surfaces to coordinate system $S_q(X_q, Y_q, Z_q)$, the two meshing surfaces Σ_2 and Σ_4 must satisfy

$$\mathbf{r}_q^{(2)} - \mathbf{r}_q^{(4)} = 0 \quad (3.20)$$

$$\mathbf{n}_q^{(2)} \times \mathbf{n}_q^{(4)} = 0 \quad (3.21)$$

, in which $\mathbf{r}_q^{(2)}$ and $\mathbf{r}_q^{(4)}$ are vectors while $\mathbf{n}_q^{(2)}$ and $\mathbf{n}_q^{(4)}$ are unit normal vectors of respective tooth surfaces illustrated in Figs. 3.18.

In the 3-D space, Eqs. 3.20 and 3.21 include six scalar equations. By the given equation

that for unit normal vectors $|\mathbf{n}_q^{(2)}| = |\mathbf{n}_q^{(4)}| = 1$, only five independent scalar equations need to be solved:

$$x_q^{(2)} - x_q^{(4)} = 0$$

$$y_q^{(2)} - y_q^{(4)} = 0$$

$$z_q^{(2)} - z_q^{(4)} = 0$$

$$n_{qy}^{(2)} n_{qz}^{(4)} - n_{qz}^{(2)} n_{qy}^{(4)} = 0$$

$$n_{qz}^{(2)} n_{qx}^{(4)} - n_{qx}^{(2)} n_{qz}^{(4)} = 0$$

Considering meshing equations Eqs. 3.15 (gears 2 and 4), 3.17 and 3.18 simultaneously, 9 independent equations are used to solve 10 variables including $u_c, \theta_c, \psi_s, \phi_s, z_t, \phi_2', u_4, \theta_4, \psi_s'$ and ϕ_4' . $u_c, \theta_c, \psi_s, \phi_s$ and z_t are variables for deriving shaved gear (gear 2); u_4, θ_4 and ψ_s' are variables for deriving involute gear (gear 4). By inputting values of ϕ_2' directly, the relation between real rotating angles $\phi_4'(\phi_2')$ can be calculated. Transmission error is defined as the differences between the real and the theoretical rotation angles, which can be represented as:

$$\Delta\phi_4'(\phi_2') = \phi_4'(\phi_2') - T_2\phi_2'/T_4 \quad (3.22)$$

, where T_2 and T_4 are tooth numbers of gears 2 and 4 respectively, and $T_2\phi_2'/T_4$ is the theoretical rotation angle of gear 4. An example is provided for illustration.

Example 3.6

Data of gears 2 and 4 are listed in Table 3.3, and the shaving machine parameters are listed in Table 3.2. Firstly, gear 2 is shaved with only lead crowning ($a_c = 0$). With different values of gear assembly error, the transmission errors are calculated and plotted as Fig. 3.19.

The transition of transmission errors are very sharp so that the noise and vibration of this gear pair will be large during meshing. By shaving gear 2 with double crowning ($a_c = 1.4 \times 10^{-3}$), the transmission errors are significantly improved as shown in Fig. 3.20.

3.3.2 Design optimization for robustness

In the constructed model for calculation of transmission error, many parameters can be tuned to observe their influences. They can be further divided into four categories: modification of shaving cutter, assembly errors of shaving cutter, assembly errors of gears and machine setting parameters, which are illustrated in the fishbone diagram illustrated as Fig. 3.21. Taguchi Method is adopted as the tool to investigate the system robustness of the gear shaving process.

Fundamental data of the gear pair for simulation are listed in Table 3.3. To plan the simulations, factors from different categories and their levels must be considered. As listed in Table 3.4, eleven factors and three levels for each factor were specified. The simulations of transmission error analysis are planned according to the L36 ($2^{11} \times 3^{12}$) orthogonal array. The arrangements and results (S/N ratios) of the simulations are listed in Table 3.5. In the analyses, the value of transmission error was considered as the product quality, which was expected to be “smaller the better”, and the formula for calculating the S/N ratio (Taguchi, [24]) is

$$S/N = -10 \text{Log} \frac{\sum_{i=1}^n y_i^2}{n} \quad (3.23)$$

, in which n and y_i denote the number and result of simulation performed for each set of parameters in Table 3.5. Since the variation of the calculated transmission error from the same input is zero, the step of averaging can be skipped. Taking simulation 1 as an example, the S/N can be calculated as:

$$S/N = -10 \text{Log} \frac{(1.2279)^2}{1} = -1.7838$$

by using Eq. 3.23.

The factors' responses can also be obtained from Table 3.5. For instance, the mean S/N of parameter A of level 1 can be calculated by:

$$\begin{aligned}
 A_1 &= \frac{1}{12}(R_1 + R_4 + R_7 + R_{10} + R_{13} + R_{16} + R_{19} + R_{22} + R_{25} + R_{28} + R_{31} + R_{34}) \\
 &= \frac{1}{12}[(-1.7838) + (-11.5664) + (-5.0211) + 0 + 7.1367 + (-4.3953) + (-2.4226) \\
 &\quad + (-10.1193) + 0 + 7.5297 + (-5.1572) + (-16.4801)] \\
 &= -3.5233
 \end{aligned}$$

, in which R_i denotes the i -th simulation result. Similarly, those of level 2 and 3 can be obtained as -8.9130 (level 2) and -7.0376 (level 3). The effect of A is then calculated by subtracting the min from max.

$$Effect = (-3.5233) - (-8.9130) = 5.3897$$

After reorganizing, the factor response table and graph are shown in Table 3.6 and Fig. 3.22 respectively. It is obvious that the combination of factors A1, B1, C2, D2, E1, F3, G3, H3, I2, J2 and K1 can produce the best quality, namely, the shaving process with this set of parameters can manufacture the gear pair of the least transmission error. The ranking of the factor sensitivity (from the highest to the lowest) is K1, A1, J2, I2, H3, D2, B1, F3, E1, C2, and G3. The improvements on transmission error can be validated by the results shown in Fig. 3.23. The dashed line represents the original set of parameter marked with shadow in Table 3.4 while the solid line represents the improved one. With the improved parameters, the peak-to-peak values of transmission error become significantly decreased and the curves also become smoother, which means that vibrations and noises can be reduced when the optimized gear pair is operating.

3.4 Concluding remarks

In this chapter, the transverse shaving of the traditional gear shaving machine has been simulated, and the gear tooth surface of shaved gear has also been constructed. The effects of machine setting parameters and cutter assembly errors on the work gear surface and the tooth

lead crowning have been investigated through numerical examples. For the crowning mechanism, the crowning effect is shown to be sensitive to the angle θ between guideway and horizontal as well as the horizontal distance d_h between pivot and pin. The horizontal and the center distance errors Δh and ΔE_0 are also proved significant to gear tooth crowning. The results can be used as instructions for design, assembly and calibration of gear shaving machine and shaving cutter.

To have a double crowned gear shaved by traditional gear shaving machine for better performance in transmission error, four categories of parameter need to be considered: modification of shaving cutter, assembly errors of shaving cutter, assembly errors of gears and machine setting parameters. It has been proved that the gear pair with optimized parameters indeed possesses better quality in transmission. Besides, among the eleven selected parameters, the coefficient a_c concerning the modification of shaving cutter and the angle θ between the guide way and horizontal on the shaving machine contribute the most to product quality (transmission error).



Table 3.1 Parameters of work gear and shaving cutter.

Parameter description	Parameter value
Work gear	
Number of teeth (T_2)	36
Normal module on pitch circle (m_{pn2})	2.65
Normal circular tooth thickness on pitch circle (s_{pn2})	4.858mm
Normal pressure angle on pitch circle (α_{pn2})	20°
Helical angle on pitch circle (β_{p2})	10° L.H.
Outer diameter	105.9mm
Face width	28.4mm
Shaving cutter	
Number of teeth (T_2)	73
Helical angle on pitch circle (β_{ps})	22° R.H.
Face width	25.4mm
Normal circular tooth thickness on pitch circle (s_{pns})	3.348mm

Table 3.2 Machine setting parameters in gear shaving.

Machine setting parameters	
Angle between guideway and horizontal (θ)	2°50'
Vertical distance between pivot and pin (d_v)	188mm
Horizontal distance between pivot and pin (d_h)	545mm
Distance between pivot and center of work (C)	385mm

Table 3.3 Basic data of the gear pair (Example 3.6).

Basic data	Gear 2	Gear 4
Module (m_n)	2.65	2.65
Tooth number (T_i)	36	36
Helix angle (β_i)	10° L.H.	10° R.H.
Pressure angle (α_n)	20°	20°

Table 3.4 Factors and their levels in transmission error analysis

Factor		Unit	Level		
			1	2	3
A	θ	degree	1°50'	2°50'	3°50'
B	d_v	mm	500	545	590
C	d_h	mm	350	385	420
D	C	mm	150	188	226
E	$\Delta\gamma_v$	degree	-0.02	0	0.02
F	$\Delta\gamma_h$	degree	-0.02	0	0.02
G	ΔE	mm	-1	0	1
H	Δv	degree	-0.02	0	0.02
I	Δh	degree	-0.02	0	0.02
J	ΔE_o	mm	-1	0	1
K	a_c	-	0.0001	0.0005	0.001

Table 3.5 The S/N ratios of the transmission error analyses.

No.	1				2			3			4	S/N
	θ	d_v	d_h	C	$\Delta\gamma_v$	$\Delta\gamma_h$	ΔE	Δv	Δh	ΔE_0	a_c	
	A	B	C	D	E	F	G	H	I	J	K	
1	1	1	1	1	1	1	1	1	1	1	1	-1.7838
2	2	2	2	2	2	2	2	2	2	2	2	-1.7838
3	3	3	3	3	3	3	3	3	3	3	3	-10.6055
4	1	1	1	1	2	2	2	2	3	3	3	-11.5664
5	2	2	2	2	3	3	3	3	1	1	1	-2.3489
6	3	3	3	3	1	1	1	1	2	2	2	-5.0211
7	1	1	2	3	1	2	3	3	1	2	2	-5.0211
8	2	2	3	1	2	3	1	1	2	3	3	-20.0087
9	3	3	1	2	3	1	2	2	3	1	1	-4.0242
10	1	1	3	2	1	3	2	3	2	1	3	0
11	2	2	1	3	2	1	3	1	3	2	1	0.6389
12	3	3	2	1	3	2	1	2	1	3	2	-12.3083
13	1	2	3	1	3	2	1	3	3	2	1	7.1367
14	2	3	1	2	1	3	2	1	1	3	2	-13.3246
15	3	1	2	3	2	1	3	2	2	1	3	-24.0182
16	1	2	3	2	1	1	3	2	3	3	2	-4.3953
17	2	3	1	3	2	2	1	3	1	1	3	-18.1906
18	3	1	2	1	3	3	2	1	2	2	1	8.3860
19	1	2	1	3	3	3	1	2	2	1	2	-2.4226
20	2	3	2	1	1	1	2	3	3	2	3	-15.3050
21	3	1	3	2	2	2	1	1	1	3	1	7.5373
22	1	2	2	3	3	1	2	1	1	3	3	-10.1193
23	2	3	3	1	1	2	3	2	2	1	1	-2.5605
24	3	1	1	2	2	3	1	3	3	2	2	-4.8046
25	1	3	2	1	2	3	3	1	3	1	2	0
26	2	1	3	2	3	1	1	2	1	2	3	-11.5493
27	3	2	1	3	1	2	2	3	2	3	1	5.8249
28	1	3	2	2	2	1	1	3	2	3	1	7.5297
29	2	1	3	3	3	2	2	1	3	1	2	-16.1962
30	3	2	1	1	1	3	3	2	1	2	3	-11.2518
31	1	3	3	3	2	3	2	2	1	2	1	-5.1572
32	2	1	1	1	3	1	3	3	2	3	2	-5.0117
33	3	2	2	2	1	2	1	1	3	1	3	-17.0885
34	1	3	1	2	3	2	3	1	2	2	3	-16.4801
35	2	1	2	3	1	3	1	2	3	3	1	-1.3159
36	3	2	3	1	2	1	2	3	1	1	2	-17.0768

Table 3.6 Factor response table for the transmission error analyses.

	A	B	C	D	E	F	G	H	I	J	K
Level 1	-3.5233	-5.4453	-6.8664	-6.7792	-5.9369	-7.5113	-6.6523	-6.9550	-8.3829	-8.8092	1.6553
Level 2	-8.9130	-6.0746	-6.1161	-5.0610	-7.2417	-6.7247	-6.6952	-7.6961	-4.6305	-5.0177	-7.2805
Level 3	-7.0376	-7.9540	-6.4914	-7.6337	-6.2953	-5.2378	-6.1264	-4.8227	-6.4605	-5.6470	-13.8486
Effect	5.3897	2.5086	0.7503	2.5726	1.3048	2.2735	0.5688	2.8734	3.7524	3.7915	15.5039
Ranking	2	7	10	6	9	8	11	5	4	3	1



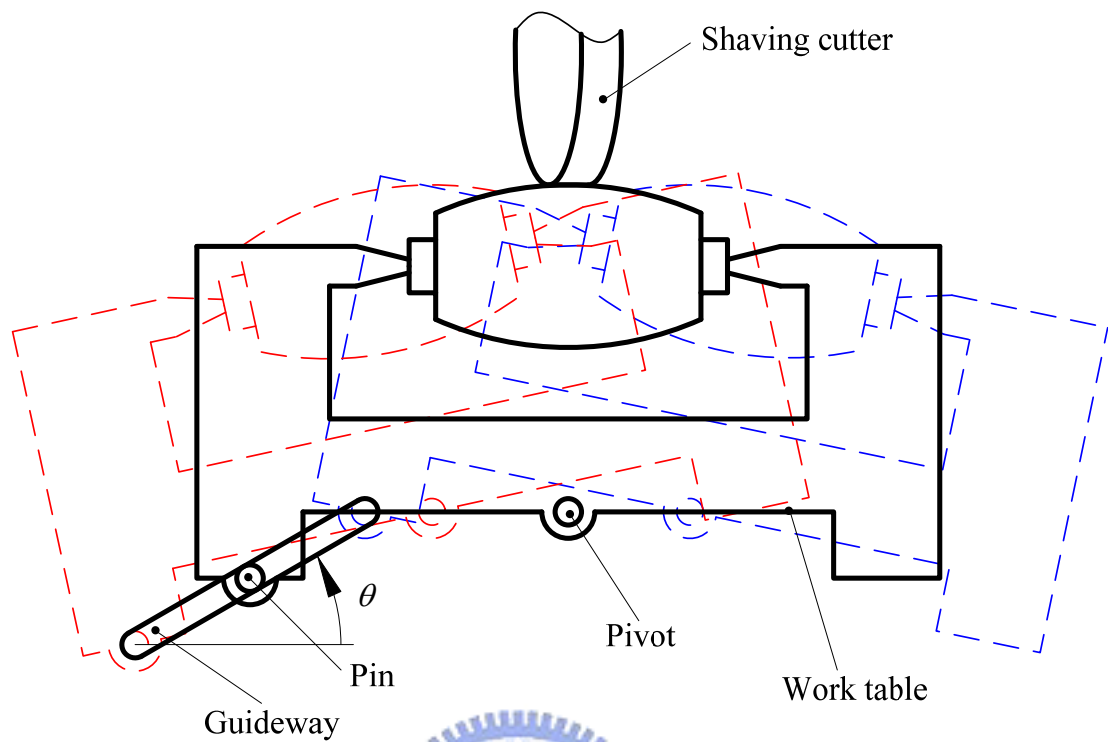


Figure 3.1 Crowning mechanism of the traditional shaving machine.

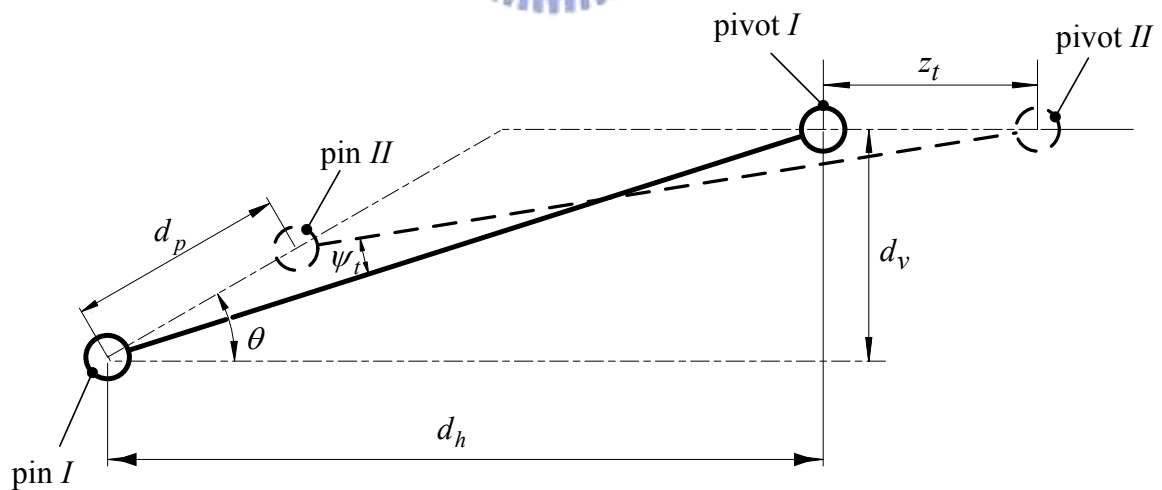


Figure 3.2 Parametric representation of the crowning mechanism.

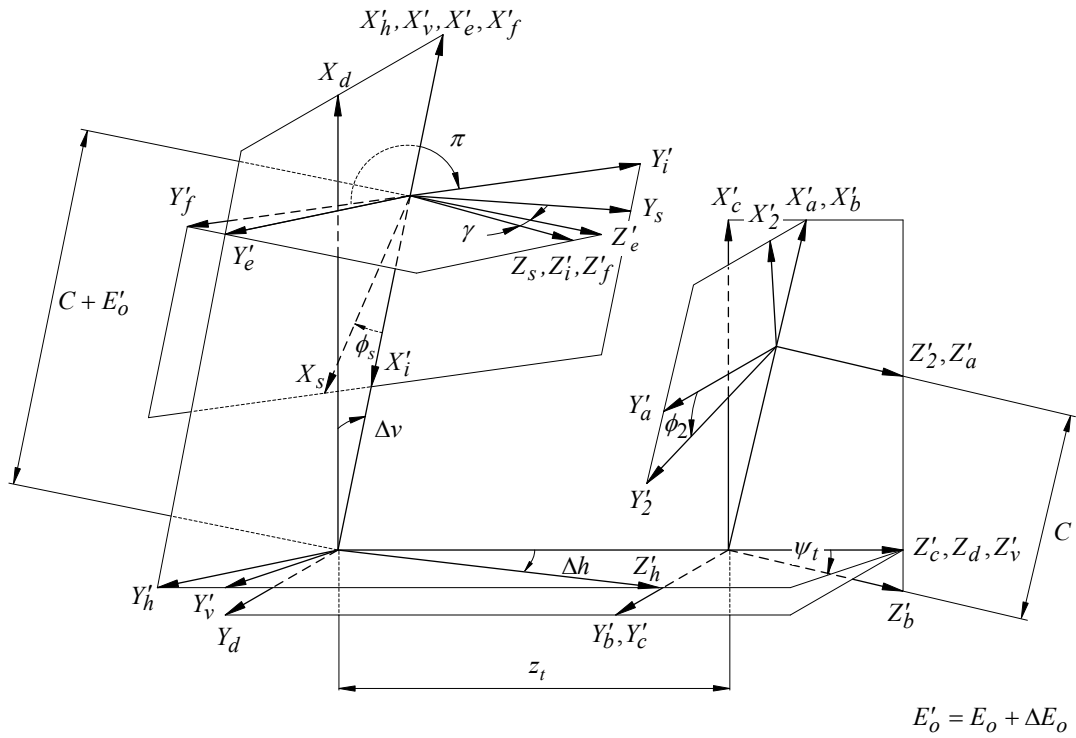


Figure 3.3 Coordinate system of the gear shaving machine with considerations of cutter assembly errors.

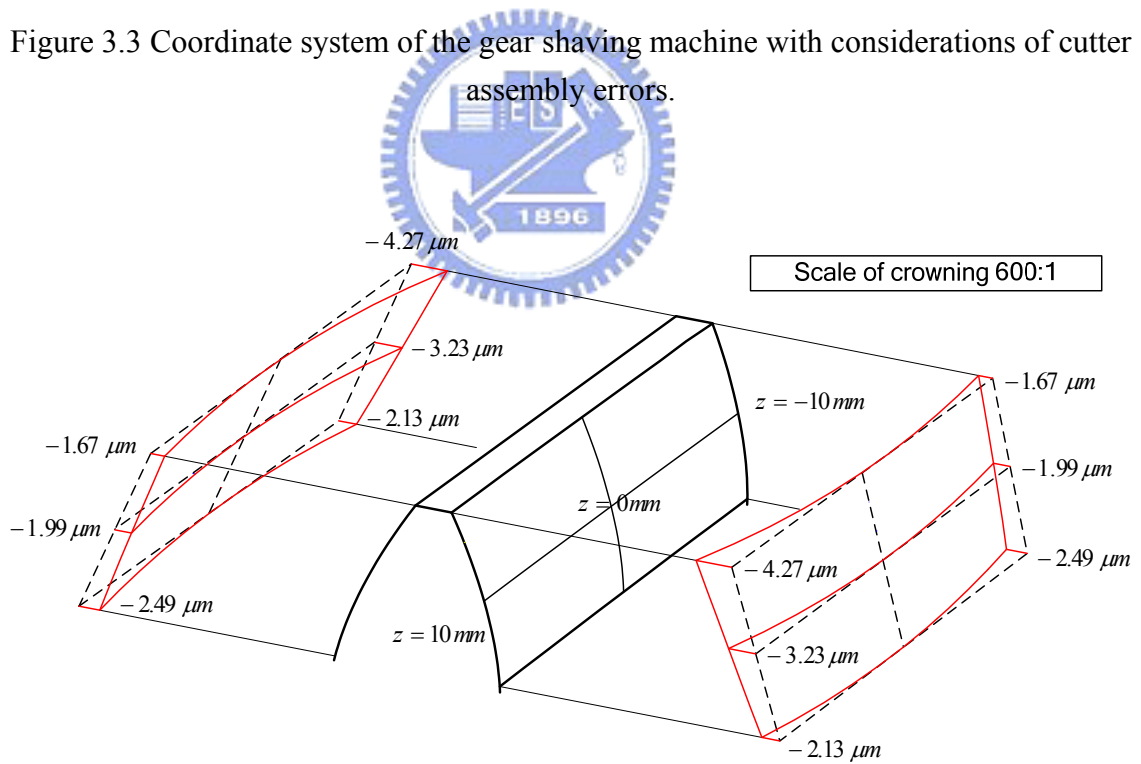


Figure 3.4 Lead crowning of the shaved gear.

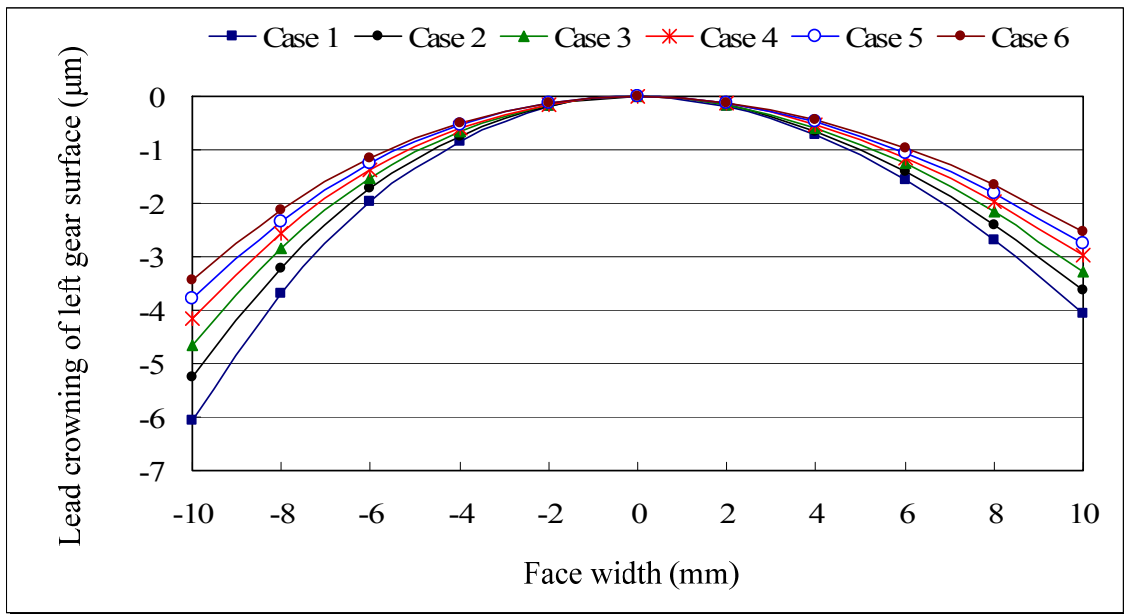


Figure 3.5 Lead crowning under different conditions ($d_v=188mm, C=385mm, \theta=2^\circ 50'$, $d_h=350\sim 600mm, \Delta d_h=50mm$).

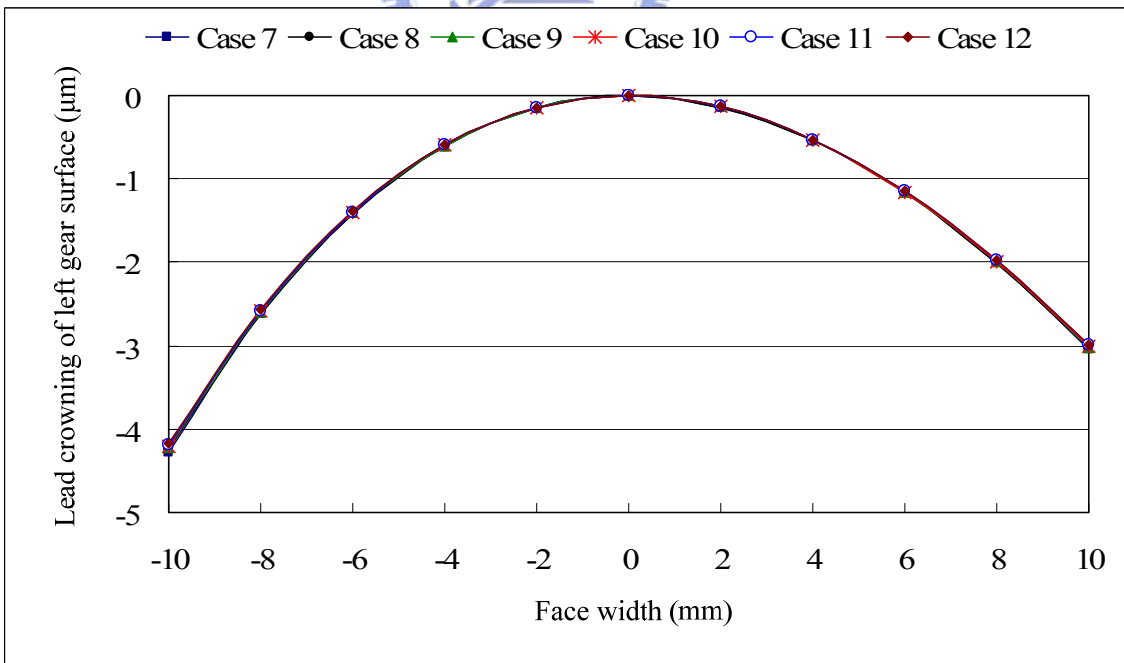


Figure 3.6 Lead crowning under different conditions ($d_h=545mm, C=385mm, \theta=2^\circ 50'$, $d_v=50\sim 300mm, \Delta d_v=50mm$).

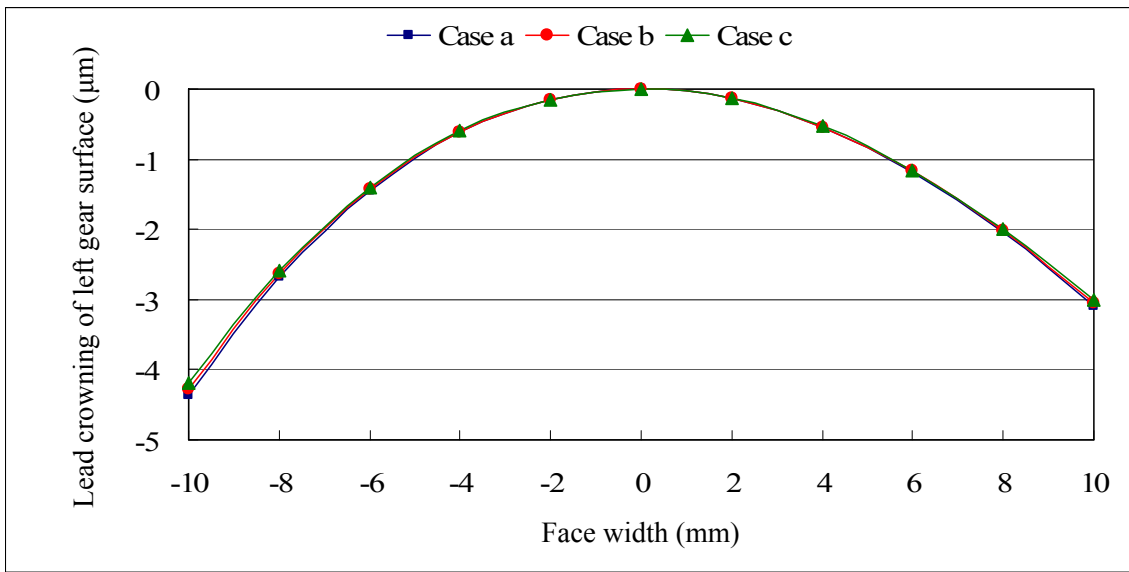


Figure 3.7 Lead crowning under different conditions ($d_v=188mm$, $d_h=545mm$, $\theta=2^\circ50'$, $C=200\sim400mm$, $\Delta C=100mm$).

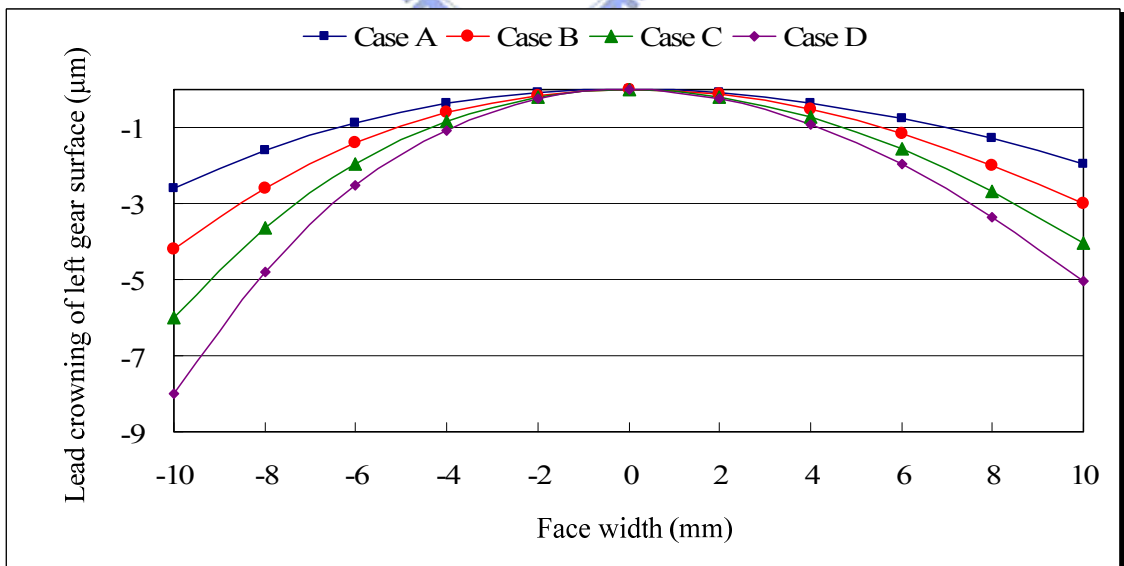


Figure 3.8 Lead crowning under different conditions ($d_v=188mm$, $d_h=545mm$, $C=385mm$, $\theta=1^\circ50'\sim4^\circ50'$, $\Delta\theta=1^\circ$).

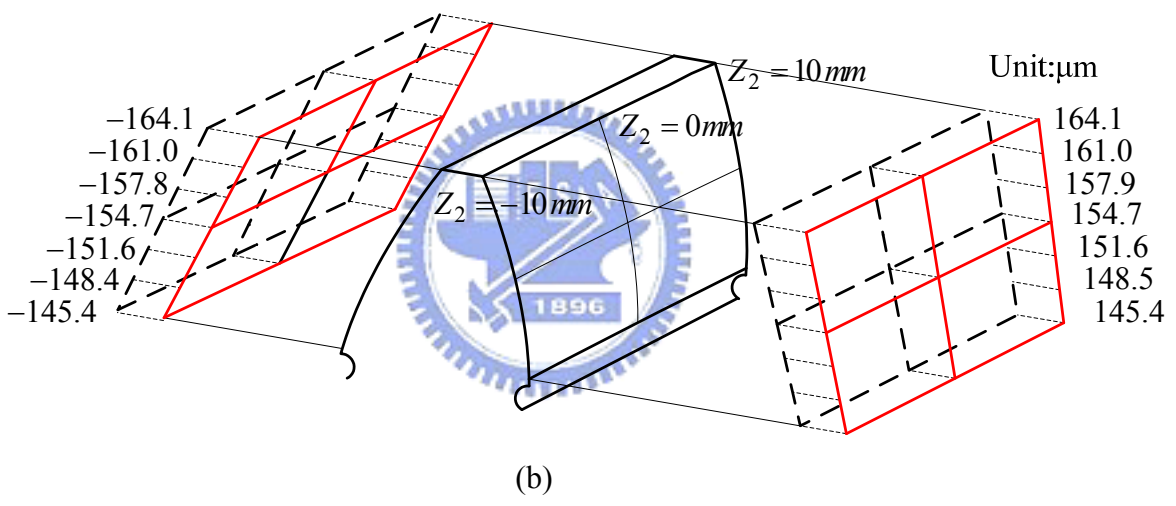
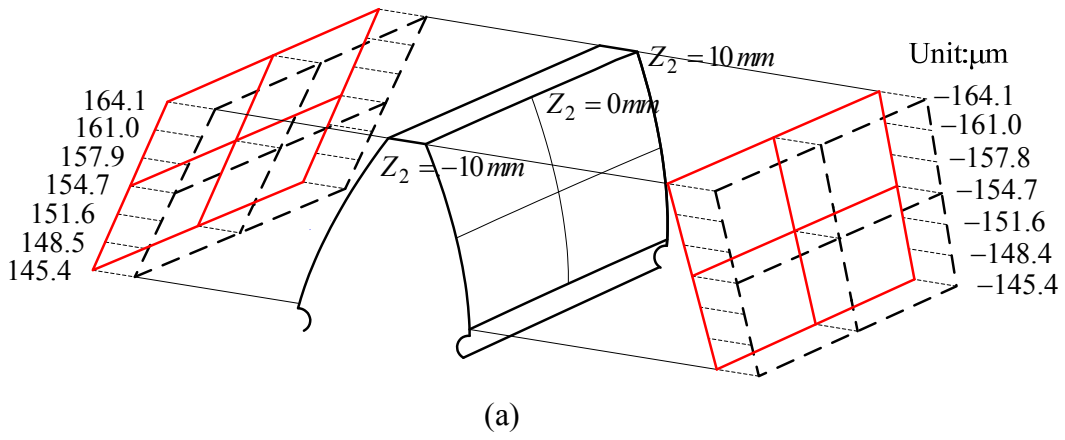


Figure 3.9 Variations of circular tooth thickness from vertical error (a) $\Delta\nu = 0.02^\circ$ (b) $\Delta\nu = -0.02^\circ$.

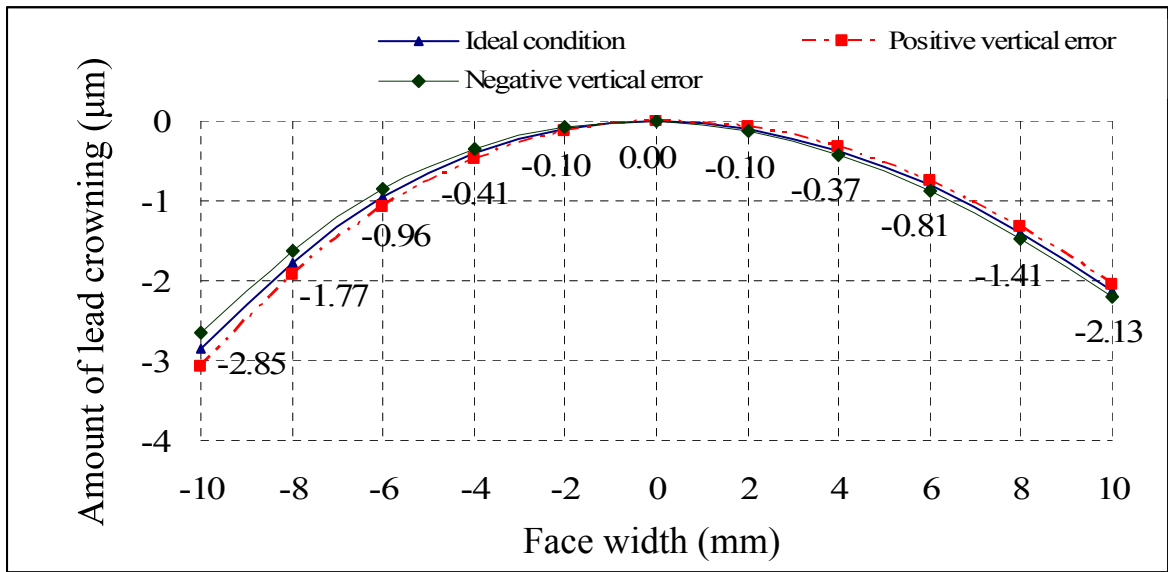


Figure 3.10 Tooth lead crowning affected by vertical cutter assembly error.

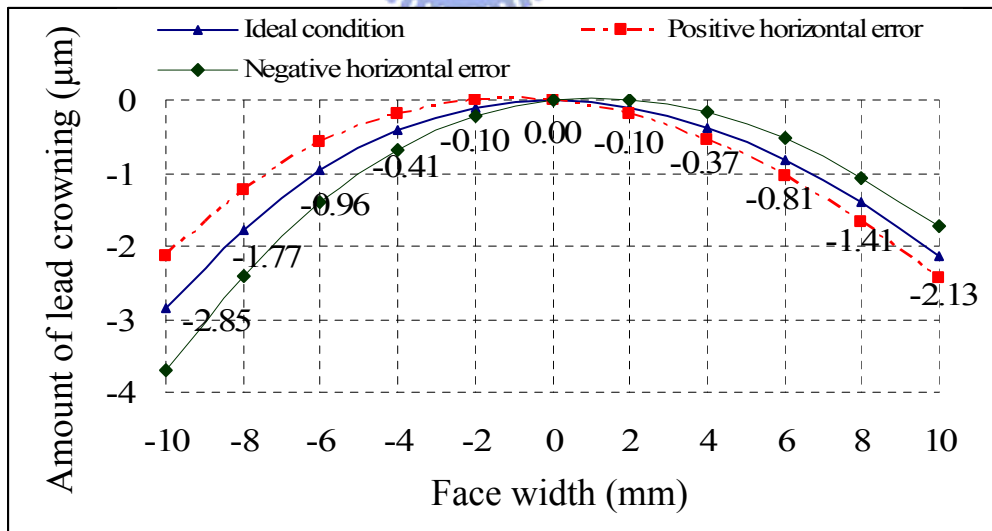


Figure 3.11 Tooth lead crowning affected by horizontal cutter assembly error.

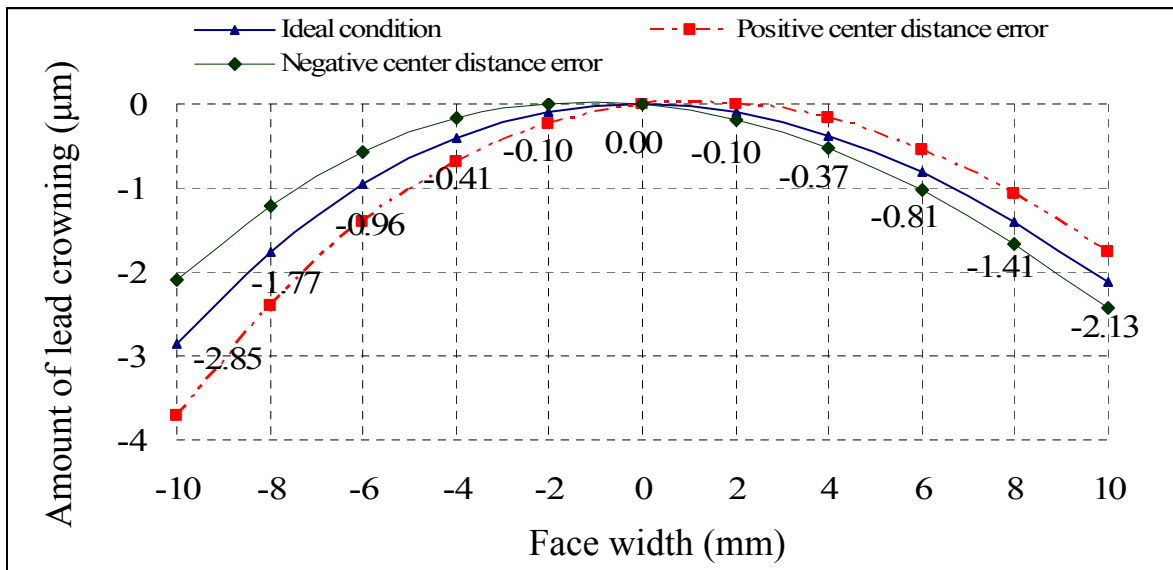


Figure 3.12 Tooth lead crowning affected by cutter assembly error of the center distance.

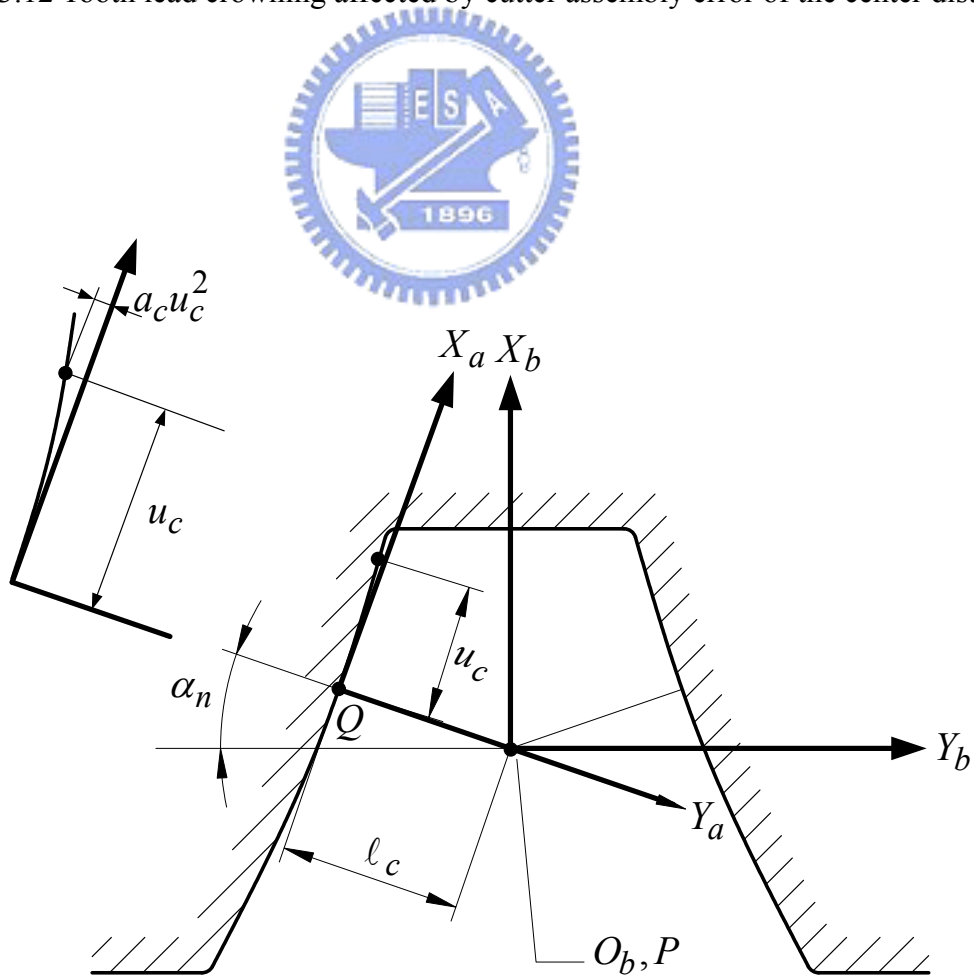


Figure 3.13 Normal section of the parabolic rack cutter.

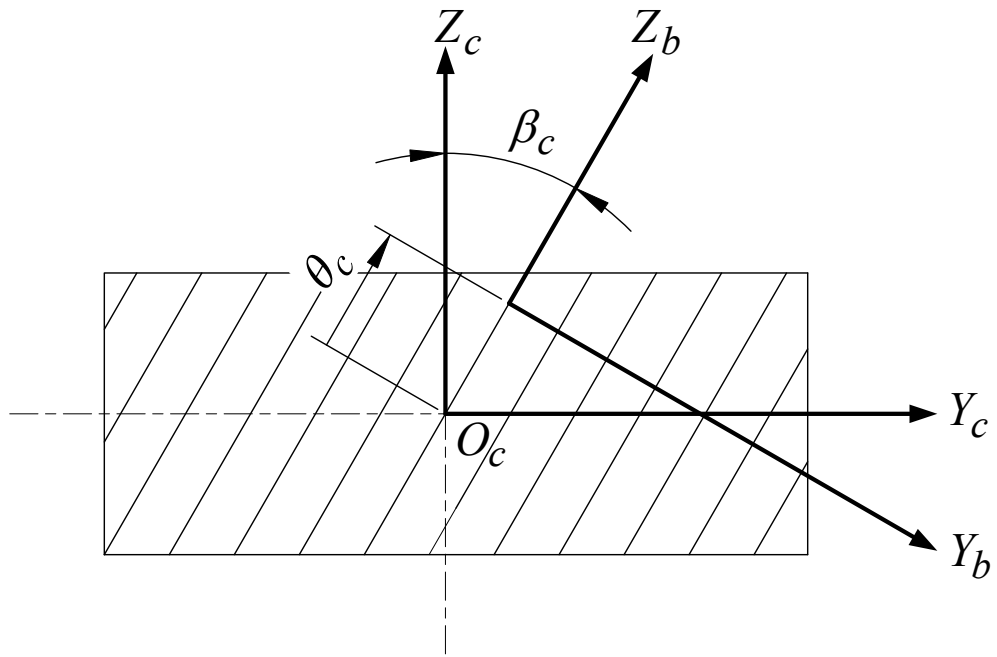


Figure 3.14 Coordinate systems of the rack cutter from normal to axial section.

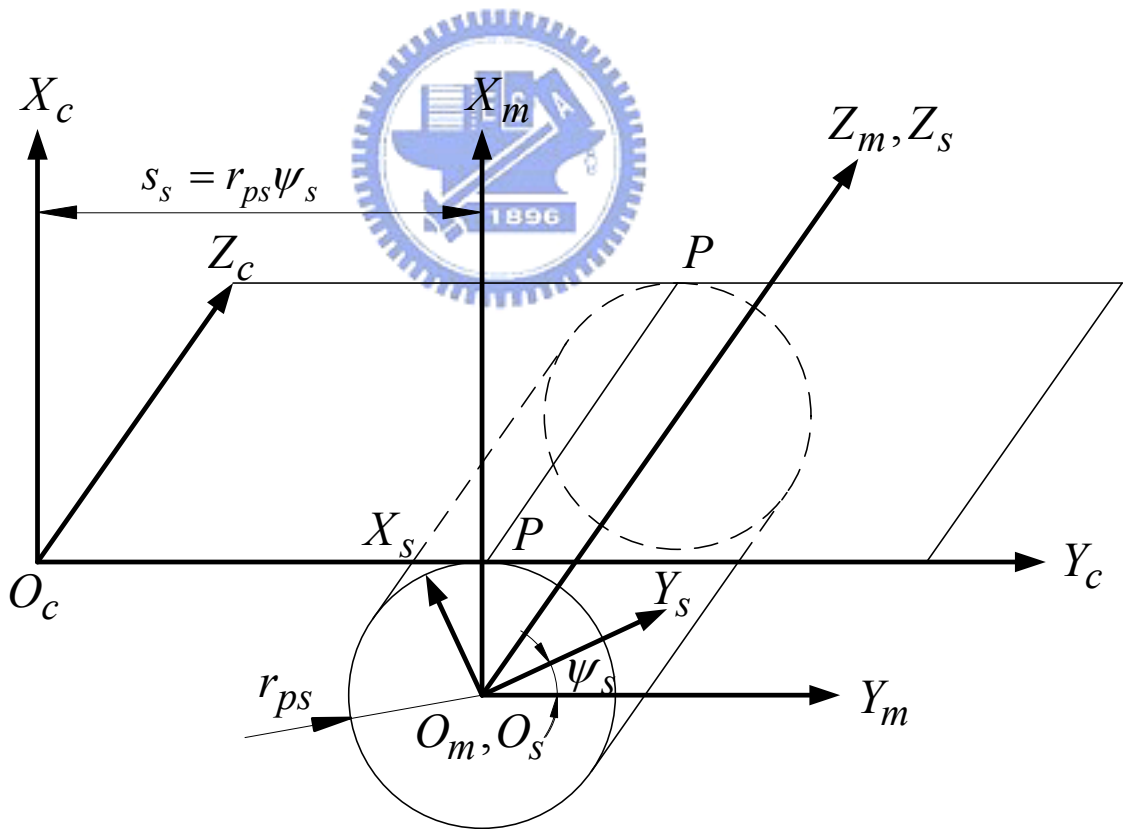


Figure 3.15 Coordinate systems of the generating motion between the rack cutter and the shaving cutter.

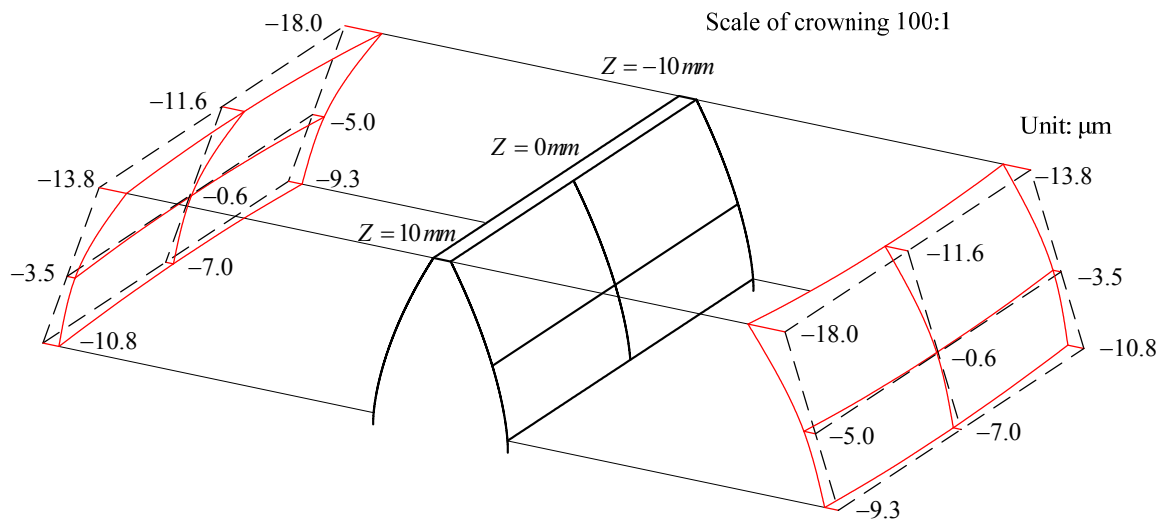


Figure 3.16 Double crowning of the saved gear.

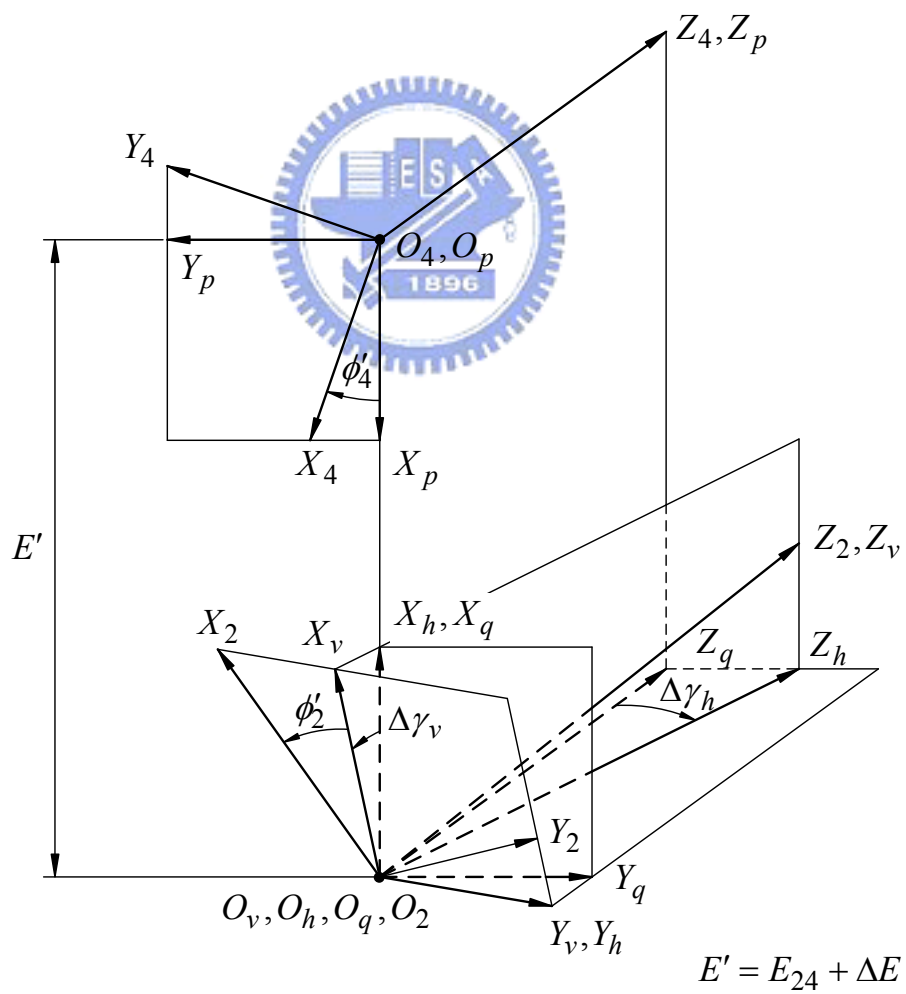


Figure 3.17 Coordinate systems of the meshing gear pair.

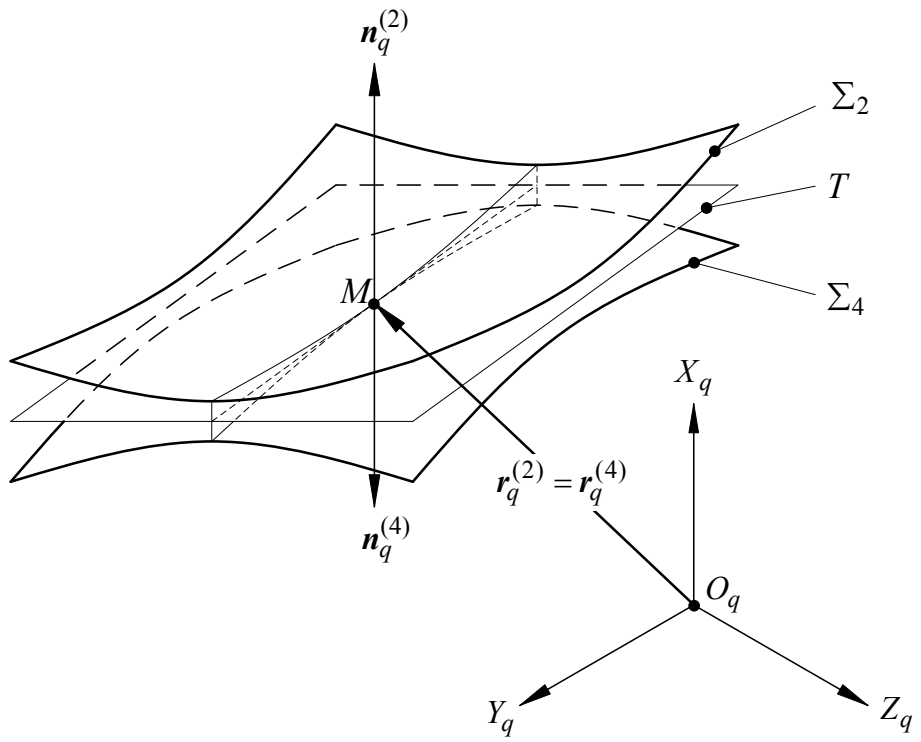


Figure 3.18 Meshing of the two gear tooth surfaces.

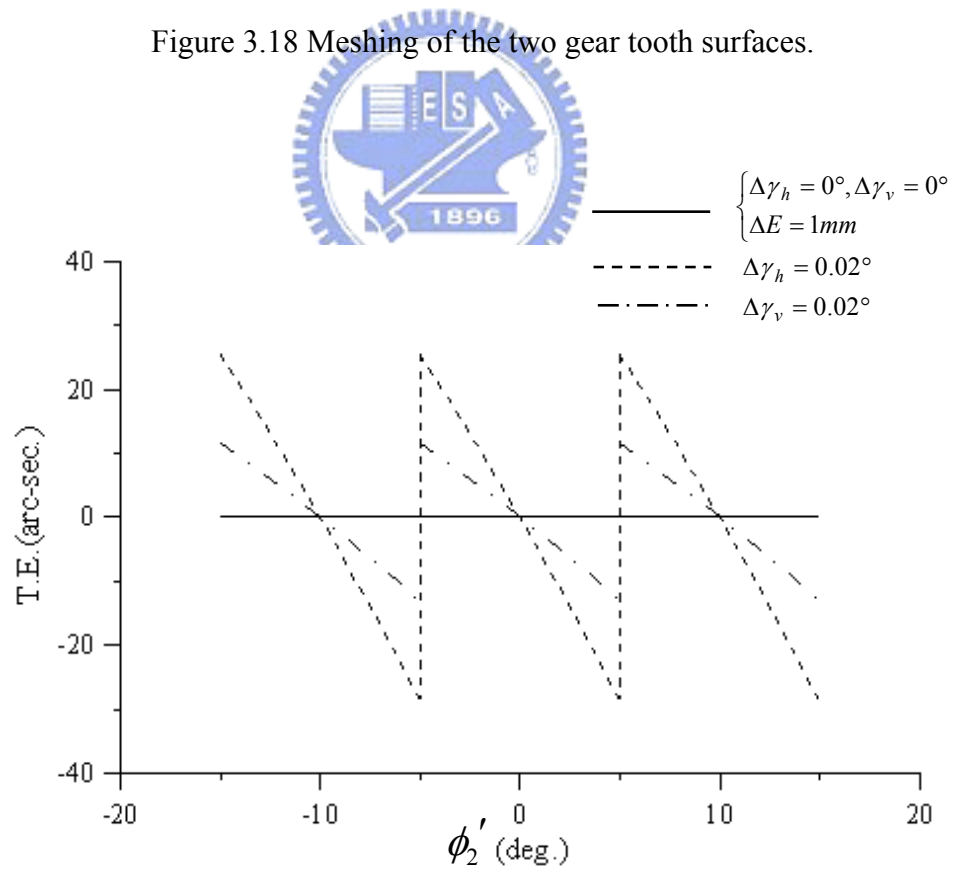


Figure 3.19 Transmission error of the gear pair (gear 2 lead crowned only).

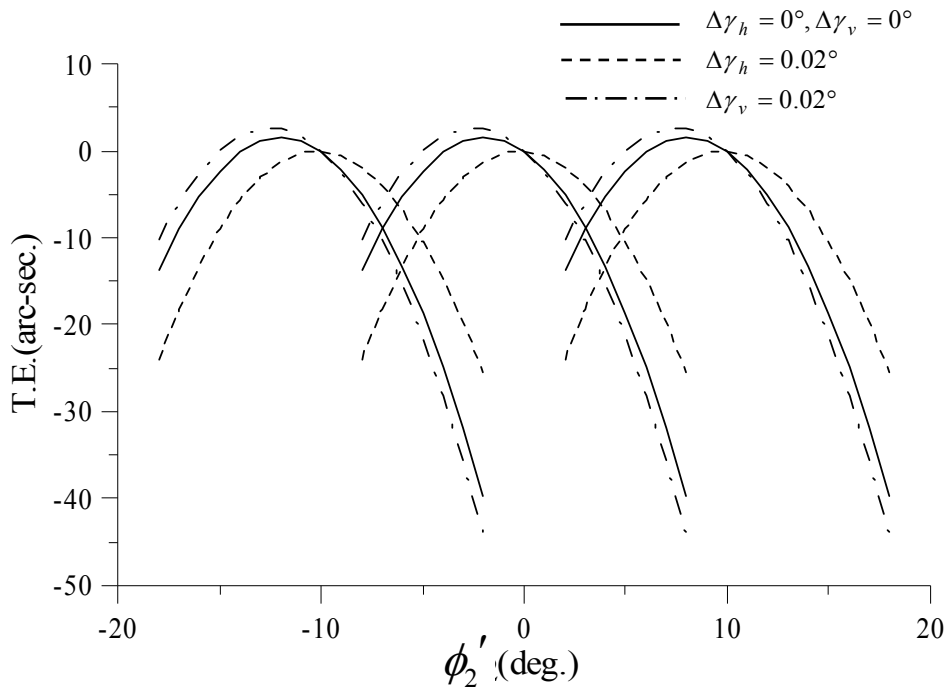


Figure 3.20 Transmission error of the gear pair (gear 2 double crowned).

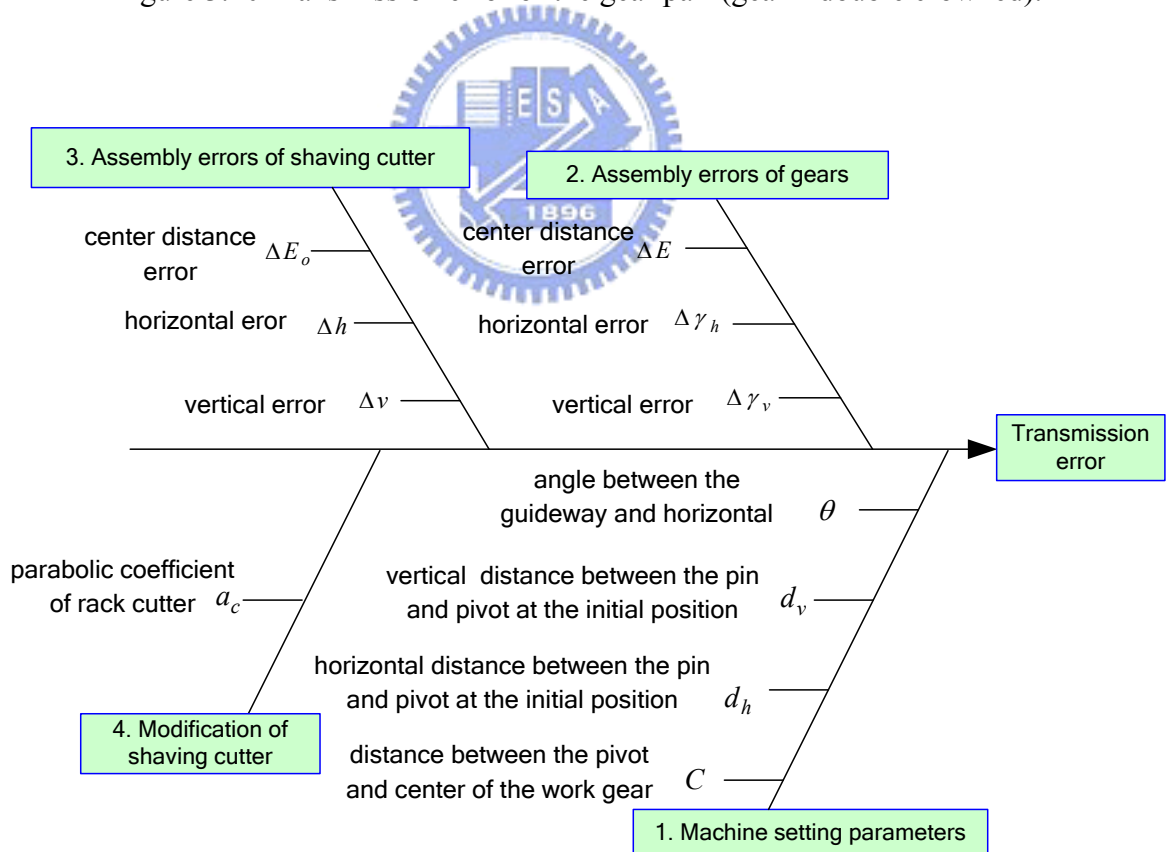


Figure 3.21 Fishbone diagram of the factors.

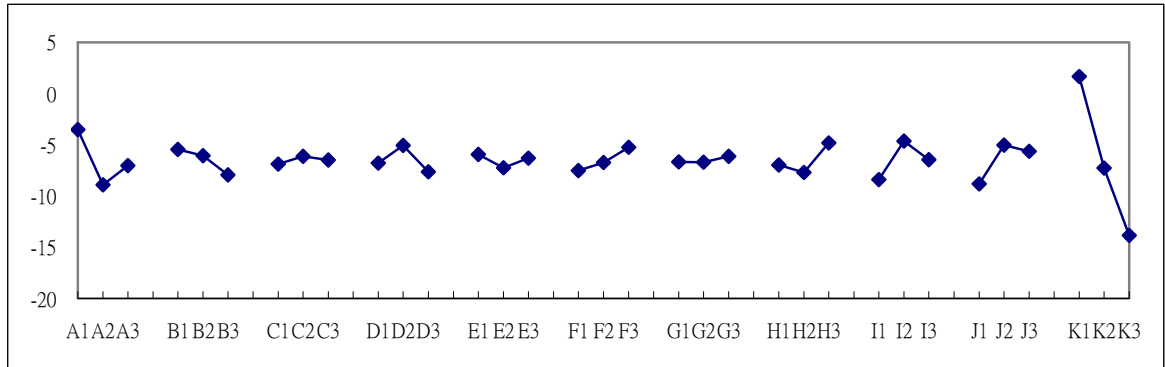


Figure 3.22 Factor response graph for the transmission error analyses.

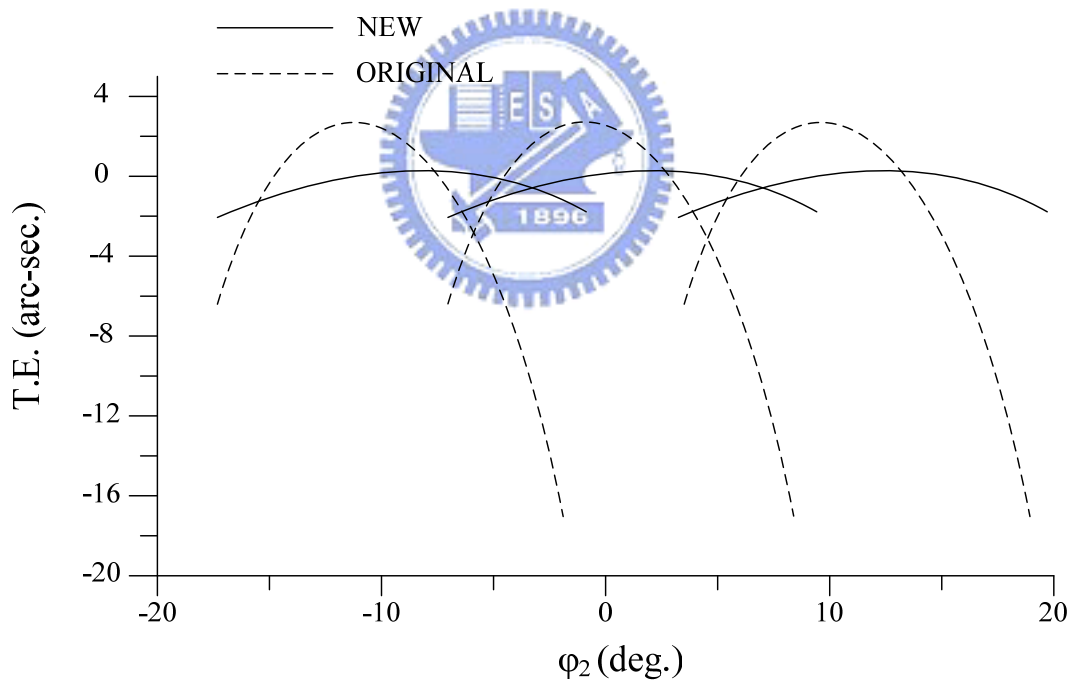


Figure 3.23 Transmission errors caused by original and optimized parameters.

CHAPTER 4

PLUNGE GEAR SHAVING WITH TOOTH CROWNING

Gears are the most important components in transmission systems. Modifications of gear teeth (gear tooth crowning) can accommodate errors and deformations encountered in the manufacture, assembly, and operation of gear pairs. Among the four basic shaving methods, plunge shaving is the most advanced gear finishing technique which only needs radial infeed. Its advantages include increased productivity, accuracy, long tool life, and a simple machine structure (Bianco, 2000). The basic meshing condition of 3D crossed-axis helical gear pair was first derived by Litvin (1994), and it has been widely adopted as the fundamental assumption for simulation of gear shaving. For shaving methods other than plunge shaving, the gear tooth crowning is accomplished by tooth modifications of the shaving cutter and the coordinated motions between cutter and gear. For the plunge shaving method, however, it only depends on the surface geometry of the plunge shaving cutter. Traditionally, the cutter surface geometry results from a cutter re-sharpening machine by trial and error. Focusing on the surface geometry of shaving cutter, what's really significant is precision of the region between SAP (start of active profile) and EAP (end of active profile) as shown in Fig. 3.1. In gear shaving, SAP of cutter tooth shaves the gear tooth root while EAP shaves the gear tooth tip. In this chapter, the analytical description of the gear with tooth crowning is first constructed by B-spline surface fitting. Then, the grinding wheel profile is parameterized and optimized for minimizing the surface deviations of theoretical and ground (from re-sharpening machine) tooth surfaces of the plunge shaving cutter. Efficiency is greatly improved by avoiding the traditional trial and error method, and the constructed mathematical model of plunge shaving cutter can be further utilized as the base for extending researches.

4.1 Surface interpolation of modified gear tooth

To integrate the modified gear tooth surfaces into the analytical process, especially for those with both lead and profile crowning, B-spline surface interpolation is selected for its ease of manipulation. In practice, the sampling points of the modified surface can be obtained by CMM (Coordinate Measuring Machine) or from other sources. In this paper, for studying purposes, the most commonly used numerical model is adopted for generation of interpolating points: the tooth flank is modified in profile (root to tip) and lead (side to side) directions independently as shown in Fig. 4.2 (Wagaj, 2002). The magnitude at the tip a_t and the gear roll angle at the start α_t define the boundaries of the tip relief. Between these two points, the profile follows a linear trajectory. Similarly, the magnitude a_r and the starting roll angle α_r define the starting point of a root modification. The amount of lead crowning is denoted by h .

A B-spline representation enables the simulation of surface irregularities and the control of small tooth geometric modifications, such as rounding and reliving. Given a grid of sampling points $D_{k,\ell}$ ($0 \leq k \leq m$ and $0 \leq \ell \leq n$) and orders p and q (degrees $p-1$ and $q-1$), it can be represented as below (Piegl, 1997):

$$D_{k,\ell} = \sum_{i=0}^m \sum_{j=0}^n N_{i,p}(s_k) N_{j,q}(t_\ell) P_{i,j} \quad (4.1)$$

where s_k 's and t_ℓ 's are the chosen parameter values; $N_{i,p}(s_k)$ ($N_{j,q}(t_\ell)$) is the i -th (j -th) B-spline basis function of order p (q); and $P_{i,j}$'s ($0 \leq i \leq m$ and $0 \leq j \leq n$) are the control points. Once the numbers of sampling points m and n are selected, then the B-spline orders p and q are limited by Eq. 4.2:

$$p \geq \frac{3m+1}{m+1}, \quad q \geq \frac{3n+1}{n+1} \quad (4.2)$$

, that is, $p \geq 3$ and $q \geq 3$.

Solving Eq. 4.1, $P_{i,j}$'s can be obtained, and the interpolated B-spline surface Σ_2^I can be represented as follows:

$$\Sigma_2^I(u, v) = \sum_{i=0}^m \sum_{j=0}^n N_{i,p}(u) N_{j,q}(v) P_{i,j} \quad (4.3)$$

where u and v denote the surface parameters; 2 denotes the surface of gear tooth; and I denotes the surface obtained by interpolation.

B-spline interpolation can be implemented using the MATLAB Spline Toolbox[®] by specifying a set of data points, and either knot sequences or orders of the interpolated surface. The process of obtaining the B-spline surface is illustrated in Fig. 4.3. For example, to interpolate the gear tooth surfaces described in Tables 4.1 and 4.2, including three target gear tooth surfaces (standard Σ_{S2} , lead crowned Σ_{L2} , and double crowned Σ_{D2}), three sets of sampling points must be acquired from the model shown in Fig. 4.2. In order to obtain gridded data points for interpolations, the target surfaces are sampled in the cylindrical coordinate system (represented by R_2 , θ_2 and Z_2) for the nature of the cylindrical gear, as shown in Fig. 4.4.

By specifying the number of sampling points m and n in the R_2 and Z_2 coordinates as well as the respective orders p and q , three interpolated tooth surfaces can be expressed as $\Sigma_{S2}^I(R_2, Z_2)$, $\Sigma_{L2}^I(R_2, Z_2)$, and $\Sigma_{D2}^I(R_2, Z_2)$. Three sets of data points (30×30 in R_2 and Z_2 coordinates for each set) are also sampled from the three target surfaces for error analysis. The interpolation error E^I is defined as a 30×30 matrix composed of values of arc length between the respective points (with the same values of radius and at the same axial cross-section) uniformly sampled from the target surface Σ_2 and the interpolated surface Σ_2^I . Each element $e_{i,j}^I$ of E^I can be expressed as Eq. 4.4:

$$e_{i,j}^I = r_{i,j} \left(\tan^{-1} \left(\frac{y_{i,j}}{x_{i,j}} \right) - \tan^{-1} \left(\frac{y_{i,j}^I}{x_{i,j}^I} \right) \right), \quad i, j = 1, 2, \dots, 30 \quad (4.4)$$

where $r_{i,j}$ denotes the value of radius; $x_{i,j}, y_{i,j}$ and $x_{i,j}^I, y_{i,j}^I$ denote the points on Σ_2 and Σ_2^I , respectively; and the maximum e_{\max}^I as well as the mean e_{mean}^I can be obtained.

Based on the error analysis in this section, E^I is not sensitive at all to the parameters in the Z_2 coordinates, including n and q . Even with lead crowning, the non-linearity remains quite small compared with that caused by profile crowning. Table 4.3 presents six conditions of Σ_{S2}^I . Increasing m and p improve the values of e_{mean}^I and e_{\max}^I , which are commonly required to be less than 10^{-3} mm. Although the errors are the same in conditions 5 and 6, the parameters in condition 6 are preferable for higher differentiability. Errors of surface Σ_{L2}^I are similar to that of Σ_{S2}^I . Nevertheless, for surface Σ_{D2}^I , under conditions similar to condition 6, m must increase to 14, as shown in Fig. 4.5, because of higher non-linearity due to profile crowning.

The interpolated surfaces Σ_{L2}^I and Σ_{D2}^I are compared with Σ_{S2}^I for validations as shown in the topographic charts Figs. 4.6 and 4.7. The topographic errors between top and root on the left and right tooth flanks are calculated for points of specific radiuses and Z cross-sections. Σ_{S2}^I is presented in straight solid lines as the base of comparison, while Σ_{L2}^I and Σ_{D2}^I are presented in dashed lines. In Fig. 4.6, Σ_{L2}^I is shown with lead crowning only and in Fig. 4.7, Σ_{D2}^I is shown with both lead and profile crownings. Note that the values of the topographic differences are all represented in arc length.

4.2 Topographic error analysis of the plunge shaving cutter

The tooth surface of the shaving cutter is usually finished last using a cone grinding wheel on the shaving cutter re-sharpening machine. Because the topographic accuracy of the plunge shaving cutter maps directly onto the work gear, it is important to identify the

topographic error of the ground tooth surfaces Σ_{S1}^G , Σ_{L1}^G and Σ_{D1}^G in comparison to the theoretical Σ_{S1}^T , Σ_{L1}^T and Σ_{D1}^T where 1 denotes the surface of shaving cutter tooth; G and T denote the surfaces derived from the re-sharpening machine and the interpolated surfaces, respectively.

The basic meshing condition for the crossed helical gear set (Litvin, [3]) is used to calculate the basic geometric data for the shaving cutter. It needs the following eight basic items: the tooth number Z_1 , the normal circular tooth thickness s_{pn1} , the helix angle β_{p1} of the shaving cutter; the tooth number Z_2 , the normal circular tooth thickness s_{pn2} , the helix angle β_{p2} of the work gear, and the normal module m_{pn} and pressure angle α_{pn} , of the shaving cutter and work gear. Fig. 4.8 shows the coordinate system of the CNC shaving machine (Hsu, 2006). Considering coordinate transformation

$$\begin{aligned} \mathbf{r}_1 &= [x_1 \quad y_1 \quad z_1 \quad 1]^T = \mathbf{M}_{12}(\phi_2) \mathbf{r}_2(R_2, Z_2) \\ \mathbf{n}_1 &= [n_{x1} \quad n_{y1} \quad n_{z1}]^T = \mathbf{L}_{12}(\phi_2) \mathbf{n}_2(R_2, Z_2) \end{aligned} \quad (4.5)$$

and meshing equation

$$f(R_2, Z_2, \phi_2) = \mathbf{n}_h \cdot \mathbf{v}_h^{(12)} = 0 \quad (4.6)$$

simultaneously, the theoretical tooth surface of shaving cutters Σ_{S1}^T , Σ_{L1}^T and Σ_{D1}^T can be derived from surfaces Σ_{S2}^I , Σ_{L2}^I and Σ_{D2}^I . \mathbf{M}_{12} and \mathbf{L}_{12} are matrices for transforming position and unit normal vectors (\mathbf{r}_2 and \mathbf{n}_2) of surfaces Σ_{S1}^T , Σ_{L1}^T and Σ_{D1}^T from coordinate system S_2 (gear) to S_1 (shaving cutter), and $\mathbf{v}_h^{(12)}$ denotes the vector of relative velocity on auxiliary coordinate system S_h .

Likewise, as shown in Fig. 4.9, the ground surfaces of shaving cutters Σ_{S1}^G , Σ_{L1}^G and Σ_{D1}^G can be obtained by coordinate transformations from S_g (grinding wheel) to S_s (shaving

cutter)

$$\begin{aligned}\mathbf{r}_s &= [x_s \quad y_s \quad z_s \quad 1]^T = \mathbf{M}_{sg} \mathbf{r}_g \\ \mathbf{n}_s &= [n_{xs} \quad n_{ys} \quad n_{zs}]^T = \mathbf{L}_{sg} \mathbf{n}_g\end{aligned}\quad (4.7)$$

and the meshing equation

$$g(u_g, \theta_g, \phi) = \mathbf{n}_m \cdot \mathbf{v}_m^{(sg)} = 0 \quad (4.8)$$

An example is provided for illustration. Note that all the topographic errors are all calculated in the axial cross-section rather than normal one.

Example 4.1

For interpolated gear tooth surfaces Σ_{S2}^I and Σ_{D2}^I (see Tables 4.1 and 4.2), the corresponding data of plunge shaving cutter and grinding wheel are presented in Tables 4.4.

Obtaining theoretical tooth surfaces Σ_{S1}^T and Σ_{D1}^T as well as ground tooth surfaces Σ_{S1}^G and Σ_{D1}^G through Eqs. 4.5 to 4.8, the topographic errors are calculated by

$$e_{i,j}^{Topo} = r_{i,j} \left(\tan^{-1} \left(\frac{y_{i,j}^T}{x_{i,j}^T} \right) - \tan^{-1} \left(\frac{y_{i,j}^G}{x_{i,j}^G} \right) \right), \quad i=1,2,\dots,5, j=1,2,\dots,9 \quad (4.9)$$

and illustrated in Figs. 4.10 and 4.11 by 5×9 grids of specified radiuses and Z cross-sections, in which theoretical surfaces are presented in straight solid lines, while the corresponding ground ones are shown in dashed lines. From SAP to EAP. of the cutter tooth, errors between Σ_{D1}^T and Σ_{D1}^G (Fig. 4.11) are less than those between Σ_{S1}^T and Σ_{S1}^G (Fig. 4.10). This is because of the nature of a grinding wheel with cone angle; that is, it presents a parabolic shape on the pitch line of a shaving cutter tooth, so that a specific amount of lead crowning can be compensated.

4.3 Design optimization of the cone-grinding wheel

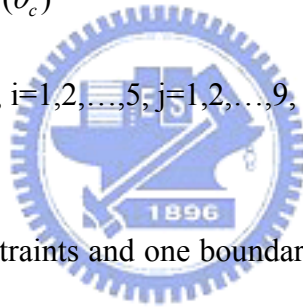
Compared with the setting parameters of the shaving cutter re-sharpening machine, the

cone angle θ_c of the grinding wheel results in more influences on topographic errors of the final product. Traditionally, θ_c is modified back and forth for the desired accuracy, which is time-consuming. In this section, two examples are provided for illustrating design optimization by adjusting θ_c (Example 4.2) and the profile of the grinding wheel (Example 4.3).

Example 4.2

The objective of this example is to minimize the topographic errors between the theoretical tooth surface and the ground one. The flowchart is shown in Fig. 4.12, and the process is integrated by the MATLAB Optimization Toolbox. The problem is formulated as:

$$\begin{aligned} &\text{find } \theta_c \\ &\text{that minimizes } \sum_{i=1}^5 \sum_{j=1}^9 e_{i,j}^{Topo}(\theta_c) \\ &\text{subject to } e_{i,j}^{Topo} < 10^{-3} \text{ mm}, i=1,2,\dots,5; j=1,2,\dots,9, \\ &\text{and } 1^\circ \leq \theta_c \leq 30^\circ. \end{aligned}$$



Considering 45 inequality constraints and one boundary constraint, the design variable θ_c is modified iteratively to obtain the optimum of topographic error. The process of calculating $e_{i,j}^{Topo}$ based on θ_c is considered as $e_{i,j}^{Topo}(\theta_c)$, and the Sequential Quadratic Programming (SQP) algorithm is adopted, where information of finite difference is used instead of gradients. The minimum and maximum searching steps are 0.001 and 0.1 degree. For standard surfaces Σ_{S1}^T and Σ_{S1}^G shown in Fig. 4.13, the topographic errors are minimized when θ_c is modified from 10° (initial value) to 1° (optimum value), which is active for the boundary constraint $1^\circ \leq \theta_c \leq 30^\circ$. In practice, it's very difficult to make a grinding wheel with cone angle less than 1° so that the topographic error can't be improved any more by only adjusting θ_c . For double crowned tooth surfaces Σ_{D1}^T and Σ_{D1}^G , the errors are still large at SAP and EAP (Fig. 4.14) due to profile crowning. To eliminate the errors, the profile of the grinding

wheel also needs to be modified.

Example 4.3

Based on Fig. 4.9, the profile of grinding wheel is parameterized as shown in Fig. 4.15. Coordinate system S_g' is attached to the unmodified profile. Within the effective length $L_A + L_B$ ($L_A=4.2mm$, $L_B=5.5mm$), the profile with four sections are defined by w_A , h_A , w_B and h_B . Represented in S_g' , the four points A_2 , A_1 , B_1 and B_2 are fitted by a B-spline curve with order 4. To improve the topographic errors between Σ_{D1}^T and Σ_{D1}^G , the process of optimization is divided into two levels. The problem formulation for level 1:

find θ_c

that minimizes $\sum_{j=1}^9 e_j^{Topo}(\theta_c)$ on the pitch line of tooth surface

subject to $e_j^{Topo} < 10^{-3} mm$, $j=1,2,\dots,9$ on the pitch line of tooth surface,

and $0.5^\circ \leq \theta_c \leq 30^\circ$.



The minimum and maximum searching steps are 0.001 and 0.1 degree, and the first level converges efficiently to $\theta_c = 2.382^\circ$, and the problem formulation of level 2:

find $\mathbf{x} = [w_A, h_A, w_B, h_B]$

that minimizes $\sum_{i=1}^5 \sum_{j=1}^9 e_{i,j}^{Topo}(\mathbf{x})$

subject to $e_{i,j}^{Topo} < 10^{-3} mm$, $i=1,2,\dots,5$, $j=1,2,\dots,9$,

and $10^{-4} < w_A < L_A - 10^{-4}$; $0 < h_A < 3$; $10^{-4} < w_B < L_B - 10^{-4}$; $0 < h_B < 3$ (unit: mm).

Following the similar concepts of programming in Example 4.2, the optimum design is presented in Table 4.5, in which the minimum and maximum searching steps are 0.0001 and 0.1 mm. The profile of the grinding wheel is considered straight sided initially. When it reaches optimum, the profile is modified for conjugation to the shaving cutter. The

topographic errors between Σ_{D1}^T and Σ_{D1}^G are shown in Fig. 4.16, where the errors are all controlled below $10^{-3}mm$.

Experiment of Example 4.3 has been conducted for validation of the proposed method. Fig. 4.17 shows the plunge shaving cutter with an enlarged view of the cutting edges. Fig. 4.18 shows the pre-shaved gear with an enlarged view of the obviously scalloped tooth surfaces measured as shown in Fig. 4.19. Firstly, the shaving cutter is ground by the grinding wheel on the re-sharpening machine (Fig. 4.20), on which the grinding wheel are modified first by the dresser according to the calculated cone angle and profile parameters. Then, the gear is plunge shaved on NACHI shaving machine with the setup shown in Fig. 4.21. Materials of gear and cutter are SCM435 and M2, and the operating speed as well as plunge infeed are set as 150 RPM and 1mm/min, respectively. The shaved gear is measured as shown in Fig. 4.22 and the mean values of tooth crowning are recorded in Table 4.6. It is found that:

1. most of the scallops are eliminated and the surface roughness is greatly improved, especially in the lead direction;
2. the amounts of modifications, though with little deviations, are close to the original design values;
3. larger modifications are induced on left flank compared with right flank; this is because the left flank is the driving one in shaving with larger cutting force;
4. efficiency is greatly improved by adopting the proposed method instead of trial and error.

4.4 Concluding remarks

Design and manufacture of the plunge-typed gear shaving cutters has always been a challenge, especially for those used to manufacture gears with tooth crowning. This chapter proposes a method for design and manufacture of the plunge shaving cutter for gears with tooth crowning analytically, rather than trial and error. By integrating B-spline interpolation, differential geometry, and design optimization, the goal is achieved. To interpolate gears with

both lead and profile crownings (double crowned), more sampling points are needed in the radial direction. In manufacturing a shaving cutter, the lead modification can be compensated by adjusting the cone angle, and the profile modification can be implemented by modifying the profile of the grinding wheel. Efficiency is greatly improved by avoiding traditional trial and error method through the proposed one. Besides, an analytical description of the modified gear tooth surface is also constructed, which can be utilized for extending research on serrations and shaving process.



Table 4.1 Basic data of the target surfaces.

Gear data		
Diameter of base circle	d_{b2}	119.618mm
Diameter of addendum circle	d_{add2}	126.71mm
Diameter of root circle	d_{r2}	119.33mm
Diameter of pitch circle	d_{p2}	123.915mm
Normal pressure angle in pitch circle	α_{pn2}	14.5°
Face width	fw_2	18mm
Gear tooth number	Z_2	79
Helix angle in pitch circle	β_{p2}	17°
Normal circular tooth thickness	s_{pn2}	2.32mm



Table 4.2 Data of gear tooth modification (crowning) of the target surfaces.

Parameter	Σ_{S2}	Σ_{L2}	Σ_{D2}
a_i	0	0	6e-3mm
α_i	N/A	N/A	31.8°
a_r	0	0	6e-3mm
α_r	N/A	N/A	28.2°
h	0	6e-3mm	6e-3mm

Table 4.3 Conditions and errors of B-spline surface interpolation ($\Sigma_{S_2}^I$).

Parameter	Condition					
	1	2	3	4	5	6
m (R_2 coordinate)	3	4	4	5	5	5
n (Z_2 coordinate)	3	3	3	3	3	3
p (R_2 coordinate)	3	3	4	3	4	4
q (Z_2 coordinate)	3	3	3	3	3	4
$e_{mean}^I (10^{-3} mm)$	9.805	1.721	1.193	0.645	0.185	0.185
$e_{max}^I (10^{-3} mm)$	15.6745	4.55	1.795	1.8539	0.0679	0.0679



Table 4.4 Data of cutter and grinding wheel for Example 4.1.

Plunge shaving cutter		
Normal circular tooth thickness	s_{pn1}	2.464mm
Tooth number	Z_1	139
Helix angle in pitch circle	β_{p1}	20°
Face width	f_{w1}	20mm
Diameter of start of active profile (SAP.)		225.922mm
Diameter of end of active profile (EAP.)		219.537mm
Operating center distance	E_o	173.04mm
Operating crossed angle	γ_o	3.002°
Grinding wheel and grinding machine		
Operating cone pitch radius	R_c	350mm
Cone angle	θ_c	10°
Pressure angle	α	4.675°
Operating radius	r_o	111.03mm

Table 4.5 Results of the second level optimization in Example 4.2.

	Initial design	Optimum design
w_A	0.1 mm	0.561 mm
h_A	0 mm	0.056 mm
w_B	0.1 mm	0.538 mm
h_B	0 mm	0.235 mm

Table 4.6 Achieved tooth modifications of gear after the experiment for validating Example 4.3.

	Left flank ($10^{-3}mm$)		Right flank ($10^{-3}mm$)	
	Design	Real	Design	Real
Profile				
Tip	6	6.9	6	5.2
Root	6	6.1	6	5.1
Lead	6	5.8	6	5.4



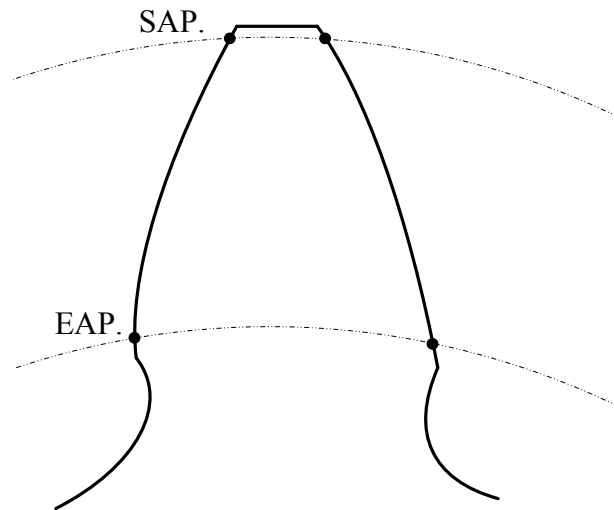


Figure 4.1 SAP and EAP of a shaving cutter tooth.

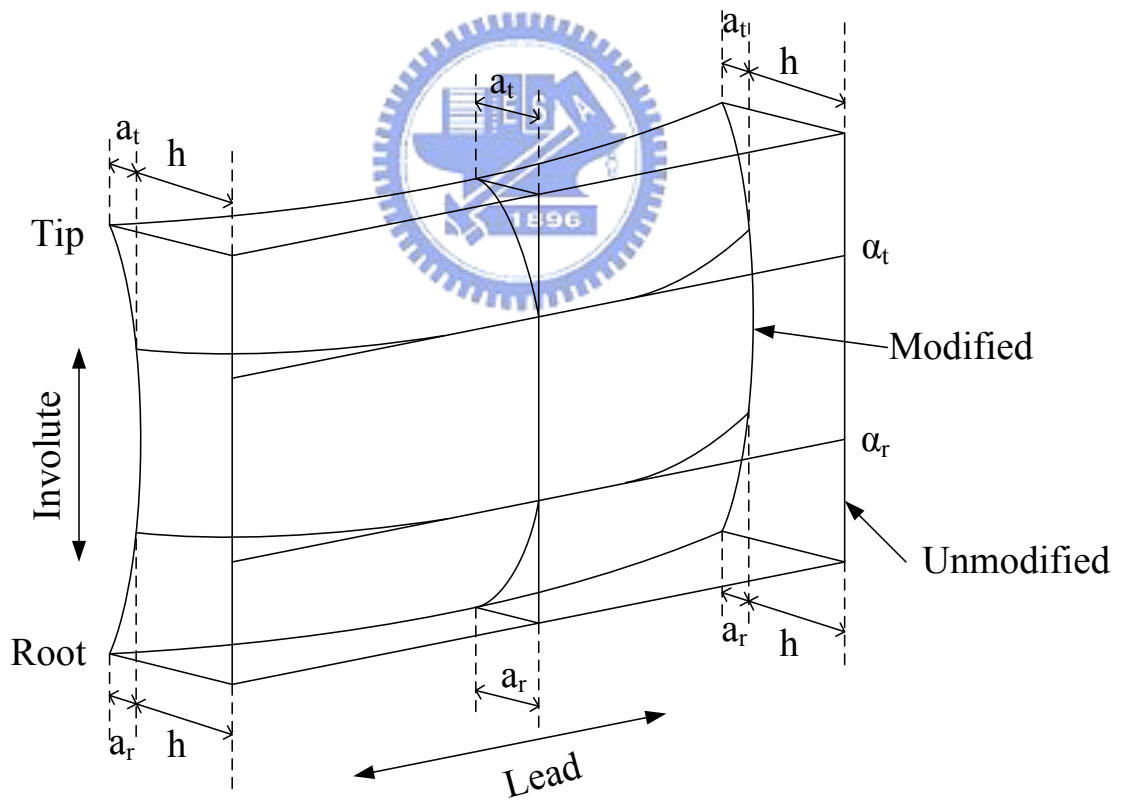


Figure 4.2 Model of gear tooth crowning (Wagaj, 2002).

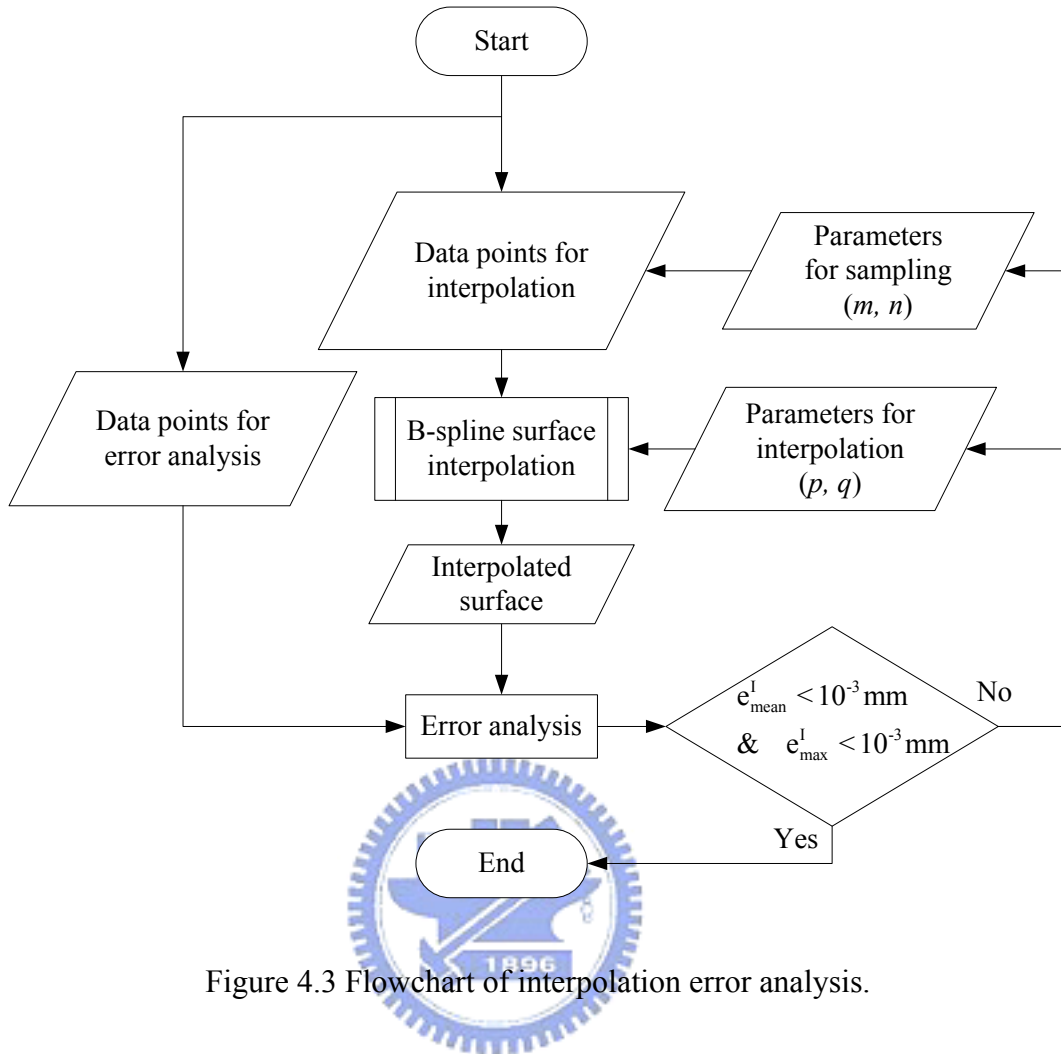


Figure 4.3 Flowchart of interpolation error analysis.

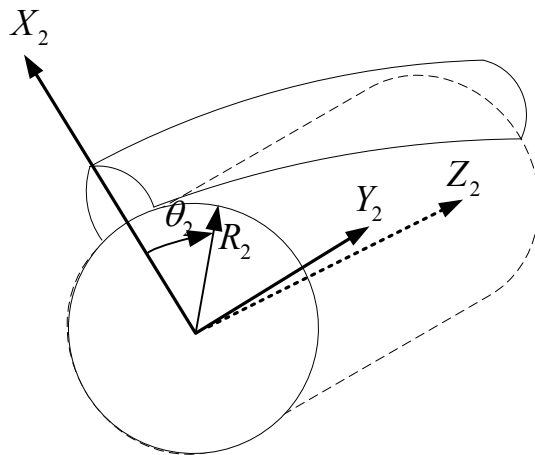


Figure 4.4 Cylindrical coordinate used for sampling data points.

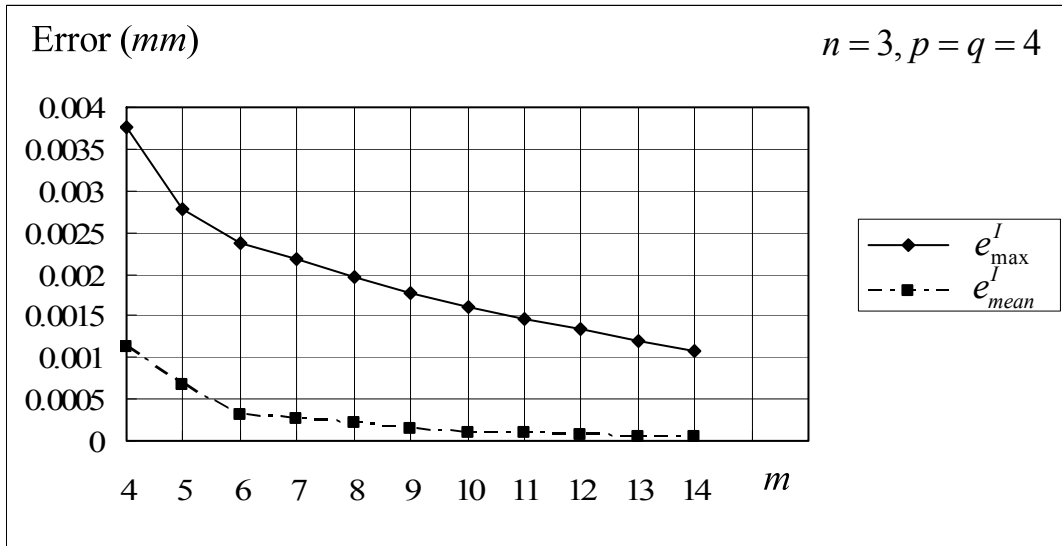


Figure 4.5 Interpolation error of Σ_{D2}^I by changing m ($n=3, p=q=4$).

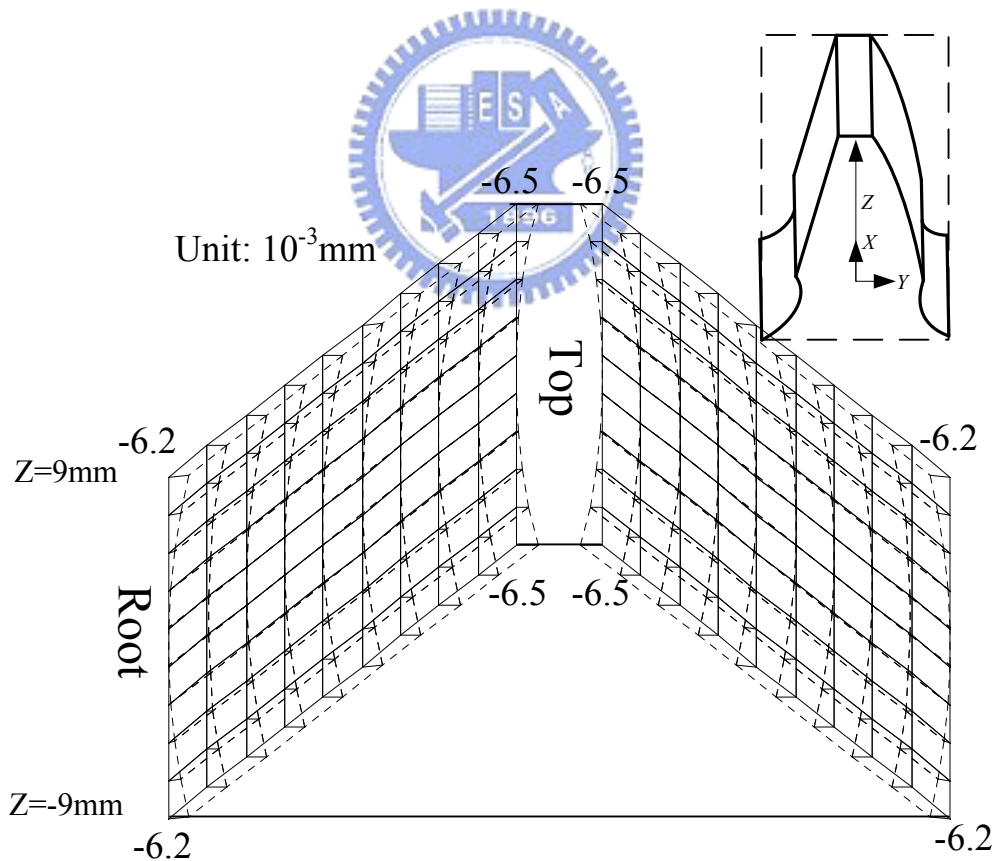


Figure 4.6 Validations of interpolated surfaces (Σ_{S2}^I vs. Σ_{L2}^I).

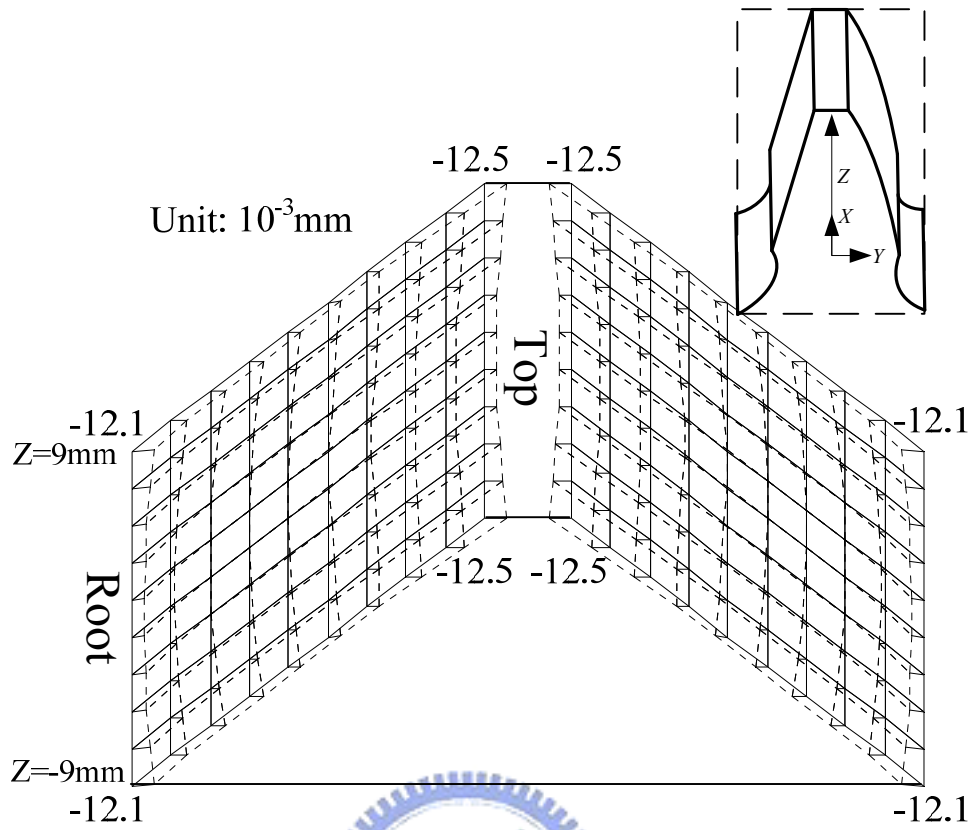
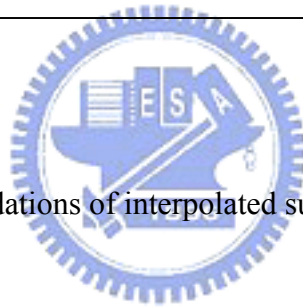


Figure 4.7 Validations of interpolated surfaces ($\Sigma_{S_2}^I$ vs. $\Sigma_{D_2}^I$).



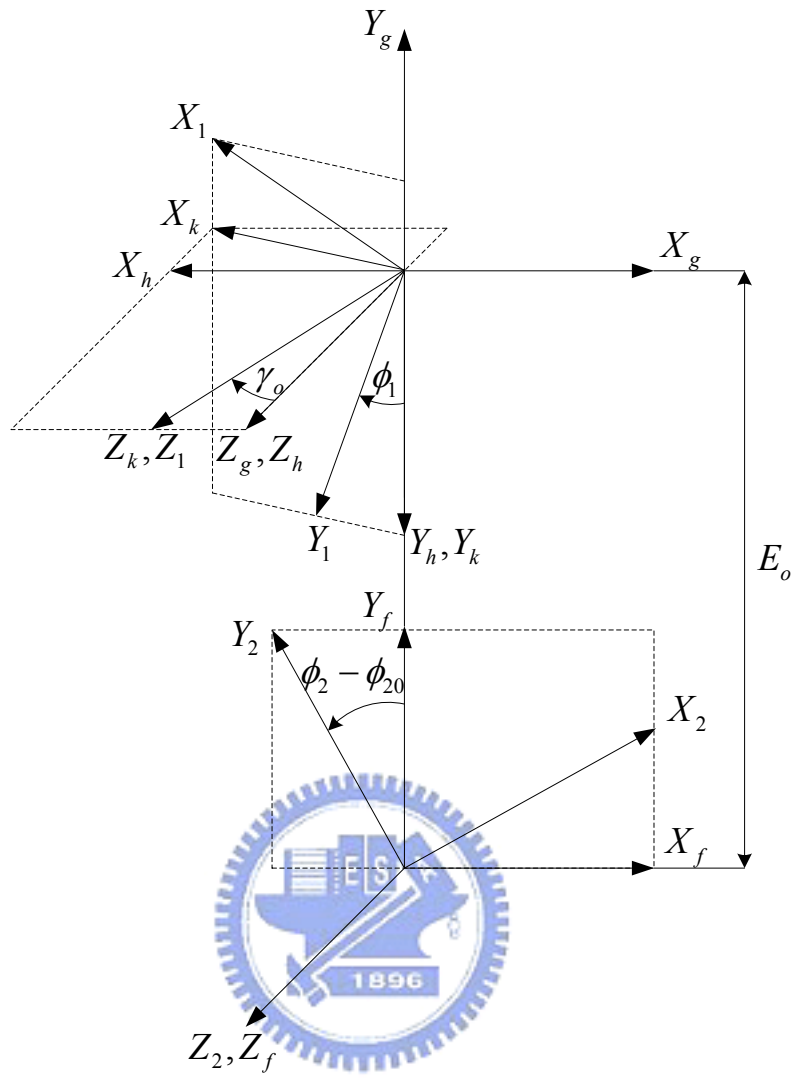


Figure 4.8 Coordinate systems of gear shaving machine

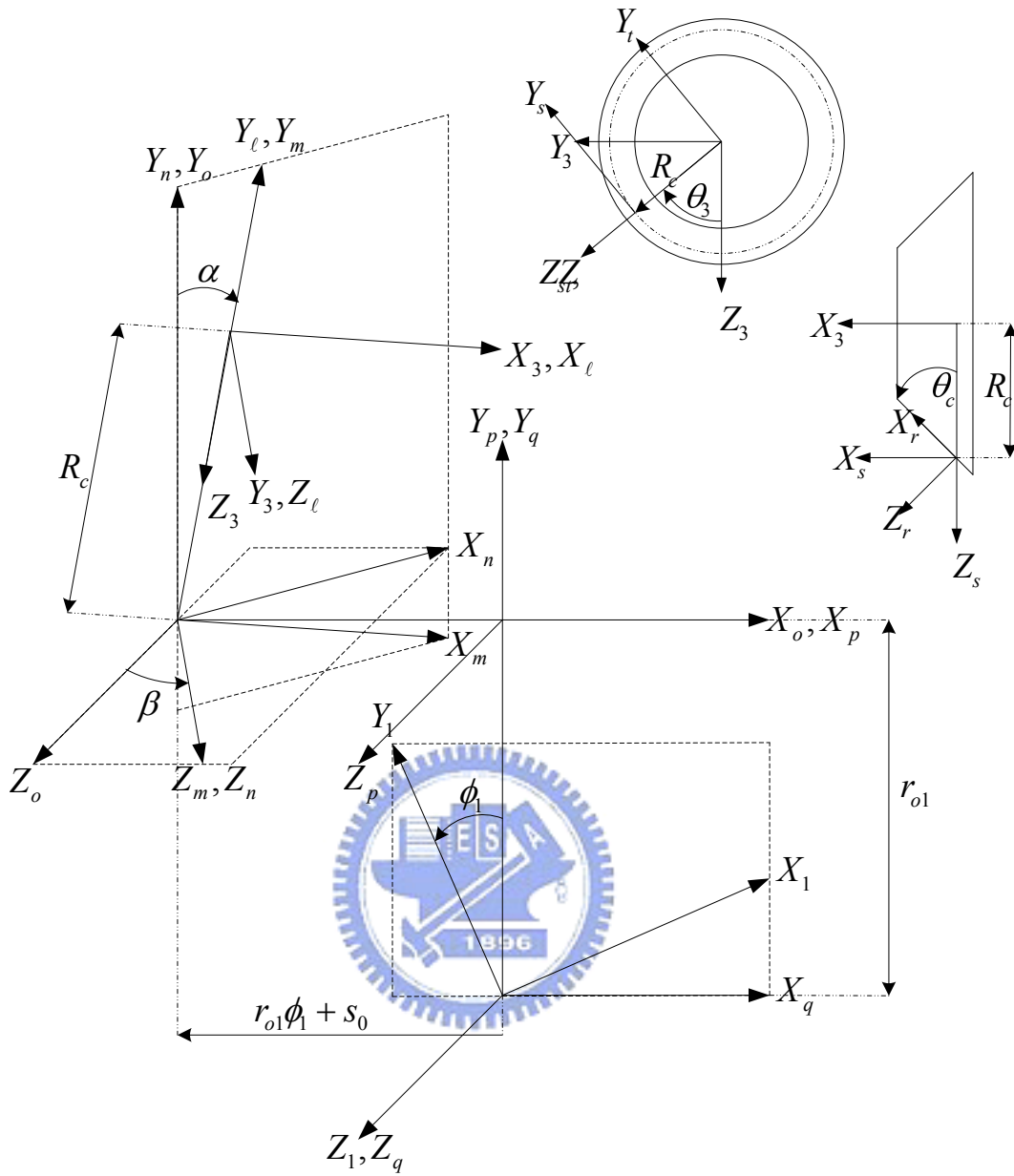


Figure 4.9 Coordinate systems of shaving cutter re-sharpening machine.

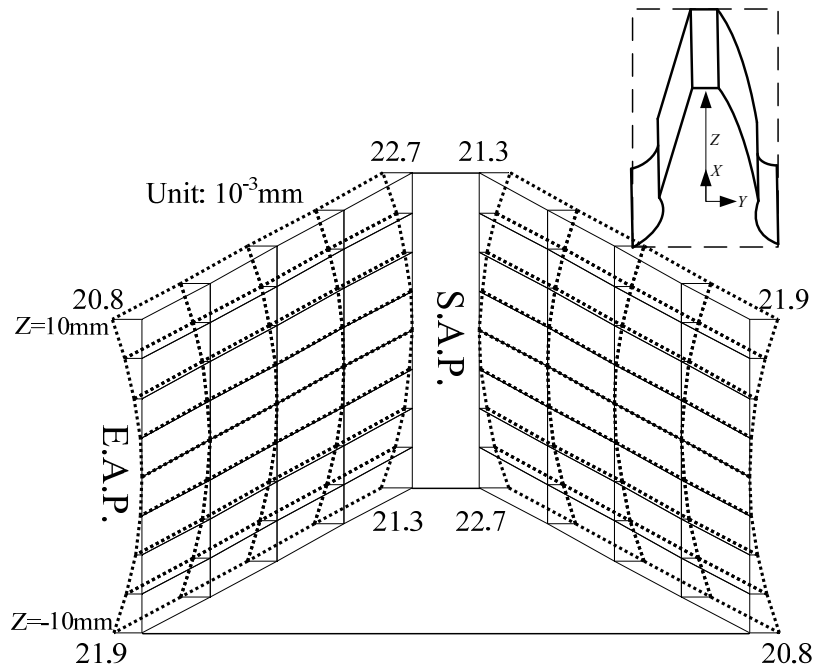


Figure 4.10 Topographic errors between theoretical and ground shaving cutter tooth surfaces

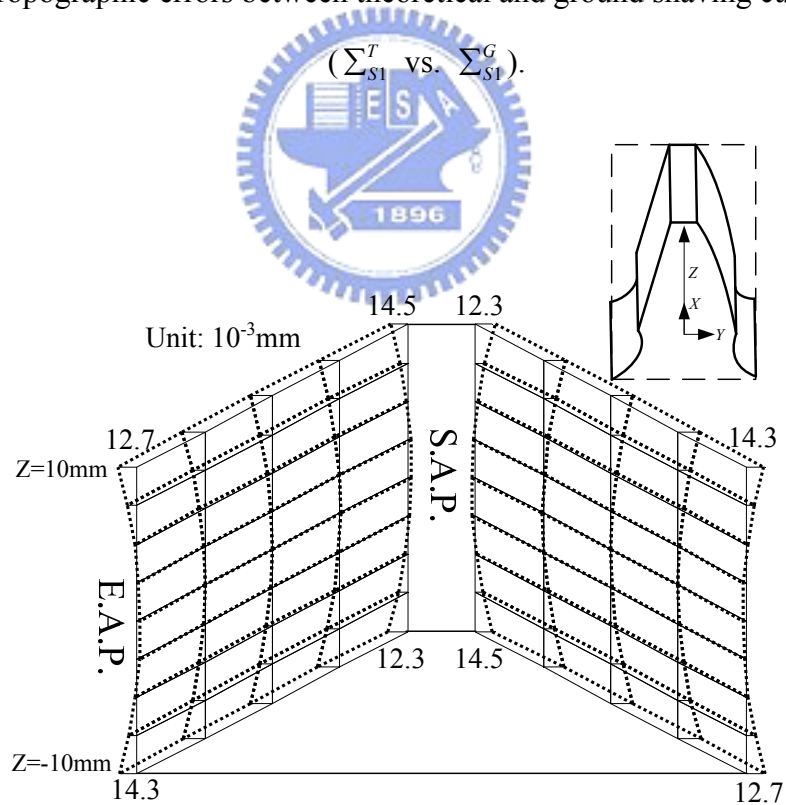


Figure 4.11 Topographic errors between theoretical and ground shaving cutter tooth surfaces

$$(\sum_{D1}^T \text{ vs. } \sum_{D1}^G).$$

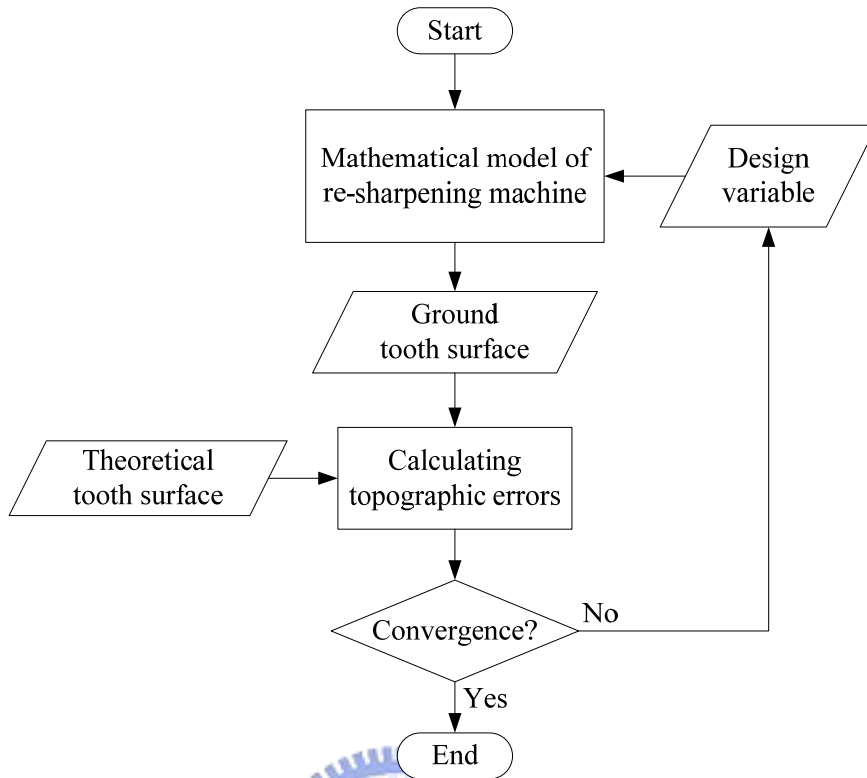


Figure 4.12 Flowchart of design optimizations of the cone grinding wheel.

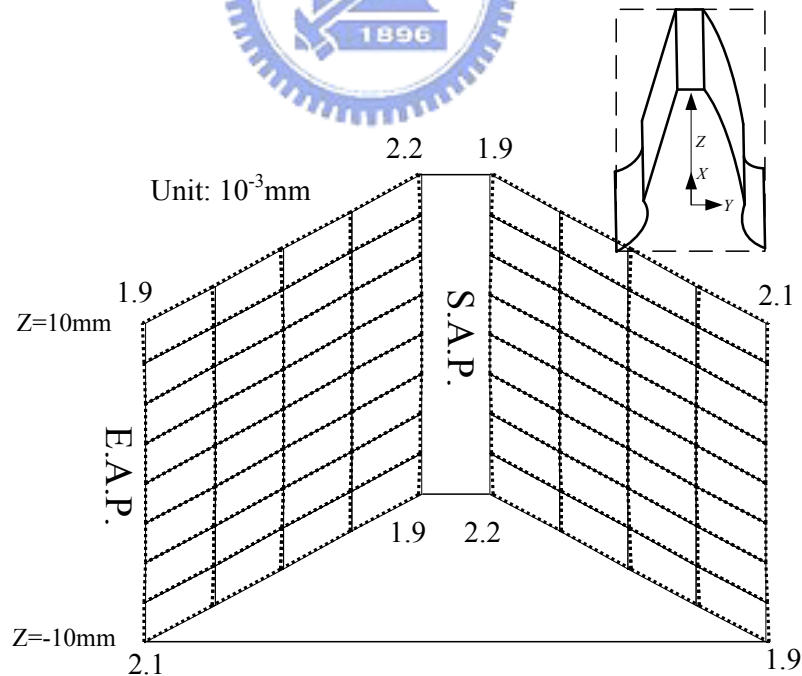


Figure 4.13 Topographic errors between theoretical and ground shaving cutter tooth surfaces optimized by θ_c (Σ_{S1}^T vs. Σ_{S1}^G).

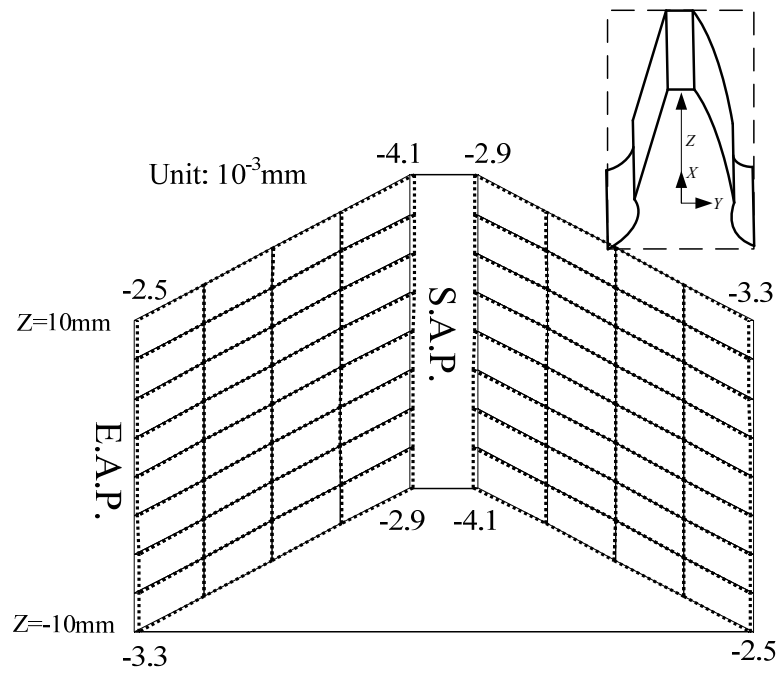


Figure 4.14 Topographic errors between theoretical and ground shaving cutter tooth surfaces

optimized by θ_c (Σ_{D1}^T vs. Σ_{D1}^G).

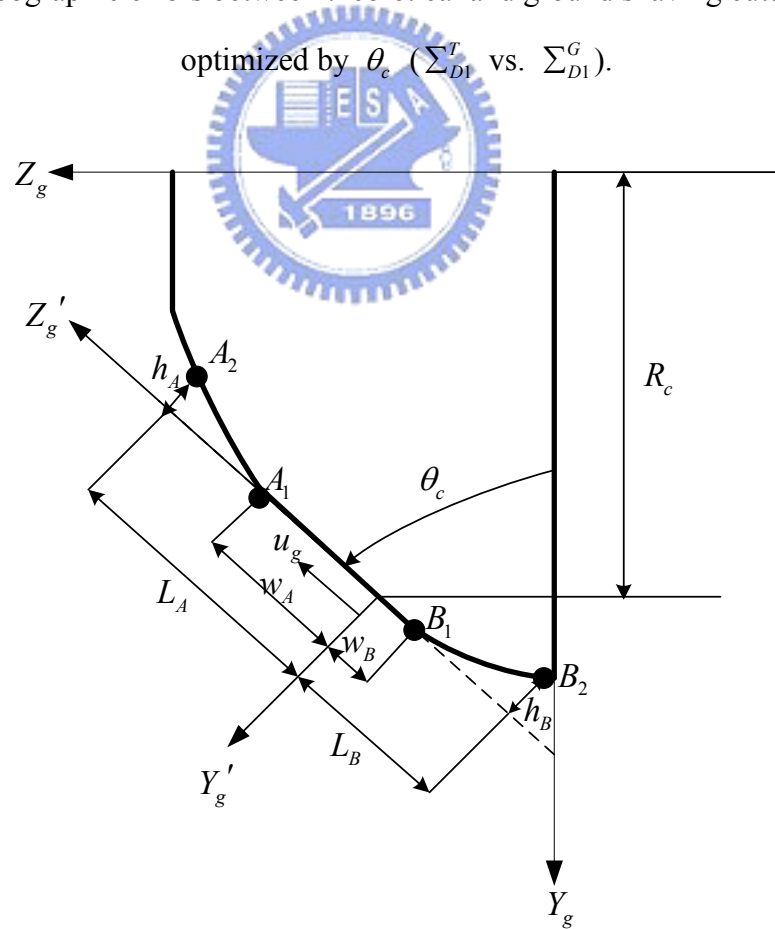


Figure 4.15 Parameterized profile of grinding wheel for optimization.

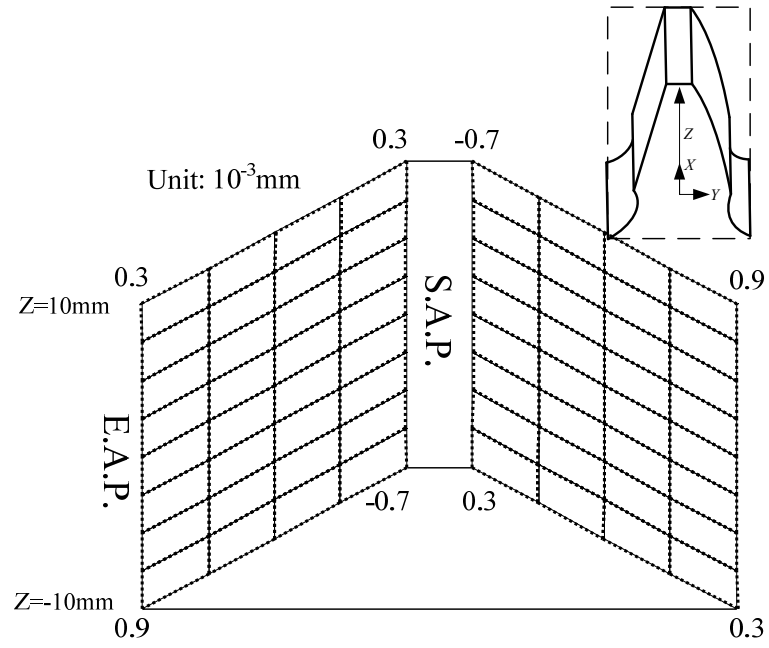
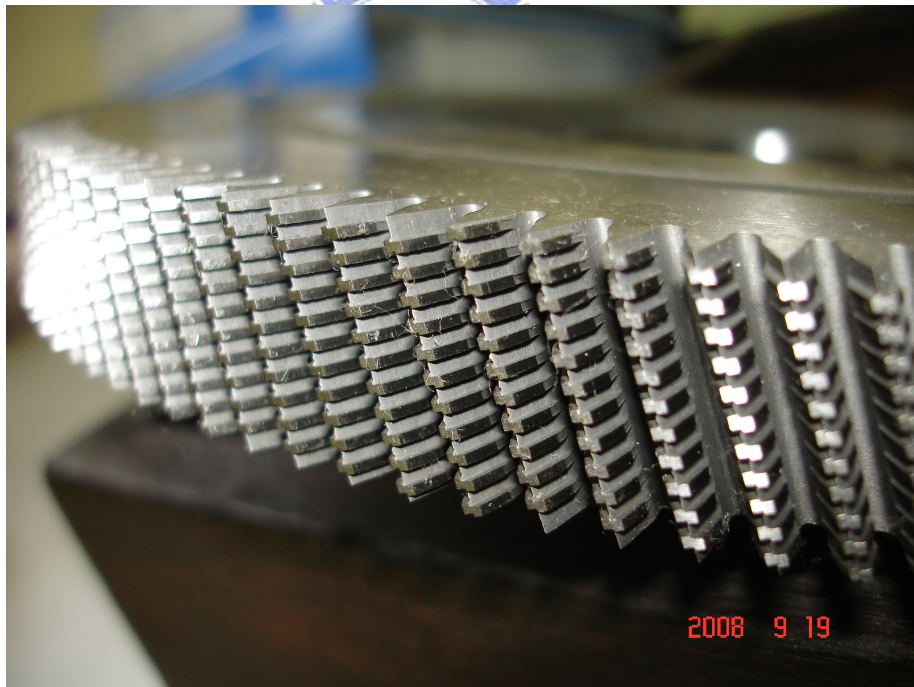


Figure 4.16 Topographic errors between theoretical and ground shaving cutter tooth surfaces by profile optimization (\sum_{D1}^T vs. \sum_{D1}^G).





(a)



(b)

Figure 4.17 Plunge shaving cutter used in the experiment (a) overview (b) scaled view.



(a)



(b)

Figure 4.18 Pre-shaved gear used in the experiment (a) overview (b) detailed view.

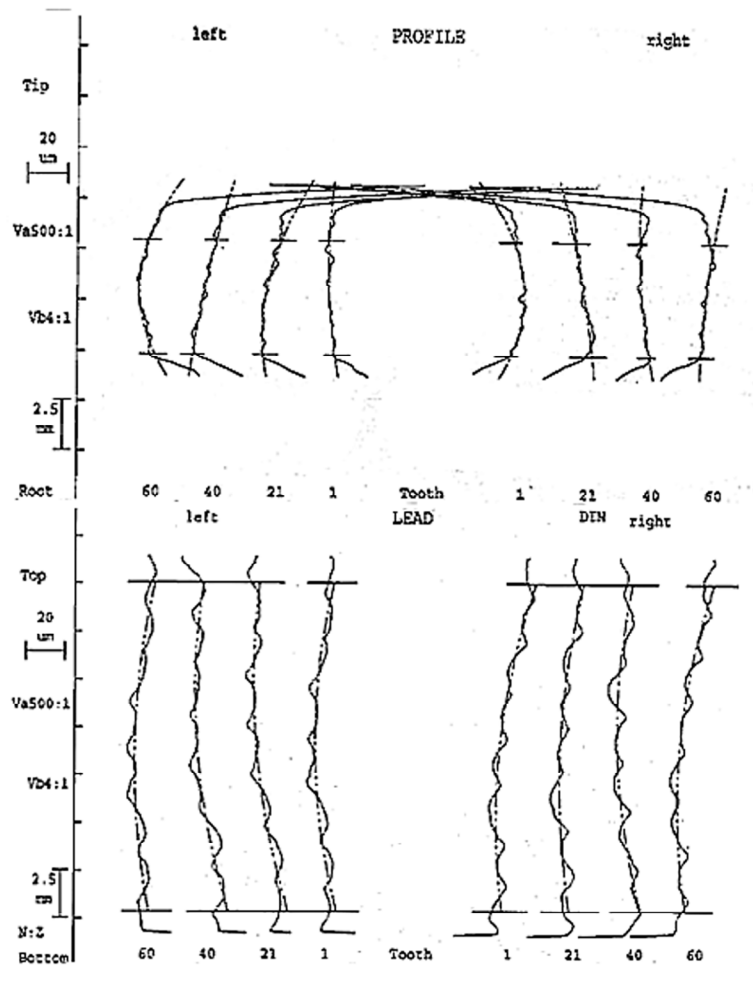


Figure 4.19 Measured data of the pre-shaved gear used in the experiment.

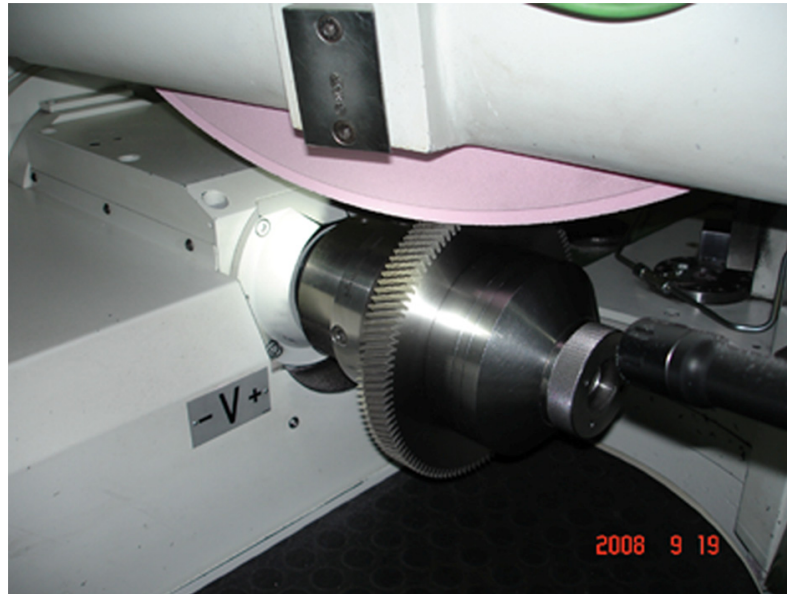
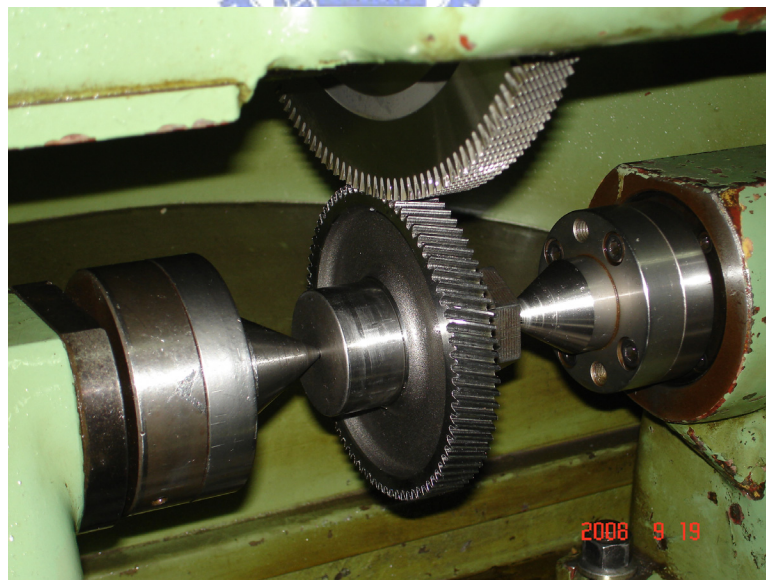


Figure 4.20 Plunge shaving cutter ground by the grinding wheel of the re-sharpening machine.





(a)



(b)

Figure 4.21 NACHI shaving machine used in the experiment (a) machine overview (b) cutter and work gear setup.

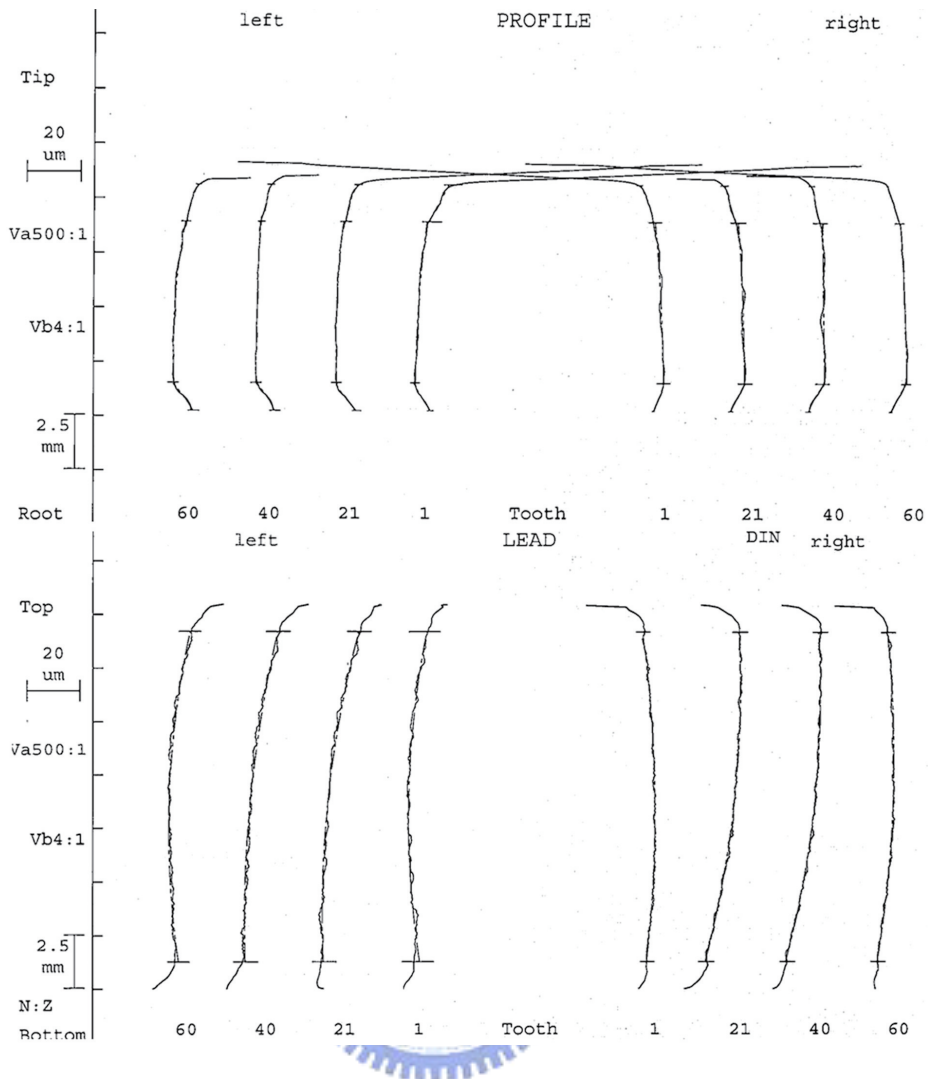


Figure 4.22 Measured data of the shaved gear after the experiment.

CHAPTER 5

DESIGN OF SERRATIONS ON GEAR PLUNGE SHAVING CUTTER

The plunge shaving cutter infeed movement towards the gear is radial to the gear axis without transverse movement. The stroke of the cutter is very short and the shaving time using this method is the shortest. The shaving cutter tooth surfaces have serrations extending from the top land to the root fillet of the teeth whose sharp edges exert a cutting action on the work gear due to the relatively lengthwise sliding motion. Serrations are an important feature for all shaving cutters, but for plunge cutters their importance is vital. The serrations related to such type of cutter must have a helical pattern and they have to be manufactured with a very high precision CNC slotting machine in order to obtain the best results. Thus, the surface roughness of the work gear after shaving is affected primarily by the arrangement of these serrations. In this chapter, an method for optimizing the serration displacement is proposed.

5.1 Design parameters for the shaving cutter serrations

As described by Hsu[10] and shown in Fig. 5.1, plunge shaving is characterized by a radial feed stroke without transverse feed. The serrations in consecutive shaving cutter teeth must be shifted longitudinally so that the cutting marks on the work gear move in a lengthwise direction. The plunge shaving cutter serrations are staggered in a helix as shown in Fig. 5.2. Thus, the design parameters for the serrations of the shaving cutter are the serration pitch p_s , the helix direction of the serrations, and the number of starts z_{os} , which indicates the number of serration pitches moved in the lengthwise direction when the shaving cutter is rotated once fully.

When the work gear meshes with the shaving cutter, the same tooth of the work gear meshes with the shaving cutter teeth every N_2 teeth. Since the number of teeth N_1 of the

shaving cutter might not be an integer multiple of the number of teeth N_2 of the work gear, the same work gear tooth will mesh with different shaving cutter teeth. For example, if the number of work gear teeth is 15 and the number of shaving cutter teeth is 157 (and the shaving cutter's initial contact tooth is labeled tooth #1), the same tooth of the work gear is meshed with the shaving cutter at tooth #1, #16, #31, #46, ..., #151, #9, #24, ..., in sequence. That is, the consecutive cutting marks on the same tooth of the work gear shift in a lengthwise direction due to the helix arrangement of the serrations. The lengthwise distance between the consecutive cutting marks is noted by the symbol d_s , defined as serration displacement, which can be expressed as follows:

$$d_s = \begin{cases} p_s \times \text{fraction part}\left(\frac{z_{os}N_2}{N_1}\right) & \text{when } \text{fraction part}\left(\frac{z_{os}N_2}{N_1}\right) < 0.5 \\ p_s \times (\text{fraction part}\left(\frac{z_{os}N_2}{N_1}\right) - 1) & \text{when } \text{fraction part}\left(\frac{z_{os}N_2}{N_1}\right) \geq 0.5 \end{cases} \quad (5.1)$$

Fig. 5.1 shows a diagram of a shaving cutter and a work gear. If the helix of the serrations moves in a right-hand (left-hand) direction and the shaving cutter rotates in a counterclockwise direction, the directional shift of the cutting mark on the work gear surface is from left to right (right to left).

However, the above is the viewpoint from shaving cutter. If the surface roughness of gear as well as cutting efficiency need to be addressed, the 3-D mathematical model needs to be constructed.

The shaving cutter is provided with a plurality of serrations with sharp cutting edges, which are produced on a slotting machine. In Hsu's [10] model, the serrations in 3-D space were obtained by calculating the intersections of slotting cutter and the shaving cutter tooth surface and then interpolated by cubic splines to obtain the cutting edges. After these, the cutting paths were calculated for analyses. However, to achieve design optimization, the calculation cycle needs to be integrated and automated. It's too inefficient to calculate serrations by intersection method when every time the design parameters are changed. To

simplify the process, the cutting edges are directly obtained by sampling and interpolating points from the shaving cutter tooth surface obtained in the previous chapter so that tooth crowning can be considered simultaneously., as shown in Fig. 5.3(a). Moreover, the serration shift SF was calculated by Eq.5.2 at the first place:

$$SF = n_s p_s / N_1 \quad (5.2)$$

, which indicated SF was controlled by defining parameters p_s and z_{os} . In this way, the design space was relatively small, and it was also unnecessary to use two parameters. In this chapter, SF is directly defined as a continuous design parameter.

By specifying the values of p_s and SF , the cutting edges are defined in the 3-D space:

$$r_{ce} = [x_{ce} \ y_{ce} \ z_{ce} \ 1] \quad (5.3)$$

According to the coordinate system of gear shaving machine shown in Fig.4.8, the cutting paths can be calculated by:

$$r_{cp}(\phi_2) = M_{21}(\phi_2)r_{ce} \quad (5.4)$$

In the next section, a numerical example is provided for design optimization of shaving cutter serration.



5.2 Numerical examples and discussion

The trace of the plunge shaving cutter's cutting edge on the work gear during the cutting process is illustrated schematically in Fig. 5.4 (Hsu, [10]). At the beginning of a shaving cycle, the cutting edge presses into the work gear surface, moves on its tooth surface due to the relative motion, and then removes chips when contact stress reaches local ultimate stress. Whereas the front cutting edge removes chips as it moves, the top land of the serration (i.e. the tooth surface of the shaving cutter), rather than removing chips, plows into the work gear tooth surface without a cutting action and extrudes material in the direction opposite to the cutting direction. Therefore, the front cutting edge produces the desired cutting action, while the top land of the serration produces unwanted friction and material flow. The following

example illustrates the design optimization of cutter serrations.

Example 5.1

The basic data for the work gear and shaving cutter are listed in Table 5.1, while the data for the serrations are listed in Table 5.2. Fig. 5.4 shows the simulations of the first and the subsequent cutting marks in the mid-tooth height of the work gear. The distance between the cutting marks between succeeding cuts, termed the “cutting mark displacement”, is directly proportional to the serration displacement. The abscissa in Fig. 5.4 represents the cutting depth (unit: μm), while the ordinate represents the cutting mark displacement in the lengthwise direction of the work gear (unit: mm) where the cutting marks are repeated within a certain range.

Fig. 5.4 (b) and (c) show the end of the first and second cutting cycle simulation, whose higher peak are termed the “first peak” and “second peak”. The ratio between the height of the second peak and that of the first peak in the first cutting cycle is known as the “cutting-down ratio”, which is used as an index for cutting efficiency. In this example, the height of the second peak is $1.590\mu\text{m}$ and the cutting-down ratio is 0.318.

According to the basic data of work gear and shaving cutter, the cutting-down ratio is optimized. The optimum design problem is formulated:

find serration shift SF

that minimizes cutting-down ration r_c

subject to $SF \times N_1 \geq p_s$

, in which $SF = n_s p_s / N_1$ originally, and it is directly selected as the design variable rather than n_s or p_s for larger design space. The minimum and maximum searching steps are 0.001 and 0.1 mm. The cutting-down ratio has been improved from 0.318 to 0.242 (1st peak= $3.1\mu\text{m}$, 2nd peak= $0.7\mu\text{m}$) by 23.9%. The scaled views of 1st peak and 2nd peak are shown in Fig. 5.5.

5.3 Concluding remarks

In this chapter, the design concepts of shaving cutter serrations are presented, and design optimization is also achieved. The advantages of the proposed model are listed:

1. The proposed mathematical model considers the tooth modification of shaving cutter tooth derived in chapter 4.
2. The proposed mathematical model can be adopted for design optimizations because the design variables are changed to be independent of each other.
3. The cutting-down ratio has been reduced by 23.9%, which means the shaving time can be reduced by almost 1/4 per piece.



Table 5.1 Basic data for the work gear and corresponding shaving cutter.

Work gear	
Number of teeth (N_2)	13
Normal module in pitch circle (m_{pn})	1.750 mm
Normal circular tooth thickness (s_{pn2})	3.270 mm
Normal pressure angle in pitch circle (α_{pn})	20°
Outside radius (r_{o2})	27.600 mm
Form radius (r_{f2})	21.490 mm
Face width	24 mm
Helix angle in pitch circle (β_{p2})	5° R.H.
Plunge gear shaving cutter	
Number of teeth (N_1)	137
Helix angle in pitch circle (β_{p1})	10° R.H.
Face width	30 mm
Normal circular tooth thickness (s_{pn1})	0.529 mm
Operating data of shaving procedure	
Operating center distance (E_o)	130.612 mm
Operating crossed angle (γ_o)	14.722°
Cone grinding wheel	
Cone angle (θ_c)	2.961°
Pressure angle (α)	13.882°
R_c	350 mm

Table 5.2 Basic data for the serrations.

Serration pitch	1.85 mm R.H.
Number of starts	62
Serration displacement	-0.216 mm

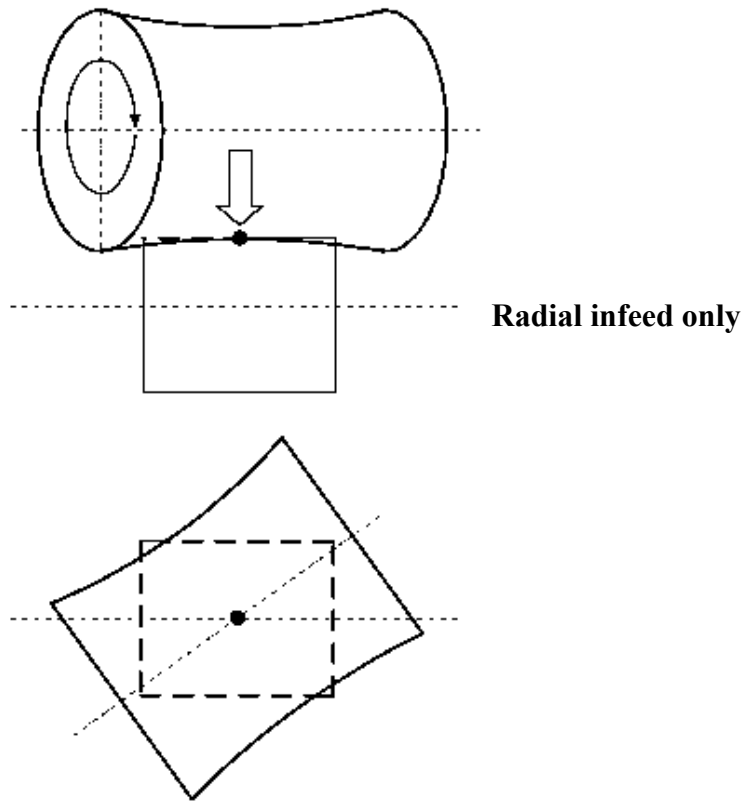


Figure 5.1 Diagram of a shaving cutter and a work gear (Hsu, 2006).

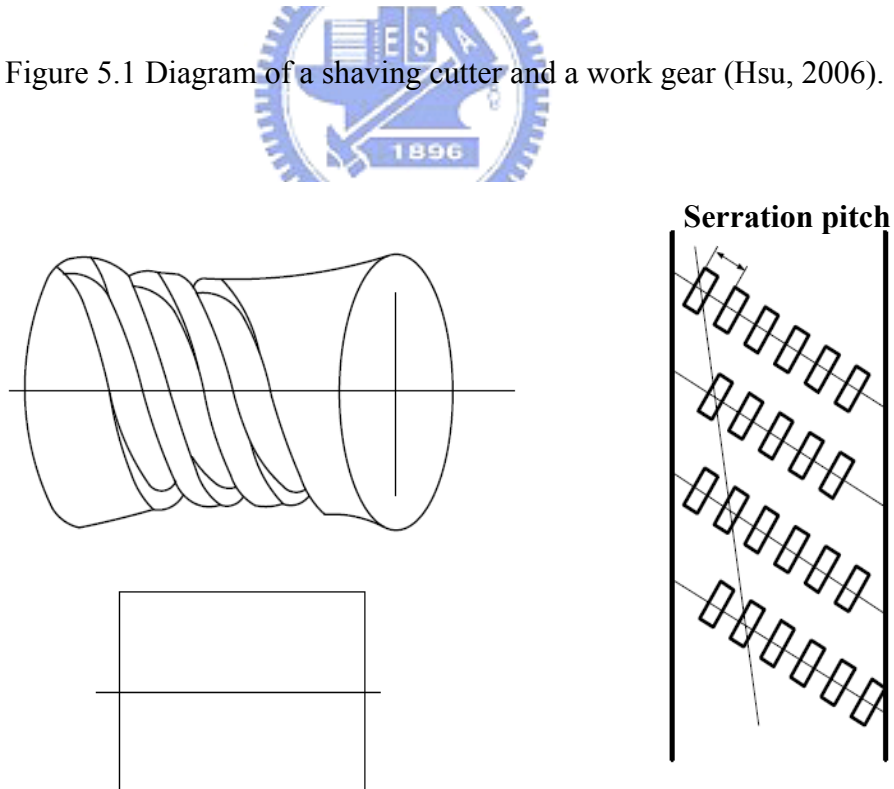


Figure 5.2 Diagram of a shaving cutter with helix-staggered serrations (Hsu, 2006).

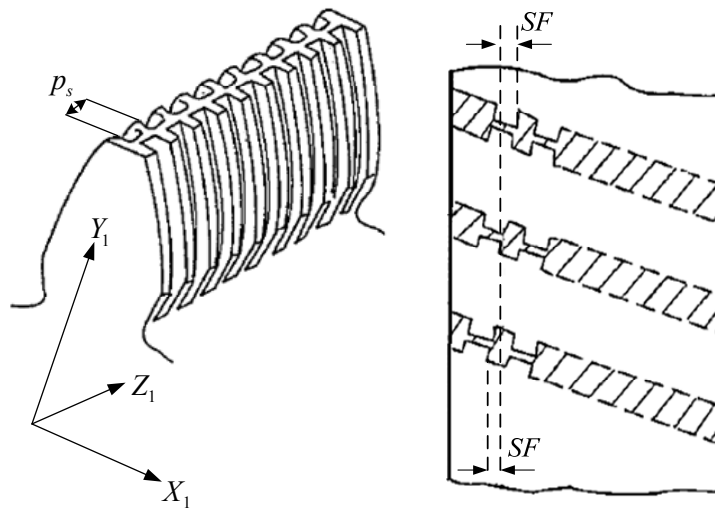


Figure 5.3. Design parameters of plunge shaving cutter serration (a) serration pitch (b) serration displacement.



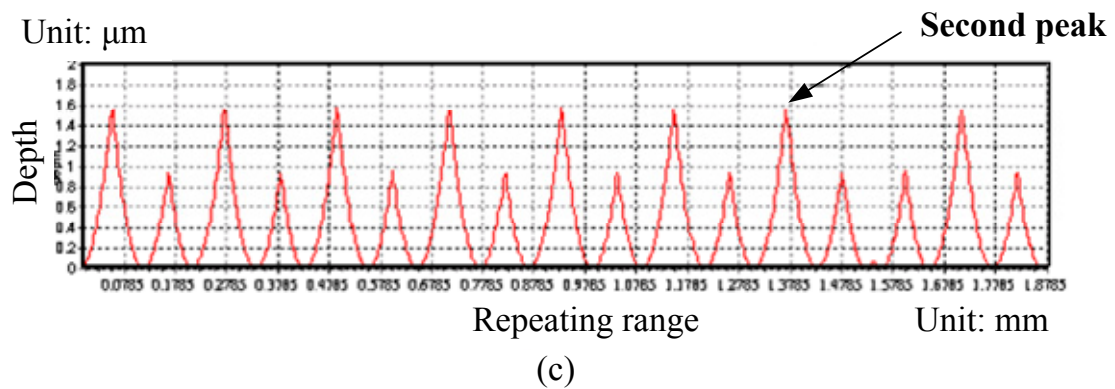
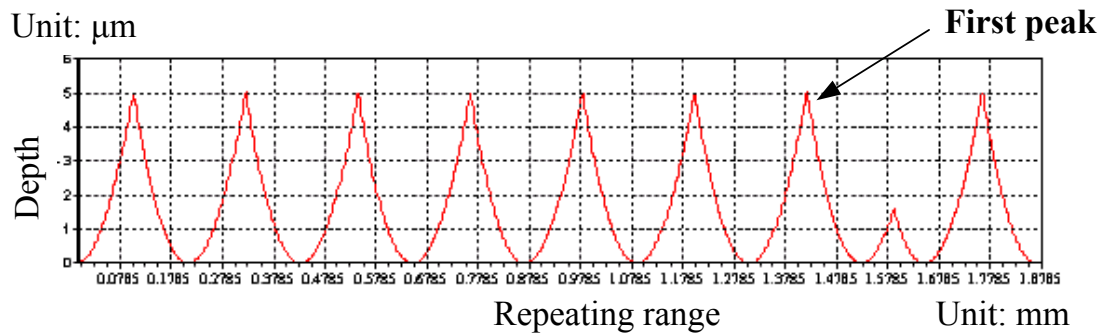
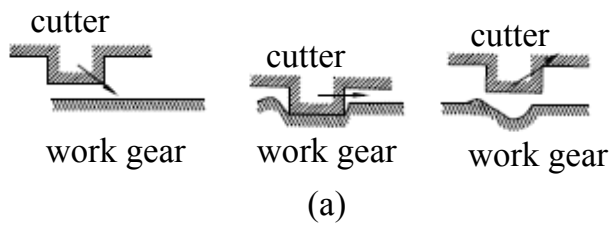
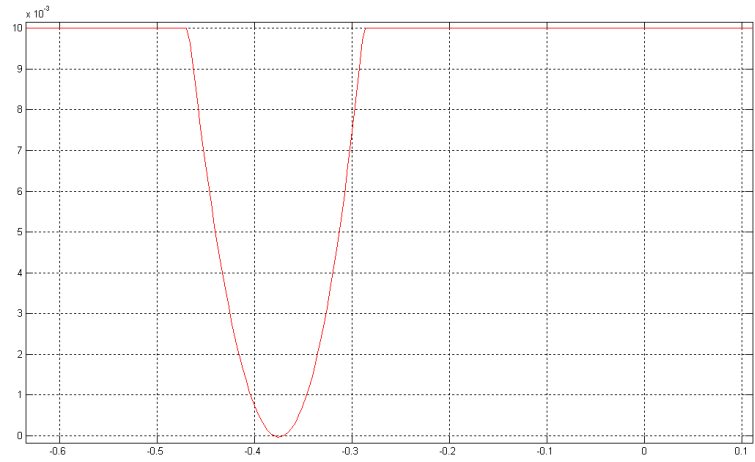
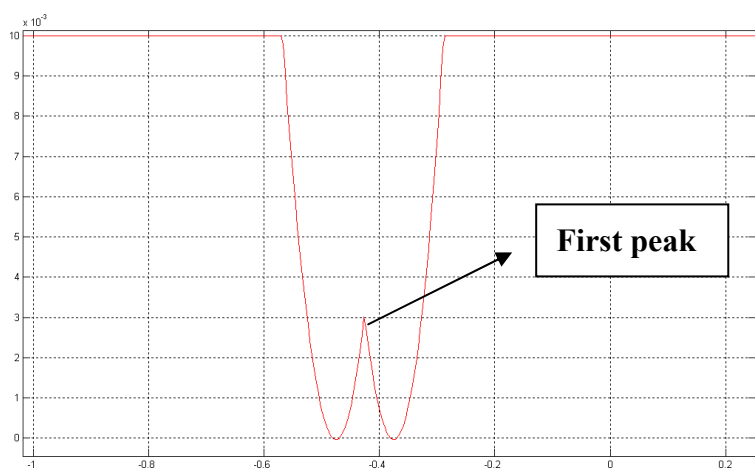


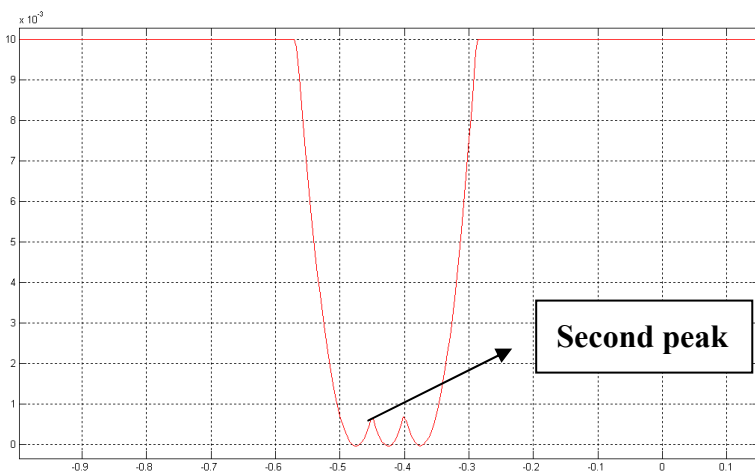
Figure 5.4 Cutting path calculations (Hsu, 2006) (a) path of the cutting edge on the work gear (b) end of the first cutting cycle simulation (c) end of the second cutting cycle simulation.



(a)



(b)



(c)

Figure 5.5 Optimized cutting-down ratio of Example 5.2 (a) 1st cut (b) 1st peak (c) 2nd peak.

CHAPTER 6

CONCLUSIONS AND FUTURE WORKS

6.1 Conclusions

This dissertation has investigated gear tooth crowning induced by transverse and plunge gear shaving. In the past, these are very time consuming because the machine setting and the shaving cutter need to be modified back and forth by trial and error. In this dissertation, mathematical models for analyses and design optimization are proposed to solve this problem. For transverse shaving, influences of machine setting parameters and cutter assembly errors have been observed. Design optimization for robustness of gear transmission error has also been accomplished. For plunge shaving, the analytical descriptions of crowned gear and hence plunge shaving cutter have been constructed so that the grinding wheel can be optimized to minimized the topographic error. The cutting trace of plunge shaving cutter has also been analyzed so that the final real tooth forms can be predicted. Besides, the shaving efficiency has also been improved. Based on the results of the numerical examples, the following conclusions have been drawn:

1. For the crowning mechanism, the crowning effect is shown to be sensitive to the angle θ between guideway and horizontal as well as the horizontal distance d_h between pivot and pin. The horizontal and the center distance errors Δh and ΔE_0 are also proved significant to gear tooth crowning.
2. To have a double crowned gear shaved by traditional gear shaving machine for better performance in transmission error, four categories of parameter need to be considered: modification of shaving cutter, assembly errors of shaving cutter, assembly errors of gears and machine setting parameters. Among the 11 selected parameters, the coefficient a_c concerning the modification of shaving cutter and the angle θ between the guide

way and horizontal on the shaving machine contribute the most to transmission error.

3. To manufacture the double crowned gear by transverse shaving, the machine setting parameter and cutter profile coefficient can be calculated and optimized beforehand without trial and error, which reduces the required time for development.
4. To interpolate gears with both lead and profile crownings (double crowned), more sampling points are needed in the radial direction. In manufacturing a shaving cutter, the lead crowning can be compensated by adjusting the cone angle, and the profile crowning can be implemented by modifying the profile of the grinding wheel.
5. The proposed mathematical model of shaving cutter serration considers the tooth modification of shaving cutter tooth.
6. The proposed mathematical model of shaving cutter serration can be adopted for design optimizations because the design variables are changed to be independent of each other.
7. To manufacture the double crowned gear by plunge shaving, the required profile of cone grinding wheel and hence the shaving cutter tooth surface can be calculated and optimized beforehand without trial and error, which reduces the required time for development; the cutter serration can also be optimized for better cutting efficiency.

6.2 Future works

Based on the mathematical models provided in this thesis for analyzing the shaving process, the following relevant research needs to be undertaken in the future:

1. New geometry and new displacement for the shaving cutter serrations should be investigated to improve the finishing effect of the plunge shaving cutter.
2. As regards the tool life of the shaving cutter, further study is needed on workpiece quality as it affects the wear of the serration.
3. Because the shaving cutter can be reground several times, future study should use the acceptable variation ratio of the contact length in the shaving cutter design to find the

regrinding range.



REFERENCES

1. Townsend, D.P., 1992. Dudley's Gear handbook: The Design, Manufacture, and Application of Gears, McGraw-Hill, New York.
2. Dugas, J. P., 1996. Gear Shaving Basics-Part I. Gear Technology, May/June, pp. 26-30.
3. Litvin, F. L., 1994. Gear Geometry and Applied Theory. PTR Prentice Hall, New Jersey.
4. Tsay, C. B., 1988. Helical Gears with Involute Shaped Teeth: Geometry, Computer Simulation, Tooth Contact Analysis, Stress Analysis. Journal of Mechanisms, Transmission, and Automation in Design, Vol. 110, pp.482-491.
5. Miao, H. C., Koga H., 1996. Design and Analysis of Plunge Shaving for Finishing Gears with Tooth Profile Modifications. ASME Power Transmission and Gearing Conference, DE, vol. 88, pp275-281.
6. Koga, H., Umezawa, K., Miao, H. C., 1996. Analysis of Shaving Processing for Helical Gears with Tooth Modification. ASME, Power Transmission and Gearing Conference, DE, vol. 88, pp265-273.
7. Kim, J. D., Kim, D. S., 1996. The Development of Software for Shaving Cutter Design. Journal of Materials Processing Technology, vol. 59, pp. 359-366.
8. Moriwaki, I., Okamoto, T., Fujita, M., Yanagimoto, T., 1990. Numerical Analysis of Tooth Forms of Shaved Gears. JSME, International Journal Series III, vol. 33, No. 4, pp. 608-613.
9. Moriwaki, I., Fujita, M., 1994. Effect of Cutter Performance on Finished Tooth Form in Gear Shaving. Journal of Mechanical Design, Transactions of the ASME, vol. 116, n. 3, pp. 701-705.
10. Hsu, R.H., 2006. Theoretical and practical investigations on the design of plunge shaving cutter. Ph.D. Dissertation, National Chung Cheng University.
11. Lin, H. J., 2006. Simulation of Gear Shaving Machines and Gear Tooth Contact Analysis. Master Thesis of National Formosa University.
12. Chang, S. L., Tsay, C. B., Tseng, C. H., 1997. Kinematic Optimization of a Modified Helical Simple Gear Train. ASME Journal of Mechanical Design, vol. 119, pp. 307-314.
13. Sundaresan, S., Ishii, K., Houser, D.R., 1991. Design Optimization for Robustness Using Performance Simulation Programs, ASME Journal of Design Automation, vol. 1, no. 32, pp. 249-256.
14. Litvin, F.L., 2001. Helical and Spur Gear Drive with Double-Crowned Pinion Tooth Surfaces and Conjugated Gear Tooth Surfaces, United States Patent, Patent No: US 6205879.
15. Wagaj, P., Kahraman, A., 2002. Influence of tooth profile modification on helical gear durability. Journal of Mechanical Design, vol. 124, pp. 501-510.
16. Kahraman, A., Bajpai, P., Anderson, N. E., 2005. Influence of tooth profile deviations on helical gear wear. Journal of Mechanical Design, vol. 127, pp. 656-663.

17. Bianco, G. , 2000. Gear Shaving. Jiuge, Beijing.
18. Litvin, F. L., Fan, Q., Vecchiato, D., Dememego, A., Handschuh, R. F., Sep, T. M., 2001. Computerized Generation and Simulation of Meshing of Modified Spur and Helical Gears Manufactured by Shaving, Computer Methods in Applied Mechanics and Engineering, vol. 190, pp.5037-5055.
19. Radzevich, S. P., 2003. Design of shaving cutter for plunge shaving a topologically modified involute pinion. Journal of Mechanical Design, vol. 125, pp. 632-639.
20. Radzevich, S. P., 2005. Computation of parameters of a form grinding wheel for grinding of shaving cutter for plunge shaving of topologically modified involute pinion. Journal of Mechanical Design, vol. 127, pp. 819-828.
21. Piegl, Les, Tiller, Wayne, 1997. The NURBS Book, 2nd edition. Springer-Verlog, Berlin.
22. Barone, S., 2001. Gear geometric design by B-spline curve fitting and sweep surface modeling. Engineering with Computers 17: 66-74.
23. Wang, Fulin, Yi, Chuanyun, Wang, Tao, Yang, Shuzi, Zhao, Gang, 2005. A generating method for digital gear tooth surfaces. The International Journal of Advanced Manufacturing Technology, vol. 28, pp. 474-485.
24. Taguchi, G., 1993. Taguchi methods: design of experiments, ASI Press, Dearborn, MI.

